Mass Spectrometric Analyses of the Lipidomes of Quiescent and Non-Quiescent Cells Reveal that Certain Dietary, Pharmacological and Genetic Interventions Delay the Chronological Aging of the Yeast *Saccharomyces Cerevisiae* by Altering Lipid Metabolism

Amanda Piano

A Thesis

in

The Department

of

Biology

Presented in Partial Fulfillment of the Requirements

for the Degree of Master of Sciences at

Concordia University

Montreal, Quebec, Canada

December 2015

CONCORDIA UNIVERSITY

School of Graduate Studies

This is to certify that the thesis prepared

By: Amanda Piano

Entitled: Mass Spectrometric Analyses of the Lipidomes of Quiescent and Non-Quiescent Cells Reveal that Certain Dietary, Pharmacological and Genetic Interventions Delay the Chronological Aging of the Yeast *Saccharomyces Cerevisiae* by Altering Lipid Metabolism

and submitted in partial fulfillment of the requirements for the degree of

Master of Sciences (Biology)

complies with the regulations of the University and meets the accepted standards with respect to originality and quality.

Signed by the final examining committee:

_____ Chair

Dr. Selvadurai Dayanandan

_____ External Examiner

Dr. Alisa Piekny

_____ Examiner

Dr. Reginald Storms

_____ Examiner

Dr. Madoka Gray-Mitsumune

_____ Supervisor

Dr. Vladimir Titorenko

Approved by _____

Chair of Department or Graduate Program Director

_____

Dean of Faculty of Arts and Science

Date _____

ABSTRACT

Mass Spectrometric Analyses of the Lipidomes of Quiescent and Non-Quiescent Cells Reveal that Certain Dietary, Pharmacological and Genetic Interventions Delay the Chronological Aging of the Yeast *Saccharomyces Cerevisiae* by Altering Lipid Metabolism

Amanda Piano, M.Sc.

Recent studies have revealed that different classes of lipids play essential roles in the intrinsically complex process of cellular aging. Although these roles of lipids is blurred by intricacy and complexity, the identification of mechanisms that link lipid metabolism to cellular aging is currently underway. The investigation of a cell's entry into and progression through a differentiated quiescent state can provide a means of linking cell cycle regulation to aging. Using yeast *Saccharomyces cerevisiae* as a model organism, I explored how the major lipid classes phosphatidic acid (PA), phosphatidylethanolamine (PE), phosphatidylcholine (PC), phosphatidylinositol (PI) and phosphatidylserine (PS), as well as mitochondria specific cardiolipin (CL) and major storage lipid triacylglycerol (TAG), are influenced during the aging process by various dietary, pharmacological and genetic interventions known to extend longevity. These interventions include a caloric restriction diet, lithocholic bile acid (LCA) and the *tor1Δ* mutation eliminating the key protein component of the pro-aging Target of Rapamycin Complex 1 (TORC1) pathway. The quantitation of different lipid classes throughout the entire lifespan was accomplished by the mass spectrometric analysis of lipids found in quiescent and non-quiescent cell populations separated by centrifugation in a Percoll density gradient. My findings revealed that there are at least three different ways of delaying aging in yeast by differently altering lipid metabolism and transport in chronologically aging cells.

Acknowledgements

I would like to thank my supervisor Dr. Titorenko for his continuous guidance and support throughout my undergraduate and graduate studies in his laboratory. I would also like to thank my committee members Dr. Madoka Gray-Mitsumune and Dr. Reginald Storms for their valuable suggestions that contributed to my research and learning experience at Concordia University, as well as past and present graduate and undergraduate students and volunteers for their support in the laboratory.

Table of Contents

List of Figures

List of Tables

List of Abbreviations

cAMP/PKA	cAMP/protein kinase A signaling pathway
CDK	cyclin dependent kinase
CFU	colony forming units
CL	cardiolipin
CLS	chronological lifespan studies
CR	caloric restriction
D	diauxic growth phase
DAG	diacylglycerol
DR	dietary restriction
ER	endoplasmic reticulum
FFA	free fatty acid
L	logarithmic growth phase
LCA	lithocholic acid
LD	lipid droplet
m/z	mass/ion charge ratio
MFQL	Molecular Fragmentation Query Language
MS	mass spectrometry
MS/MS	tandem mass spectrometry
non-CR	non-caloric restriction
NQ	non-quiescent
NL	nutrient limitation
OD_{600}	optical density at 600 nm
PD	post-diauxic growth phase
PA	phosphatidic acid
PC	phosphatidylcholine
PE	phosphatidylethanolamine
PG	phosphatidylglycerol
PI	phosphatidylinositol
PS	phosphatidylserine
PKA	protein kinase A

ppm	parts per million
Q	quiescent
RLS	replicative lifespan studies
ROS	reactive oxygen species
Sch9	serine-threonine protein kinase Sch9
SE	sterol esters
ST	stationary growth phase
TAG	triacylglycerol
TCA cycle	tricarboxylic acid cycle
TORC1	target of rapamycin complex 1
WT	wild-type strain

1 Introduction

1.1 The budding yeast *Saccharomyces cerevisiae* as an advantageous model organism for unveiling mechanisms of cellular aging in multicellular eukaryotes

The aging process has demonstrated its complexity at both the organismal and cellular level. The converging, diverging and overlap of cellular aging pathways and mechanisms, as well as the great intricacy at the multicellular level, has contributed to our blurred understanding of the complex mechanisms and processes underlying cellular aging in both individual cells and cell populations. For this reason, the budding yeast *Saccharomyces cerevisiae* is arguably one of the most important model organisms when conducting age-related research [1, 2, 3] and has been recognized as contributing to the identification of the most age-related mammalian genes when compared to other model organisms [1]. Our enhanced knowledge of the roles and functions of genes in yeast has furthered our understanding of age-related diseases and illnesses and the mechanisms with which they manifest in higher eukaryotes such as humans. Such a great advantage over other model organisms is due to budding yeast's unicellular properties, easy ability to culture, maintain and study, and its evolutionarily conserved eukaryotic cellular aging processes [4]. *S.cerevisiae'*s unicellular properties and evolutionarily conserved cellular processes and pathways provide a simplified model allowing a deeper understanding of the mechanisms and biological principals involved in multi-cellular eukaryotic aging [4]. This further insight is due to budding yeast's tractability to all levels of experimental analysis such as genetic, molecular, biochemical, cell biological, system biological and microfluidic dissection analysis [3, 5, 6, 7, 8]. The short and easily observed lifespan of *S.cerevisiae* has played a major role in the rapid identification of various molecular mechanisms and factors that modify aging, allowing a more throughout understanding of the roles of numerous genes, key nutrient and

energy-sensing signalling pathways and small molecules in defining and influencing eukaryotic longevity [2, 5]. The impact of these longevity influencing factors can be easily assayed due to *S.cerevisiae*'s ability to provide two aging models as complementing approaches to study aging.

1.2 Replicative and chronological models of yeast aging

An additional advantage when studying yeast as a model organism is aging can be easily examined by two different lifespan assays, each monitoring a different aspect of cellular aging [1, 9]. Traditionally investigated independently of each other under laboratory conditions, replicative and chronological aging lifespan assays are able to provide us with strong models of the aging process in both dividing and non-dividing cells respectively [4, 5, 9]. Replicative lifespan studies (RLS) take advantage of the asymmetric budding that takes place during yeast division in nutrient available environments and defines aging as the number of daughter cells a single mother cell can produce before cell cycle arrest [1, 2, 10] (**Figure 1.1**). Under laboratory conditions, replicative lifespan assays involve the manual removal of daughter cells from the mother cell using a micromanipulator under a dissection microscope [1, 11]. Smaller daughter buds are continuously removed and tallied until the mother cell reaches a post-replicative state, no longer able to produce daughter cells (about 20-30 divisions later), becoming senescent and eventually lyse [11] **(Figure 1.1).** RLS with yeast are valuable as they are able to provide a cellular aging model for mitotically active cells (for example lymphocytes) in multicellular organisms [2, 11]. When studying replicative lifespan in yeast, it is extremely important to note that there are multiple factors that can influence yeast's replicative lifespan such as growth conditions (nutrient availability and carbon source) and genetic background [1]. Yeast cells grown in conditions of lower glucose concentrations, in attempt to model the longevity-

extending influence of a calorie restricted diet in multicellular eukaryotic organisms, differ in their replicative lifespan extension depending on the genetic background of the strain [1]. Findings such as this have demonstrated the significant influence of various environmental and genetic factors on replicative aging [1].

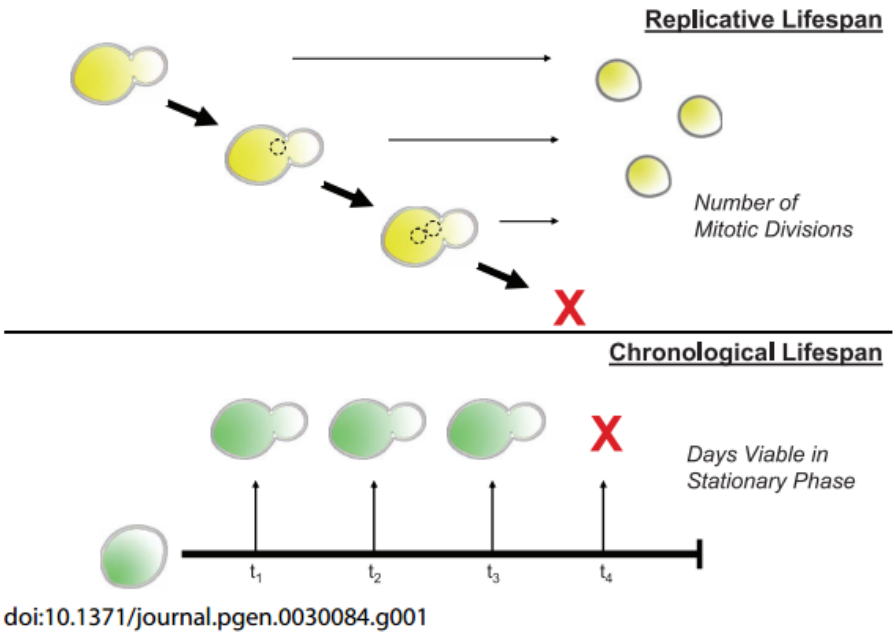

Figure 1.1 Replicative and Chronological Lifespan Studies Replicative lifespan is determined by the number of mitotic divisions or number of daughter cells a mother cell produces until cell cycle arrest. Chronological lifespan is measured by the amount of time during the stationary phase/post mitotic phase cells can maintain viability and proliferate when placed on to nutrient-rich media [1].

The second yeast aging paradigm investigates chronological lifespan by determining the length of time a cell remains viable after cell cycle arrest takes place [1, 2, 11, 12] **(Figure 1.1).** Upon nutrient limitation, yeast cell growth and division are arrested and cells enter the stationary growth phase. Chronological lifespan studies (CLS) define lifespan by the amount of time yeast cells remain viable while in this non-dividing phase. Yeast cell viability is determined by the cell's ability to re-enter the cell cycle and commence division when essential nutrients are present, indicated by the formation of a colony when placed on solid nutrient rich media [1, 2, 5,

9, 12, 13]. Liquid cultures are able to provide post-mitotically active cells arrested in their cell cycle, as once all carbon sources are exhausted, the culture enters the stationary growth phase [2, 4]. Yeast cell viability is determined at various time points throughout stationary phase by the ability to resume mitotic growth upon formation of a colony when placed on nutrient rich media, thus defining their chronological lifespan [12, 13]. The chronological lifespan model of aging in yeast is able to complement that of replicative lifespan as it provides a model that studies non-dividing cells (for example neurons and stem cells) in multicellular eukaryotic organisms [1, 5]. CLS also provide a model to investigate the mechanisms involved in apoptotic and necrotic cell death pathways [1, 5].

The replicative and chronological aging paradigms have both provided models that further investigate different aspects of aging in yeast, each with their own assay. The availability of these assays has been able to significantly advance our understanding of the cell-autonomous mechanisms responsible for orchestrating longevity-defining cellular processes within an individual cell in eukaryotic organisms [1, 2, 8, 10, 14].

1.3 Cell-autonomous mechanisms underlying chronological aging in yeast *S.cerevisiae*

As chronological lifespan studies continue to emerge, there appears to be a wealth of information demonstrating that cellular aging is not simply a programmed process of functional decline or the accumulation of molecular damage; rather it is made up of a biomolecular network composed of longevity-defining processes [5, 9]. These cellular processes include cell metabolism, growth, division, organelle biogenesis, interorganellar communication, macromolecular homeostasis, stress response and death, all taking place throughout yeast's chronological lifespan [9]. A body of evidence supports the view that there are cellular processes

prior and/or after entry into a non-proliferative state that are responsible for defining the longevity of chronologically aging yeast [5]. A biomolecular network is composed of these longevity-defining cellular processes and current research suggests several lifespan checkpoints play key roles in determining the pace of cellular aging [5, 9]. Yeast's lifespan consist of both early-life (logarithmic, diauxic and post-diauxic growth phase) and late-life (stationary growth phase) checkpoints located both prior to and after cell cycle arrest respectively [9]. The importance and presence of these checkpoints is exemplified by the addition of a longevity extending molecule only exhibiting its anti-aging effect if added at a specific checkpoint during yeast's lifespan, supporting the importance of these lifespan checkpoints in defining longevity based on the anti- or pro- aging influence on the cellular processes [5, 15]. Each checkpoint involves master regulator proteins, responsible for assessing the intracellular concentrations of intermediates and by-products of certain metabolic pathways, and are then able to respond to these intracellular conditions by influencing the rates and efficiencies the cell's cellular processes **(Figure 1.2).** Master regulator proteins are therefore responsible for regulating vital cellular processes throughout chronological lifespan by orchestrating the development and maintenance of anti- and pro- aging cellular patterns to establish a rate of chronological aging and define yeast chronological lifespan [9]. The concentration of intracellular key metabolites is influenced by factors such as diet and the addition of small molecules [5, 9]. Master regulator proteins detect a change in the concentration of key metabolites at given checkpoints and respond by modulating the rate of cellular processes, such as cell growth, division, metabolism or stress response in the network, in turn establishing the rate of chronological aging **(Figure 1.2).** Key proteins and protein complexes that play roles as checkpoint-specific master regulators include but are not limited to 1) Rim15p, Msn2p, Msn4p and Gis1p as anti-aging master regulators by their role in

stress resistance, 2) Tel1p and Rad53p as anti-aging master regulators by their ability to minimize telomere DNA damage and 3) TORC1 (Target of Rapamycin Complex 1) as a pro-aging master regulator [5] **(Figure 1.2).** An increase in the intracellular amino acids synthesized from Tricarboxylic acid (TCA) cycle intermediates, activates the TORC1 complex leading to a pro-aging cellular pattern involving protein synthesis in the cytosol, inhibition of stress genes, suppression of protein synthesis in the mitochondria and the suppression of autophagy (via Protein Kinase A (PKA), another pro-aging master regulator) [5] **(Figure 1.2).**

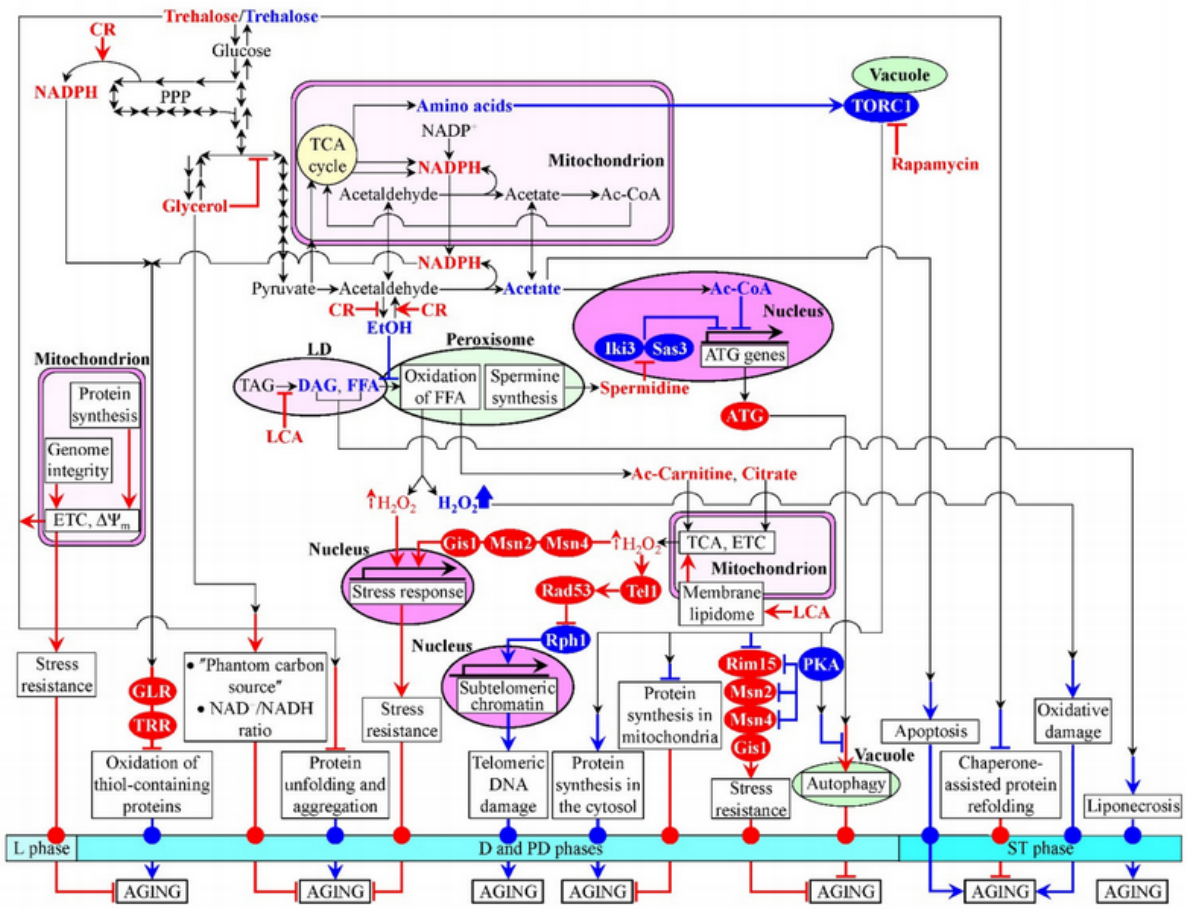

Figure 1.2 The concept of a biomolecular network underlying chronological aging in yeast. The concept of a biomolecular network includes both early (logarithmic phase (L phase), diauxic phase (D phase) and post-diauxic phase (PD phase)) and late (stationary phase (ST phase)) lifespan checkpoints. The intracellular concentrations of key intermediates and products of longevity-defining metabolic pathways are monitored by master regulator proteins or protein complexes. These master regulators then respond to age-related intracellular concentrations of key metabolites at specific time points by adjusting the rate and efficiency of cell metabolism, growth, division, organelle biogenesis, interorganellar communication, macromolecular homeostasis, stress response or death. The regulation of these cellular processes throughout lifespan orchestrates the development and maintenance of anti-aging (red) or pro-aging (blue) cellular patterns, therefore establishing the rate of cellular aging and defining yeast chronological lifespan. Anti-aging master regulators are located in the red circles and pro-aging master regulator proteins are located in blue circles. Figure reference [5].

1.4 Differentiation of yeast cells cultured in liquid media yields several cell populations that differ in their longevities

As previously mentioned, stationary-phase yeast cultures play a crucial role in the analysis of chronologically aging yeast cells as it provides post-mitotic cells that can be assayed for their viability. When cultured in nutrient-rich liquid media with glucose, yeast cells consume glucose as their primary carbon source and cell division takes place at an exponential rate [3, 4]. Upon glucose exhaustion, cells begin to cease rapid growth and begin to utilize non-fermentable carbon sources in the medium, leading to the diauxic shift [3, 4]. During the diauxic shift, the culture transitions from the logarithmic to diauxic growth phase and yeast cells begin to arrest in the G1 phase of the cell cycle (G0 state) allowing them to enter a differentiation program yielding a population of non-proliferating quiescent cells [4, 9, 16, 17].

Quiescent cells are infamously known for their ability to synchronously re-enter the cell cycle and commence cell division when placed back into nutrient rich conditions [4, 16, 17, 18]. Upon entry into the stationary phase, an environment of carbon exhaustion/starvation, yeast cultures are composed of both quiescent cells and a heterogeneous mixture of non-quiescent cells [4, 16, 17]. Differentiation into a quiescent state provides quiescent cells with various physical, physiological and biochemical characteristics displaying the reprogramming and remodelling of most intracellular structures and processes [3, 4, 16, 17]. The quiescent cell population is composed of mainly unbudded daughter cells or young mother cells that have only budded once, with a thickened cell wall, uniform in size and maintain a higher density than non-quiescent cells [16, 17]. The significant difference in density allows the easy separation of the two cell populations by density centrifugation [16, 17]. The accumulation of reserve carbohydrates such as trehalose, and to a lesser extent glycogen, accounts for quiescent cell's increase in density [16,

17, 18]. The increase of intracellular trehalose, a non-reducing disaccharide, provides the cell with the ability to survive situations of desiccation and freezing [18]. Trehalose accumulation contributes to the stress tolerance of cells by preserving membranes in a liquid crystalline phase as well as stabilizing proteins and preventing their aggregation during heat shock [18]. Quiescent cells have shown resistance to various types of stresses including: chronic oxidative, thermal and osmotic stress while maintaining functional mitochondria with a high respiratory efficiency and low levels of reactive oxygen species (ROS) [16, 17]. The maintenance of viability (determined by high metabolic activity when monitored with a fluorescent reporter molecule), reproductive capacity (determined by the cell's ability to form colonies on fresh media) and genomic stability are also key characteristics of quiescent cells [4, 16, 17].

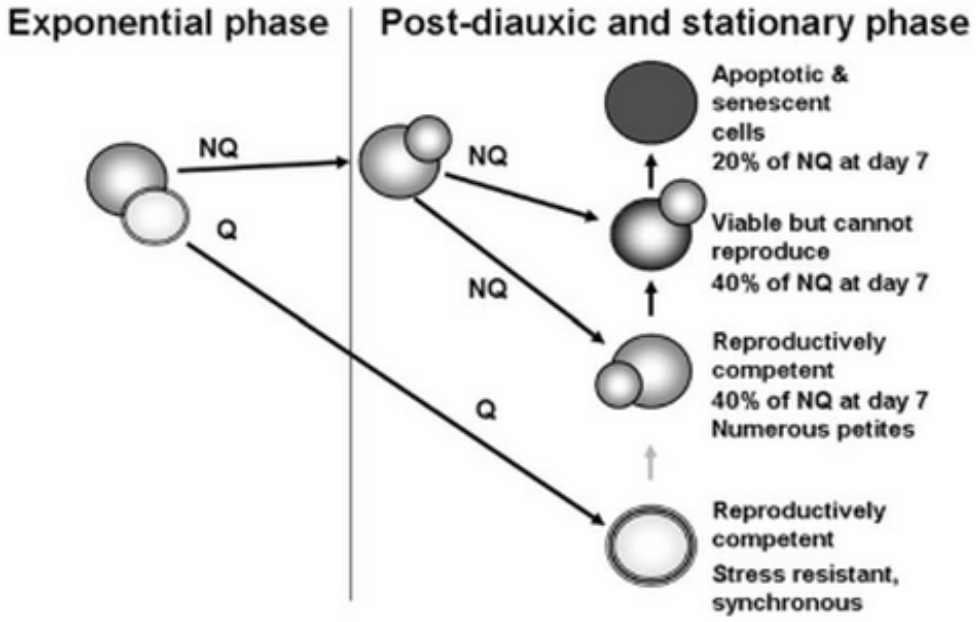

Figure 1.3 Model of quiescent (Q) and non-quiescent (NQ) cell differentiation during diauxic shift in glucose rich medium. During Post-diauxic and stationary phase, both quiescent and non-quiescent cell populations are present. Non-quiescent cells are comprised of three cell types, varying in their reproductive competence and viability, which are replenished at a slower rate by age-related differentiation of quiescent cells [4]. Figure Reference [4].

The stationary phase's non-quiescent cell population is comprised of old mother cells that have budded multiple times [4, 5, 16]. The less dense non-quiescent cell population is a heterogeneous mixture of cells that vary in viability and reproductive competence [4, 16, 17] **(Figure 1.3).** This heterogeneous mixture is made up of 3 cell types which include 1) viable and reproductively competent cells that begin to exhibit genomic instability, high levels of ROS and mitochondria that are unable to respire; 2) viable but reproductively incompetent cells that are believed to derive from the previously mentioned viable, reproductively competent non-quiescent cells and lastly; 3) apoptotic and senescent cells that may have originated from the reproductively incompetent non-quiescent cells [4, 16, 17] **(Figure 1.3).** Quiescent cells, under standard conditions are believed to replenish the non-quiescent cell population over time at a

slower rate as they begin to lose their quiescent cell characteristics such as genomic stability, mitochondrial function, reproductive competence and viability [4, 19] **(Figure 1.3).**

Quiescent cells maintain their viability and reproductive competence for a longer period of time when compared to non-quiescent cells due to the numerous structural, metabolic and physiological features that quiescent cells acquire upon their differentiation during the diauxic shift. Nutrient availability plays an important role in the differentiation of quiescent cells as quiescent cell differentiation takes place once the cell is faced with a nutrient limited and stressful environment.

1.5 The characteristic structural, metabolic and physiological features of quiescent yeast cells are orchestrated by a network of nutrient-sensing signalling pathways

As previously established, quiescent yeast cells undergo a drastic remodelling of their characteristics at the morphological, biochemical and physiological level upon exit from the cell cycle during the G1 phase in nutrient starved conditions [18]. These quiescent cell traits provide cells with the ability to survive long periods of starvation or stress and re-enter the proliferating state upon re-feeding [18]. Key nutrient-sensing pathways ensure quiescent cells acquire and maintain their quiescent-cell characteristics better adapting them to nutrient limited or stressful environments increasing their chances for survival [18]. The evolutionarily conserved core nutrient signalling pathways that ensure proper entry into quiescence and the acquiring of quiescent cell characteristics includes the Protein Kinase A (PKA), Target of Rapamycin Complex 1 (TORC1), Sucrose non-fermenting 1 (Snf1) and Pho85 signalling pathways [18]. These key signalling pathways display several points of overlap that ensure the appropriate response to nutrient starvation ensuring survival [18].

The PKA signalling pathway plays an important role as a positive regulator of cellular growth and a critical player in deciphering when to enter quiescence [18]. The heterotetrameric protein kinase PKA complex includes 2 catalytic subunits with 2 regulatory subunits acting as pseudosubstrates [19, 20]. The presence of cAMP (cyclic-adenosine monophosphate), in glucose rich environments, causes the regulatory subunits of PKA to bind cAMP therefore releasing PKA's catalytic subunits, allowing the phosphorylation of target proteins involved in ribosomal biogenesis, cellular growth, stress response and metabolism [18, 19]. PKA-signalling network promotes growth by inducing ribosome biogenesis by way of the controlled expression of ribosomal protein genes, rDNA genes and Ribi (ribosomal biogenesis) genes while inhibiting transcription factors that repress growth [18]. Upon glucose exhaustion, decreasing levels of cAMP lead to the negative regulation of the PKA pathway [18, 19]. The down regulation of PKA leads to the expression of genes associated with stress resistance, the inhibition of cell growth and cell cycle progression by the regulation of G1-S phase progression and the inhibited mobilization of reserve carbohydrate glycogen and stress protecting trehalose, allowing quiescent yeast cell to obtain their characteristics essential for proper entry into a quiescent state [18, 19]. Yeast cells with uncontrolled PKA activity are unsuccessful in acquiring most physiological characteristics of quiescent cells upon entry into stationary phase, while PKA deficient yeast cells are locked into a G0-like state as growth is arrested, demonstrating the critical role of PKA upon entry into quiescence [18].

TORC1 is a highly conserved pro-aging pathway in yeast that plays a critical role in the cell's decision on when to enter quiescence [18]. TORC1 activity relies on both the quality and quantity of multiple nutrients in the environment and can be inhibited by various environmental conditions such as starvation for carbon, nitrogen or amino acids and the presence of noxious

stress such as acetic acid, high salt, redox stress or high temperatures [18, 21]. The TORC1-Sch9 nutrient signalling branch of the TORC1 pathway plays an important role in lifespan regulation during chronological aging as the deletion of protein kinase SCH9 in yeast mimics the longevity extending effects of a calorie restricted diet and a TOR1 deletion [21]. Upon starvation for essential nutrients such as carbon, nitrogen or phosphate, yeast cells arrest growth and division, and then enter into the stationary phase [21]. TORC1's inhibition mimics the effects of nutrient starvation as they both lead to decreased protein synthesis and ribosomal biogenesis, changes in gene transcription, induction of autophagy, G1 cell cycle arrest and entry into quiescence [18, 21].

The Snf1 protein kinase signalling pathway is a central controller of energy homeostasis largely dependent on the presence of glucose [18, 19, 20]. The presence of glucose causes the auto-inhibition between the catalytic and regulatory subunits of Snf1p, a heterotrimeric AMP-activated kinase at the centre of the Snf1 pathway, inactivating its protein kinase function [19, 20]. The absence of glucose relieves this inhibition allowing Snf1p to be a functional protein kinase. Snf1p activation under declining glucose levels, promotes respiratory metabolism, gluconeogenesis, glycogen accumulation, autophagy and peroxisome biogenesis due to its ability to take part in the transcription of 400 genes, either by inhibiting transcriptional repressors or stimulating transcriptional activators, along with controlling transcriptional machinery [18, 20]. During the diauxic shift, when the preferred carbon source (glucose) is depleted, Snf1p plays a critical role in ensuring the expression of numerous genes involved in the metabolism of alternative carbon sources, such as gluconeogenesis and respiration, ensuring the yeast cell acquires the appropriate metabolic machinery and traits as a quiescent cell maintaining viability throughout the nutrient depleted stationary phase [18]. The role of Snf1p during the diauxic shift

is important upon entry into quiescence as it provides the cell with the appropriate metabolic machinery and cellular traits to maintain viability and increased chances for survival throughout stationary phase.

The cyclin-dependent kinase (CDK), Pho85, plays a major role in regulating intracellular phosphate metabolism but has also demonstrated an important role in other cellular processes such as sensing other environmental changes and cell cycle control [19, 20]. Pho85 associates with 10 cyclins, directing it to various target substrates [18, 19, 20]. Pho80, the best studied cyclin, makes up the Pho80-Pho85 cyclin-CDK complex which in the presence of external phosphate inhibits phosphate starvation and the secretion of phosphatases which retrieve and metabolize extracellular phosphate from phosphate limited environments [18, 19, 20]. The Pho80-Pho85 complex can also activate cyclin Cln3, allowing the progression over START in G1 of the cell cycle in phosphate rich environments [20]. Therefore, the inactivity of the Pho80-Pho85 complex in phosphate deprived conditions prior to entry into quiescence leads to G1 cell cycle arrest.

The proper preparation of a yeast cell structurally, metabolically and physiologically is crucial for the cell's survival when placed in nutrient-limited or stressful environmental conditions. Extracellular environmental conditions play a critical role upon entry into quiescence. Nutrient conditions outside the yeast cell are relayed by a major complex and intricate network of signalling pathways into the cell to allow the cell's preparation for the best chances of survival. The evolutionarily conserved PKA, TORC1, Snf1 and Pho85 signalling pathways have all demonstrated a much greater regulatory role upon entry into quiescence in addition to their better known roles in cellular energy and building. The integration and overlap of these key signalling pathways, forming a network, ensures survival upon nutrient starvation

and entry into quiescence [18] **(Figure 1.4).** These pathways converge at key nodes by common target proteins which play a critical role in the proper establishment of the quiescent program, ensuring the best chances of survival for the cell under nutrient starved and stressful conditions **(Figure 1.4).**

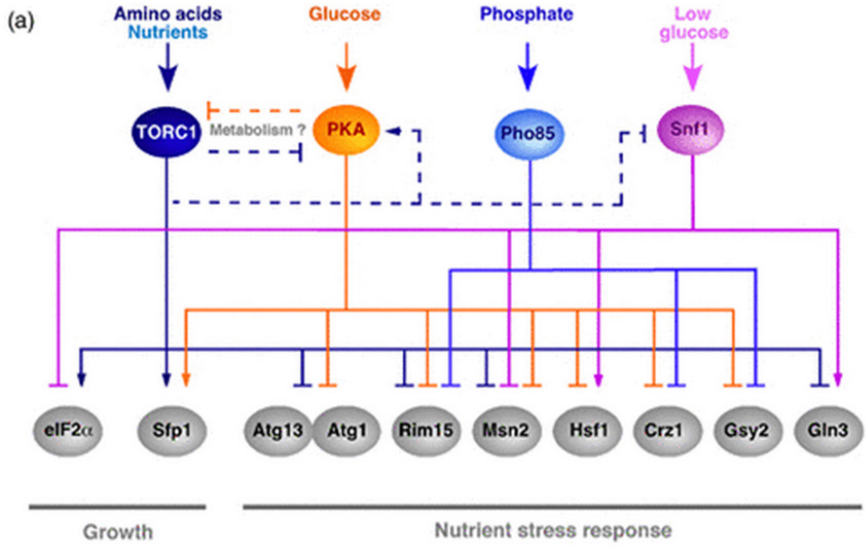

Figure 1.4 Key nutrient-signalling pathways converge at critical key nodes ensuring the proper establishment of a quiescent program. The key evolutionarily conserved nutrient-signalling pathways PKA, TORC1, Snf1 and Pho85 share common target proteins (grey circles) that play important roles in cell growth and nutrient stress response. The overlap of positive (arrows) or negative (bars) interactions ensures the appropriate cellular response to nutrient starvation, ensuring the cells best chance of survival. Figure and legend reference [18].

1.6 Synthesis, turnover and regulation of different lipid classes in yeast cells

Lipids have demonstrated greater roles in the cell in addition to their commonly associated roles in energy storage and as structural elements of yeast. Lipids play critical roles in cellular processes such as mediators of membrane fusion, apoptosis, cell signalling, membrane trafficking, anchoring membrane proteins, reservoir of 2nd messengers, provide pre-cursors of macromolecules, modification of membrane association and function as molecular chaperones [22, 24]. Yeast provide a great research model when studying lipid metabolism due to their

highly conserved eukaryotic lipid pathways which display a strong homology with higher eukaryotes [22, 23, 24]. The investigation of lipid biosynthesis, degradation and storage while aiding in the determination of the gene-enzyme relationship and how they influence lipid synthesis and turnover in multi-cellular organisms is possible due to yeast as a simplified model organism [22]. Glycerophospholipid synthesis in yeast is a complex dynamic process that is regulated by genetic and biochemical mechanisms and is tightly interrelated with the synthesis and regulation of other major glycerophospholipid classes [23].

Major yeast membrane glycerophospholipids include phosphatidylcholine (PC), phosphatidylethanolamine (PE), phosphatidylinositol (PI), and phosphatidylserine (PS) while major mitochondrial membrane glycerophospholipids include phosphatidylglycerol (PG) and cardiolipin (CL), demonstrating the cell's non-uniform lipid distribution and the varying glycerophospholipid profile of organelles dependant on the organelle's structure or function [23, 25]. Triacylglycerols (TAG) and the sterol esters (SE) are the primary constituents at the core of the Lipid Droplet (LD), a storage organelle composed of a monolayer of phospholipids and a small amount of proteins that house these neutral lipids [24]. The accumulation of free fatty acids (FFA) and sterols can have toxic effects on the yeast cell; therefore they are converted to TAG and SE respectively and stored in the LD to avoid this toxic result [24]. Neutral lipids are not suitable as membrane components therefore they remain in the LD until they are required by the cell for energy or as a precursor of membrane lipid synthesis [24].

Lipid synthesis takes place in multiple cellular organelles such as the endoplasmic reticulum (ER), mitochondria and lipid droplet, but all glycerophospholipid and TAG synthesis requires PA as a precursor [22, 23, 24]. Phospholipid and TAG synthesis branch off into 2 major lipid biosynthesis pathways from PA via CDP-DAG (CDP-diacylglycerol) and DAG

(diacylglycerol) respectively [22, 23, 24]. CDP-DAG, a liponucleotide intermediate, acts as a direct precursor in the synthesis of PI and PS in the ER [22, 24]. Further modification of PS in the mitochondria allows the synthesis of PE [22, 24]. PE is then available for the ER directed synthesis of PC, demonstrating a highly interrelated lipid synthesis pathway within the cell as the synthesis of one lipid at times relies on the presence of one or multiple lipids as a precursor [22, 24]. CDP-DAG is also a precursor of CL synthesis in the mitochondria with PG as its precursor [22, 23, 24] **(Figure 1.5).**

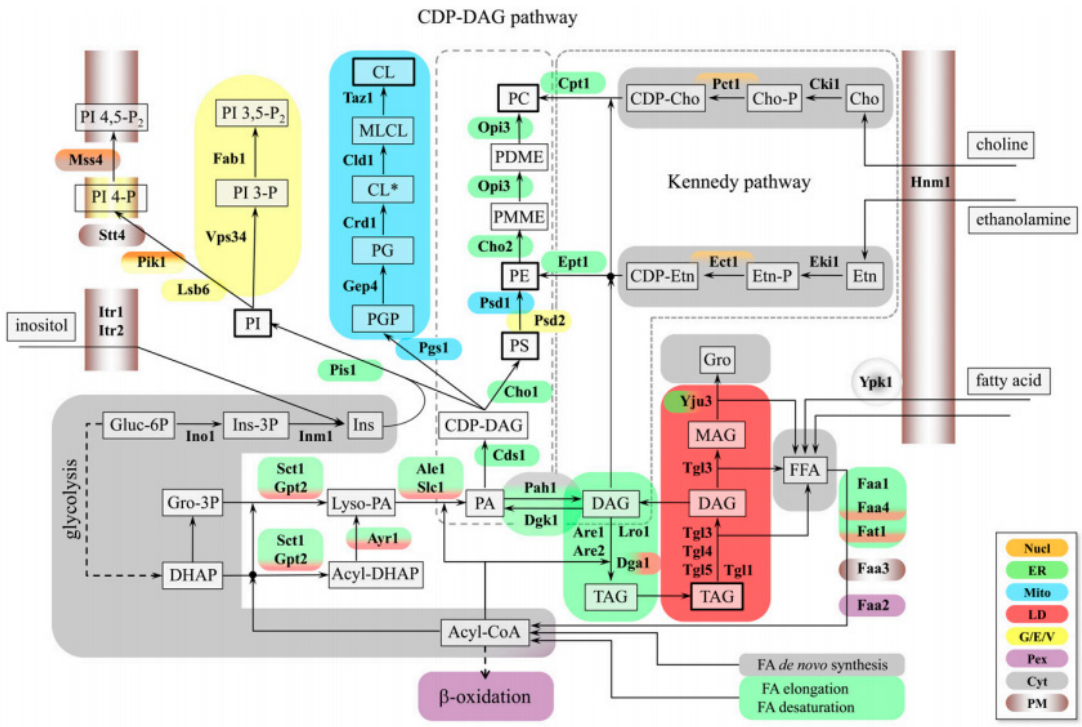

Figure 1.5 Major yeast lipid synthesis pathways and their subcellular localization. All glycerophospholipid and TAG (triacylglycerol) synthesis shares PA as common precursor. The CDP-DAG (CDP-diacylglycerol) lipid synthesis branch leads to the direct synthesis of PI (phosphatidylinositol) and PS (phosphatidylserine) in the ER (endoplasmic reticulum). PS synthesis allows the synthesis of PE (phosphatidylethanolamine) in the mitochondria, which can then serve as a precursor for the synthesis of PC (phosphatidylcholine) in the ER. PC and PE can also be synthesized via the Kennedy Pathway in the presence of DAG and exogenous choline and ethanolamine. CDP- DAG is also the precursor of PG (phosphatidylglycerol) in the mitochondria, eventually leading to the synthesis of CL (cardiolipin) after a few modifications. The DAG branch from PA leads to the synthesis of TAG in the ER, eventually packaging TAG into LDs (lipid droplets) where it is readily available as a source of DAG to refuel the cell with PA or provide a source of FFA (free fatty acids) for lipid synthesis or β-oxidation. Figure and legend reference [22].

The second biosynthetic lipid pathway requires PA's highly regulated dephosphorylation to DAG within the ER as a necessary step required for the synthesis of PC and PE by the Kennedy Pathway, and as the precursor of TAG synthesis [22, 24]. PC and PE are also derived by the Kennedy Pathway in the presence of DAG using exogenous choline and ethanolamine, respectively, should the cell have faulty enzymes or lack the necessary precursors to synthesize PC and PE by CDP-DAG [22, 23, 24]. TAG synthesis and accumulation and leads to the

budding off of LDs from the ER [24]. The few proteins in the LD's phospholipid monolayer membrane have been identified as enzymes involved in lipid metabolism [24]. The quantity of LDs is dependent on the amount of TAG and SE synthesized, as an increase in their synthesis leads to an increase in the number of LDs [24]. Once TAG is sequestered in the LD, it is readily available for degradation to DAG and FFA, providing a source of DAG which can be phosphorylated to regenerate PA or act as a precursor to PC and PE synthesis via the Kennedy pathway [24] **(Figure 1.5).** The regeneration of PA can then provide the core precursor to further the synthesis of all lipids in the CDP-DAG lipid biosynthetic branch. TAG degradation in the LD therefore allows the synthesis of most major lipid classes via PA regeneration, and provides the cell with FFAs that are important for lipid synthesis and can enter the catabolic process of β-oxidation to fuel the TCA cycle [24].

The tight control of lipid synthesis plays a critical role in the cell as one missing enzyme or precursor leads to a cascade of events in the cell if there is no alternative route of synthesis available, such as the Kennedy Pathway in the synthesis of PC and PE. The interconnected lipid synthesis pathways also provide mechanisms that influence lipid turnover, such as the tightly controlled conversion of DAG back to PA, and vice versa, that can fuel both branches (CDP-DAG and DAG) of lipid synthesis from PA depending on various factors responsible for regulating lipid synthesis [24].

Glycerophospholipid synthesis can be regulated by various factors such as enzyme expression or the regulation of an enzyme's catalytic activities [24]. The presence of both specific and non-specific phospholipases and phosphatases play a critical role in lipid regulation by contributing to the turnover of lipids by way of their degradation [24]. Gene expression of enzymes involved in lipid synthesis is highly influenced by environmental growth conditions

such as temperature, growth medium, pH and nutrients [24]. This demonstrates the crucial role a cell's environmental conditions have on its cellular lipidome. Glycerophospholipid synthesis also relies on the phosphorylation of enzymes by protein kinases A and C, casein kinase II and cyclin-dependent kinase demonstrating an overlap between various signalling pathways and lipid synthesis [24]. With yeast's lipidome so amendable to environmental changes and influenced by various factors such as dietary changes and the addition of small molecules, changes in yeast's lipidome are expected [25].

1.7 Caloric Restriction (CR) and lithocholic acid (LCA) extend longevity of chronologically aging yeast in part by altering lipid metabolism

Lipid metabolism in yeast is a very dynamic and interrelated network due to the overlap of lipid synthesis pathways and the tightly controlled turnover rates between various lipid classes. Environmental and nutrient conditions play an important role in lipid metabolism as altering these conditions has an influence on the yeast lipidome as a whole [25]. Therefore, a change in diet, the addition of a small molecule or a change in genetic background has the power to alter the yeast lipidome, demonstrating its flexibility. A calorie restricted diet and the addition of lithocholic acid (LCA), a hydrophobic small molecule bile acid, have demonstrated longevity extending effects in chronologically aging yeast by altering the metabolism and interorganellar transport of lipids [26]. The lipid dynamics of peroxisomes, lipid droplets, mitochondria and the ER have demonstrated key roles as players in longevity-extension under a calorie restricted diet and/or treatment with LCA [26, 27].

Caloric restriction (CR) involves a low-calorie dietary regimen capable of extending lifespan in organisms across phyla and delaying age-related diseases in mouse models [27]. The

optimal glucose concentration that promotes the longest lived and most fit chronologically aging yeast has shown to be 0.2% [27]. A CR diet, conditions of 0.2% glucose, is capable of regulating longevity by various ways such as extending the chronological life span of yeast, remodelling the metabolism of trehalose and glycogen, modulating the oxidation-reduction processes in mitochondria and ROS levels, altering mitochondrial morphology, delaying mitochondria-controlled apoptosis, altering the abundance of numerous proteins involved in carbohydrate and lipid metabolism while promoting the consumption of neutral lipids deposited in lipid droplets [27].

Under non-CR conditions of 2% glucose, an increased glucose concentration increases intracellular ethanol synthesis upon glucose fermentation, provoking the suppression of peroxisome oxidation of FFA due to the lipolysis of TAG in LDs [27, 28]. The suppression of FFA oxidation allows the build-up of FFA in the LD, eventually leading to several negative feedback loops that induce the accumulation of DAG and FFA in the ER, the location of TAG synthesis [28]. This lipid accumulation within the ER leads to pre-mature aging and death of the cell due to the accelerated rate of necrosis [28]. Under conditions of calorie restriction, 0.2% glucose, lower levels of glucose evade the accumulation of ethanol within the cell, therefore averting the suppression of the peroxisomal oxidation of FFAs [28]. A CR diet avoids the negative feedback loops that result from FFA accumulation in the peroxisome, evading the accumulation of FFA and DAG in the ER [28]. The lack of this lipid accumulation in the peroxisome, LD and ER under CR conditions, avoids the accelerated necrosis found under non-CR conditions, therefore extending lifespan.

The hydrophobic bile acid, lithocholic acid (LCA), was identified as a powerful longevity-extending molecule upon conduction of a screen to yield novel anti-aging compounds

[28, 29]. The method of LCA's lifespan extending influence has shown to be independent of any major pro-aging pathways such as TOR and cAMP/PKA, as a deficiency in either of these pathways will not hinder LCA's longevity extending ability [28, 29]. LCA treatment has shown to remodel the cell's lipid dynamics under a CR diet by: 1) stimulating mitochondrial transport of acetyl-CoA, therefore limiting its availability for FFA synthesis in the ER; 2) activating TAG synthesis from FFA and DAG and in the ER and; 3) slowing down the lipolytic conversion of TAG into FFA and DAG within the LD [28]. All these cellular modifications to the lipid metabolism and synthesis by LCA avert the accumulation of FFAs in the cell, avoiding the pre-mature aging by necrosis and extending lifespan [28].

LCA localizes to the inner mitochondrial membrane (IMM) leading to the remodelling of the mitochondria's phospholipid synthesis and transport upon treatment of the cell [30]. These changes in the mitochondrial membrane include an increase in PA, PC, PS, and PG with a decrease in PE and CL [30]. The yeast cell's mitochondria also undergo an increase in size and decrease in number and IMM cristae [30]. These physical changes in the mitochondria brought about by treatment with LCA lead to a more efficient mitochondrial respiration, membrane potential maintenance and ATP synthesis as chronologically old quiescent cells age, leading to an increased chronological lifespan [30].

1.8 The objectives of studies described in this thesis

The differentiation pathways of quiescent and non-quiescent cells have shown to be influenced by multiple factors such as dietary, pharmacological and genetic intervention. A caloric restricted diet and the addition of the longevity extending molecule lithocholic acid (LCA) have shown to increase the lifespan of both quiescent and non-quiescent cells. The TORC1 signalling pathway, a key pathway accelerating aging in yeast, has also demonstrated an important role in cell cycle regulation and aging. The single-gene-deletion mutation for *tor1*Δ, which eliminates the essential Tor1p of the TORC1 protein complex, has been found to extend the lifespan of chronologically aging yeast under both CR and non-CR conditions, in synergy with the addition of LCA. With our current understanding of how these factors influence the cell cycle regulation with respect to quiescent and non-quiescent cells, it is possible to further examine how these factors alter yeast's cellular lipidome to better understand the impact of the lipidome on the aging process.

The mass spectrometric analysis and quantitation of major lipid classes PA, PC, PE, PI, PS, CL and TAG in the cell will lead to a more thorough understanding of how lipid metabolism influences the aging and differentiation process of quiescent and non-quiescent cells separated by density-gradient centrifugation.

Therefore, my first objective was to elucidate how a calorie restricted diet influences the lipidomes of quiescent and non-quiescent yeast cells that age chronologically.

My second objective was to investigate the effect of the longevity extending small molecule lithocholic acid (LCA) on the lipidomes of quiescent and non-quiescent yeast cells undergoing chronological aging.

My third objective was to examine how the TORC1 pathway, a key pro-aging signalling route, impacts the lipidomes of quiescent and non-quiescent yeast cells that age chronologically.

2 Caloric restriction, a longevity-extending dietary intervention, alters lipid compositions of quiescent and non-quiescent cells of chronologically aging yeast

2.1 Abstract

A diet known as caloric restriction (CR) has been shown to extend longevity of chronologically aging yeast [27, 28]. In studies described in this Chapter of my thesis, I used centrifugation in a Percoll density gradient to separate quiescent (Q) and non-quiescent (NQ) cells of chronologically aging yeast. The Q and NQ populations of cells were purified from yeast cultured either under CR conditions in 0.2% glucose or under non-CR conditions in 2% glucose. I employed quantitative mass spectrometry to monitor how the CR diet impacts age-related changes in the lipid compositions of purified populations of Q and NQ yeast. My findings imply that CR causes a substantial remodeling of lipid metabolism and transport in both Q and NQ cells. Based on these findings, I propose a working hypothesis on how CR delays chronological aging of yeast cells by altering lipid dynamics within different cellular organelles.

2.2 Materials and Methods

Yeast strains, media and growth conditions

The wild-type strain *Saccharomyces cerevisiae* BY4742 (*MATα his3Δ1 leu2Δ0 lys2Δ0 ura3Δ0*) from Thermo Scientific/Open Biosystems was grown in YEP medium (1% yeast extract, 2% peptone; both from Fisher Scientific; #BP1422-2 and #BP1420-2, respectively) initially containing 0.2% or 2% glucose (#D16-10; Fisher Scientific) as the carbon source. Cells were cultured at 30^{o}C with rotational shaking at 200 rpm in Erlenmeyer flasks at a "flask volume/medium volume" ratio of 5:1.

Separation of Q and NQ cells by centrifugation in Percoll density gradient

1 mL of 1.5 M NaCl (#S7653; Sigma) was placed into a 50-mL Falcon tube, and 8 mL of the Percoll solution (#P1644; Sigma) was added to this tube. The NaCl and Percoll solution was then mixed by pipetting. To form two Percoll density gradients, 4 mL of the NaCl/Percoll mixture was put into each of the two polyallomer tubes for an MLS-50 rotor for an Optima MAX ultracentrifuge (all from Beckman Coulter). The tubes were centrifuged at 25,000 × g (16,000 rpm) for 15 min at 4^{o}C in an Optima MAX ultracentrifuge. A sample of yeast cells were taken from a culture at a certain time point. A fraction of the sample was diluted in order to determine the total number of cells per mL of culture using a hemacytometer (#0267110; Fisher Scientific). For each Percoll density gradient, 1×10^{9} yeast cells were placed into a 15-mL Falcon tube and pelleted by centrifugation at 5,000 rpm for 7 min at room temperature in a Centra CL2 clinical centrifuge (Thermo IEC). Pelleted cells were resuspended in 500 µL of 50 mM Tris/HCl buffer (pH 7.5), overlaid onto the preformed gradient with a syringe and needle to avoid disrupting the gradient, and centrifuged at 2,300 × g (5,000 rpm) for 30 min at 25^{o}C in an Optima MAX ultracentrifuge. The upper and lower fractions of cells were removed with a micropipette, discarding the gradient with no visible band of cells and Percoll was removed by washing cells twice with 50 mM Tris/HCl buffer (pH 7.5) and cells were resuspended in 1 mL of 50 mM Tris/HCl buffer (pH 7.5) for cell counts and preparation for freezing of the cell pellet.

Cell number measurement of Q and NQ cells separated by centrifugation in Percoll density gradient and preparation of pellet for storage until lipid extraction

A 50 µL aliquot of the upper or lower fraction of cells recovered and washed from the Percoll gradient were diluted in order to determine the total number of cells per fraction using a

hemacytometer (#0267110; Fisher Scientific). 10 µL of serial dilutions (1:10 to $1:10^3$) of cells were applied to the hemacytometer, where each large square is calibrated to hold 0.1 µL. The number of cells in 4 large squares was then counted and an average was taken in order to ensure greater accuracy. The concentration of cells was calculated as follows: number of cells per large square × dilution factor × 10 × 1,000 = total number of cells per mL of fraction. The remaining 950 µL of the cell aliquots were washed twice with 155 mM ammonium bicarbonate (pH 8.0) in preparation for the freezing of the cell pellet at -80°C until the lipid extraction.

Lipid extraction from purified populations of Q and NQ cells

The lipid extraction of purified populations of quiescent and non-quiescent cells used Richard et al.'s modified version of Bligh and Dyer's lipid purification and extraction protocol [31]. The pelleted cell fractions kept at -80°C were thawed on ice before being resuspended in 1mL of cold nanopure water. The volume that contained 5×10^7 cells of each fraction was transferred to the appropriate 15-mL high-strength glass screw top centrifuge tube with a Teflon lined cap (#0556912; Fisher Scientific). The volume of each sample was topped off to 1 mL with cold nanopure water. To each tube the following was added: 20 µL of the internal standard mix prepared in Chromasolv HPLC (>99.9%) chloroform (Sigma-Aldrich) (**Table 2.1**), 800 uL of 425-600 µM acid-washed glass beads to break open the cells (#G8772; Sigma-Aldrich) and 3 mL of a Chromasolv HPLC (>99.9%) chloroform: methanol mixture (both from Sigma-Aldrich) at a 17:1 ratio. The samples were then vortexed vigorously for 2 hours at 4°C. At room temperature, the samples were then centrifuged in a Centra CL2 clinical centrifuge for 5 minutes separating the upper aqueous and lower organic phase which contained nonpolar lipids TAG, PC, PE and PG. The lower organic layer was transferred to another labelled 15 mL glass high-

strength centrifuge tube using a glass Pasteur pipette with careful attention not to disrupt the glass beads or upper aqueous phase. 1.5 mL of 2:1 chloroform: methanol solution was added to the remaining upper aqueous phase allowing the separation of polar lipids PA, PS, PI and CL. The samples were again vortexed vigorously at 4^{O}C for 1 hour. The non-polar organic band was kept at 4^{O}C for the duration of the second vortexing. At the end of 1 hour, the samples were again centrifuged for 5 minutes at 3,000 rpm and the lower organic phase was separated and added to the corresponding non-polar organic phase with a glass Pasteur pipette. With both lower organic phases combined, the solvent was evaporated off by nitrogen gas flow. Once all solvent was evaporated, the remaining lipid film was dissolved and resuspended in 100 µL of 1:2 chloroform: methanol and immediately transferred into 2 mL glass vials with Teflon screw tops to avoid evaporation until samples were analysed by mass spectrometry. Samples were then stored at -20^{O}C and ran on the LTQ Orbitrap Mass Spectrometer within one week of the extraction.

Table 2.1: Internal standard mix composition (modified from reference [31])

Detection Mode	Class of Lipid Standard	Lipid Chain Composition (number carbons: number double bonds on fatty acid chain)	Exact Mass Molecular Weight (g/mol)	M/Z (mass/ion charge)	Concentration in mix (mg/µL)
Negative	CL	14:0 / 14:0 / 14:0 /14:0	1274.9000	619.4157	0.10
	FFA	19:0	298.2872	297.2711	0.02
	PA	14:0 / 14:0	614.3920	591.4026	0.10
	PE	14:0 / 14:0	635.4526	634.4448	0.10
	PG	14:0 / 14:0	688.4290	665.4394	0.10
	PS	14:0 / 14:0	701.4240	678.4271	0.02
Positive	TAG	13:0 / 13:0 / 13:0	680.5955	698.6299	0.10
	PC	13:0 / 13:0	649.4683	650.4761	0.10

Internal Standards CL, PA, PE, PG, PS and PC are all from Avanti Polar Lipid, Alabaster, AL, USA. TAG Internal standard originates from Larodan, Malmo, Sweden.

Lipid identification and quantitation of Q and NQ cells using mass spectrometry

Samples were diluted 1:1 with 1:2 chloroform: methanol and 0.1% ammonium hydroxide for improved ionization efficiency. Samples were injected one at a time using a Thermo Orbitrap Velos Mass Spectrometer equipped with HESI-II ion source (Thermo Scientific) at a flow rate of 5 µL/ minute. The instrument settings for the Orbitrap used the optimized settings listed in Richard's et al.'s tune file (**Table 2.2**).

Table 2.2: Thermo Orbitrap Velos mass spectrometer's tune file instrument settings (from reference [31])

Instrument polarity	Positive	Negative
Source voltage (kV)	3.9	4
Capillary temperature (°C)	275	275
Sheath gas flow	5	5
Aux gas flow	1	1
FT-MS injection time (ms)	100	500
FTMS microscans	3	1

Data was acquired according to the Instrument Method for data-dependent acquisition for 5 minutes in both positive and negative mode by the FTMS analyser at a resolution of 100,000 for both MS and MS/MS data (**Table 2.3**).

Table 2.3: Instrument method for data-dependent acquisition (from reference [31])

Acquisition time	**5 minutes (with a 0.25 minute delay)**	
Instrument polarity	**Positive**	**Negative**
MS (Segment 1)		
Analyzer	FTMS	FTMS
Mass Range	Normal	Normal
Resolution	100,000	100,000
Data Type	Centroid	Centroid
Scan Range	400-1,200	400-1,200
Data dependent MSMS (segments 2-10)		
Analyzer	FTMS	FTMS
Resolution	30,000	30,000
Data Type	Centroid	Centroid
Activation	HCD	HCD
Activation time (ms)	0.1	0.1
Isolation width	1	1
Collision energy	35	65
Mass range	Normal	Normal
Data type	Centroid	Centroid
Scan Range	-	-

Between each sample, the line was flushed with 1:2 chloroform: methanol until the background ion detection steadied and returned back into the baseline level. Diluted internal standard mix was injected multiple times throughout the acquisition to ensure no sensitivity loss throughout the run.

Once all data was acquired, raw files were converted to open mzXML format using ProteoWizard MSConvert software (http://proteowizard.sourceforge.net/), the file format used by the Lipid Identification Software LipidXplorer (https://wiki.mpi-cbg.de/lipidx/Main_Page). Data files were then imported into the software, using the following settings (**Table 2.4**), and all lipids in the following lipids classes: PA, PC, PE, PI, PS, CL and TAG, were identified with the help of Molecular Fragmentation Query Language (MFQL) files. MFQL files were obtained

from the LipidXplorer page listed above and aided in the identification of lipids by their m/z ratio as well as their fragmentation patterns.

LipidXplorer's output data was then opened under a Microsoft Excel file and all detected lipids were quantified by comparison with the intensity of the corresponding lipid class' internal standard's known concentration in the sample. Each quantified lipid had a corresponding internal standard from the same lipid class, allowing the calculation of molar percentage of each identified lipid species and therefore lipid class.

Table 2.4 Lipid identification by LipidXplorer import settings for data acquired under positive and negative mode. (From reference [31])

	Positive Mode	**Negative Mode**
Selection Window (Da)	1	1
Time Range (sec.)	0-350	0-350
Calibration masses		
MS	0	0
MS/MS	0	0
m/z range (m/z-m/z)		
MS	140-1,200	100-400
MS/MS	200-1,400	200-1200
Resolution (FMHW)		
MS	100,000	100,000
MS/MS	30,000	30,000
Tolerance (ppm)		
MS	10	10
MS/MS	10	10
Resolution Gradient (res/(m/z))		
MS	0	-55
MS/MS	0	0
Minimum Occupation (0<1)		
MS	0.5	0.5
MS/MS	0	0
MS1 offset (Da)	0	0

Statistical analysis

Statistical analysis was performed using Microsoft Excel's (2010) Analysis ToolPack-VBA. All data are presented as mean ± SEM. The *p* values were calculated with the help of GraphPad *t* test calculator using an unpaired two-tailed *t* test.

2.3 Results

2.3.1 CR alters the intracellular concentrations of cardiolipin, a phospholipid specific for mitochondria, in Q and NQ cell populations of chronologically aging yeast

Cardiolipin (CL) is known to be synthesized only by enzymes confined to the inner mitochondrial membrane of the yeast *S. cerevisiae* [32, 33]. Therefore, in yeast cells this phospholipid resides only in mitochondria and is a signature phospholipid of these organelles [22]. Using mass spectrometry, I identified and quantitated lipids (including CL) that were extracted from purified Q and NQ cell populations of chronologically aging yeast cultured either under CR conditions in 0.2% glucose or under non-CR conditions in 2% glucose. I found that the CR diet causes the following changes in the cellular concentrations of CL in chronologically aging yeast: 1) in chronologically "young" Q cells that have not entered stationary growth phase on day 6 of culturing, CR significantly reduces the cellular concentration of CL (**Figure 2.1**); 2) in chronologically "old" Q cells that have entered stationary growth phase, CR enables them to maintain the cellular concentration of CL at a substantially higher level than that is seen in yeast cultured under non-CR conditions (**Figure 2.1**); and 3) in chronologically "young" and "old" NQ cells, CR significantly increases the cellular concentration of CL (**Figure 2.2**).

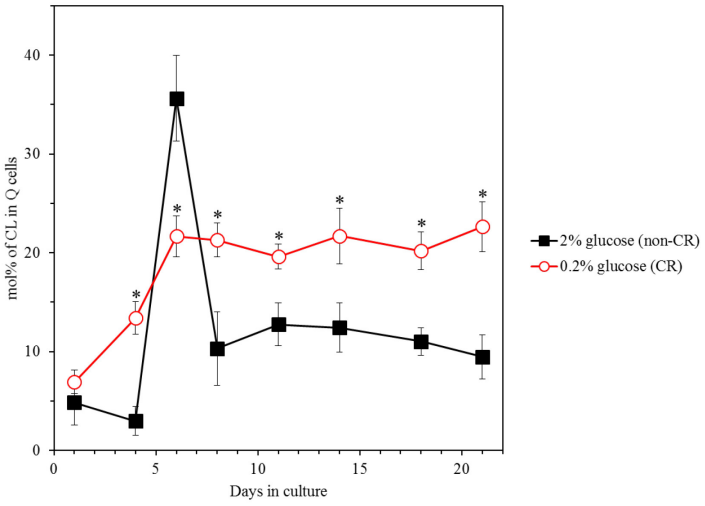

Figure 2.1. CR alters the age-related dynamics of changes in CL concentrations within Q cells. Cells were cultured in the nutrient-rich YP medium initially containing 0.2% or 2% glucose. Q cells were purified from cell cultures recovered on days 1, 4, 6, 8, 11, 14, 18 or 21 of cell culturing. Extraction of cellular lipids, as well as their mass spectrometric identification and quantitation, were carried out as described in Materials and Methods. Based on these data, the concentrations of CL were calculated in mol%. Data are presented as means ± SEM (n = 2; * $p < 0.05$).

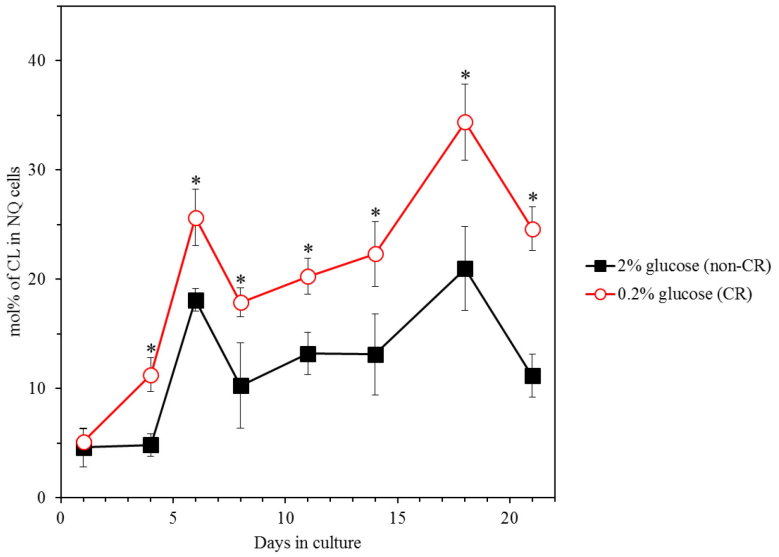

Figure 2.2. CR alters the age-related dynamics of changes in CL concentrations within NQ cells. Cells were cultured in the nutrient-rich YP medium initially containing 0.2% or 2% glucose. NQ cells were purified from cell cultures recovered on days 1, 4, 6, 8, 11, 14, 18 or 21 of cell culturing. Extraction of cellular lipids, as well as their mass spectrometric identification and quantitation, were carried out as described in Materials and Methods. Based on these data, the concentrations of CL were calculated in mol%. Data are presented as means ± SEM (n = 2; * $p < 0.05$).

My findings suggest that the ability of CR to increase cellular concentration of CL, the signature lipid of mitochondria, may be responsible in part for the CR-driven longevity extension of both Q and NQ cells.

2.3.2 CR reduces the intracellular concentrations of triacylglycerol, a neutral lipid specific for lipid droplets, in Q and NQ cell populations of chronologically aging yeast

Triacylglycerol (TAG) synthesis takes place in the ER, where it is then packaged into highly dynamic neutral lipid storage vesicles known as lipid droplets (LD) [22-24, 34]. LDs grow, fragment and shrink (due to lipolysis) and maintain high interactions with protein network machines, making them highly integrated into vital processes and defining longevity [34]. TAG's primary location in LDs make it an important lipid to quantify when determining the effect of CR and non-CR conditions on LDs in both Q and NQ cells.

Using quantitative mass spectrometry, it was possible to measure TAG concentrations in Q and NQ cells of chronologically aging yeast grown under CR or non-CR conditions, to better understand the role of TAG, and therefore of LDs, with respect to cellular aging. I found that the CR diet significantly decreases TAG concentrations throughout lifespan, both before and after cell entry into stationary phase, in both Q and NQ cells (**Figures 2.3 and 2.4,** respectively).

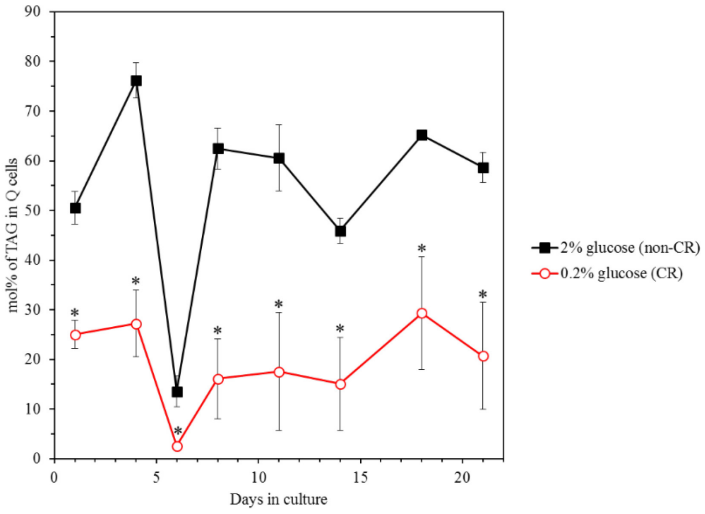

Figure 2.3. CR reduces the concentrations of TAG within Q cells. Cells were cultured in the nutrient-rich YP medium initially containing 0.2% or 2% glucose. Q cells were purified from cell cultures recovered on days 1, 4, 6, 8, 11, 14, 18 or 21 of cell culturing. Extraction of cellular lipids, as well as their mass spectrometric identification and quantitation, were carried out as described in Materials and Methods. Based on these data, the concentrations of TAG were calculated in mol%. Data are presented as means ± SEM (n = 2; * $p < 0.05$).

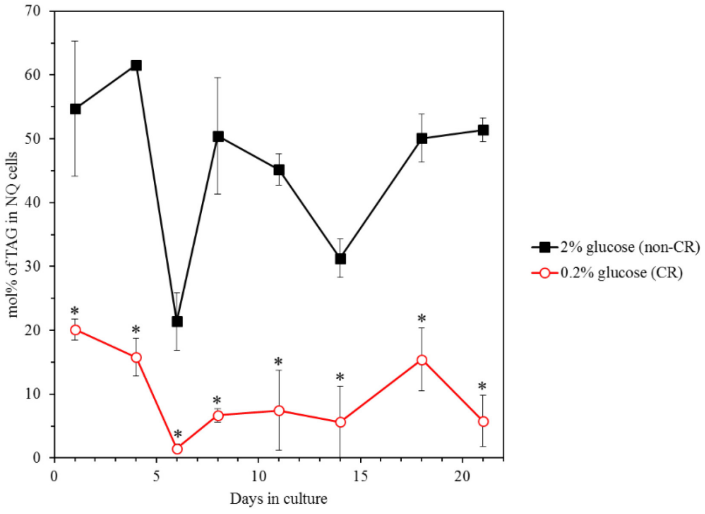

Figure 2.4. CR decreases the concentration of TAG within NQ cells. Cells were cultured in the nutrient-rich YP medium initially containing 0.2% or 2% glucose. NQ cells were purified from cell cultures recovered on days 1, 4, 6, 8, 11, 14, 18 or 21 of cell culturing. Extraction of cellular lipids, as well as their mass spectrometric identification and quantitation, were carried out as described in Materials and Methods. Based on these data, the concentrations of TAG were calculated in mol%. Data are presented as means ± SEM (n = 2; * $p < 0.05$).

It should be stressed that the entry of Q and NQ cells into stationary growth phase on day 6 of culturing under CR or non-CR conditions coincides with a dramatic drop in the concentration of TAG within these cells (**Figures 2.3 and 2.4**). My observations suggest that the ability of CR to reduce cellular concentration of TAG, a neutral lipid deposited in LDs, may be responsible in part for the CR-dependent longevity extension of both Q and NQ cells.

2.3.3 CR alters the intracellular concentrations of phosphatidic acid (PA) in Q and NQ cell populations of chronologically aging yeast

PA is a glycerophospholipid known to be synthesized in the ER [22-24]. After being formed in the ER, PA can be used as a precursor for the synthesis of the following lipid classes in yeast cells: 1) phosphatidylserine (PS) and phosphatidylinositol (PI) in the ER; 2) TAG in the ER; and 3) PG in mitochondria; to be converted to CL in mitochondria [22-24]. PA is transported to these organelles from the ER via mitochondria-ER junctions [22-24]. Using quantitative mass spectrometry, I found that the CR diet has the following effects on the cellular concentrations of PA in chronologically aging yeast: 1) in chronologically "young" Q and NQ cells that have not entered stationary growth phase on day 6 of culturing, CR does not alter PA concentrations (**Figure 2.5**); and 2) in chronologically "old" Q and NQ cells that have entered stationary growth phase, CR allows these cells to maintain the cellular concentration of PA at a significantly higher level than that observed in yeast grown under non-CR conditions (**Figure 2.6**). These findings suggest that the CR diet may delay yeast aging by maintaining a higher concentration of PA within chronologically "old" Q and/or NQ cells.

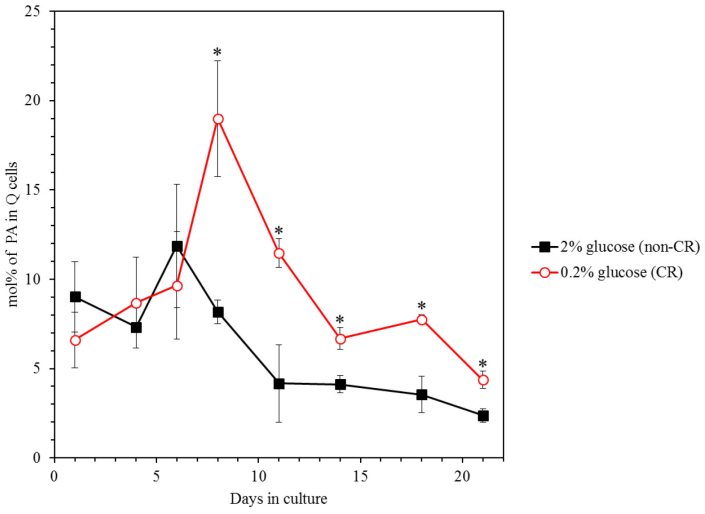

Figure 2.5. CR increases the concentrations of PA within chronologically "old" Q cells. Cells were cultured in the nutrient-rich YP medium initially containing 0.2% or 2% glucose. Q cells were purified from cell cultures recovered on days 1, 4, 6, 8, 11, 14, 18 or 21 of cell culturing. Extraction of cellular lipids, as well as their mass spectrometric identification and quantitation, were carried out as described in Materials and Methods. Based on these data, the concentrations of PA were calculated in mol%. Data are presented as means ± SEM (n = 2; * $p < 0.05$).

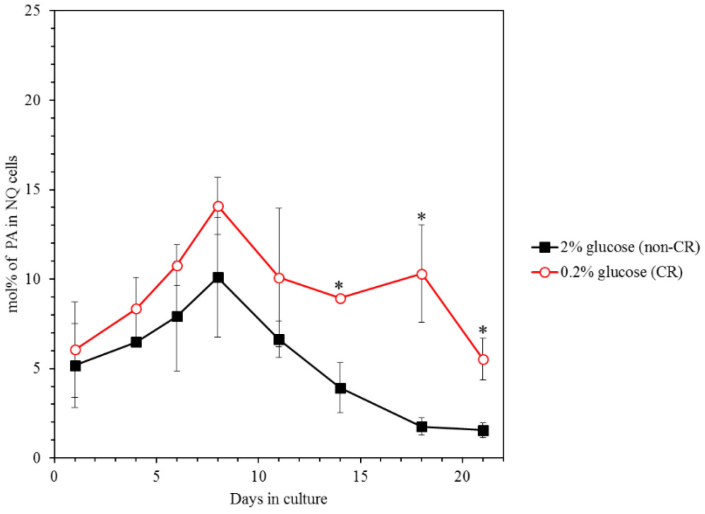

Figure 2.6. CR increases the concentrations of PA within chronologically "old" NQ cells. Cells were cultured in the nutrient-rich YP medium initially containing 0.2% or 2% glucose. NQ cells were purified from cell cultures recovered on days 1, 4, 6, 8, 11, 14, 18 or 21 of cell culturing. Extraction of cellular lipids, as well as their mass spectrometric identification and quantitation, were carried out as described in Materials and Methods. Based on these data, the concentrations of PA were calculated in mol%. Data are presented as means ± SEM (n = 2; * $p < 0.05$).

2.3.4 CR alters the intracellular concentrations of PS only in Q cell population and does not change PI concentrations in Q and NQ cell populations

Two glycerophospholipids, PS and PI, are known to be formed directly from PA in the ER of yeast cells [22-24]. With the help of quantitative mass spectrometry, I assessed the concentrations of these two PA-derived glycerophospholipids in Q and NQ cells purified from yeast cultures progressing through the chronological aging process. I discovered that the CR diet has the following effects on the cellular concentrations of PS and PI in chronologically aging yeast: 1) throughout the chronological lifespan of Q cells, the CR diet enables the cellular concentration of PS to be maintained at a substantially higher level than that observed in yeast grown under non-CR conditions (**Figure 2.7**); 2) CR does not alter PS concentrations in NQ cells recovered at various stages of chronological aging (**Figure 2.8**); and 3) CR does not change PI concentrations in Q and NQ cell populations of any chronological age (**Figures 2.9 and 2.10**, respectively). My findings suggest that the CR diet may delay aging of Q cells because a relatively high concentration of PS is maintained within chronologically "young" and "old" Q cells. However, the ability of CR to delay aging of NQ cells is unlikely due to changes in the concentration of PS within these cells. Moreover, it seems unlikely that the CR diet delays the aging of Q and NQ cells by a mechanism dependent upon altering the concentration of PI within these cells.

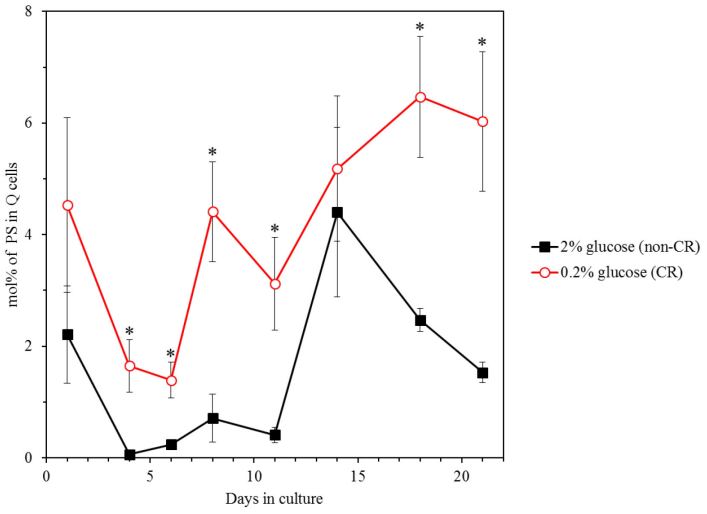

Figure 2.7. CR increases the concentrations of PS throughout the chronological lifespan of Q cells. Cells were cultured in the nutrient-rich YP medium initially containing 0.2% or 2% glucose. Q cells were purified from cell cultures recovered on days 1, 4, 6, 8, 11, 14, 18 or 21 of cell culturing. Extraction of cellular lipids, as well as their mass spectrometric identification and quantitation, were carried out as described in Materials and Methods. Based on these data, the concentrations of PS were calculated in mol%. Data are presented as means ± SEM (n = 2; * $p < 0.05$).

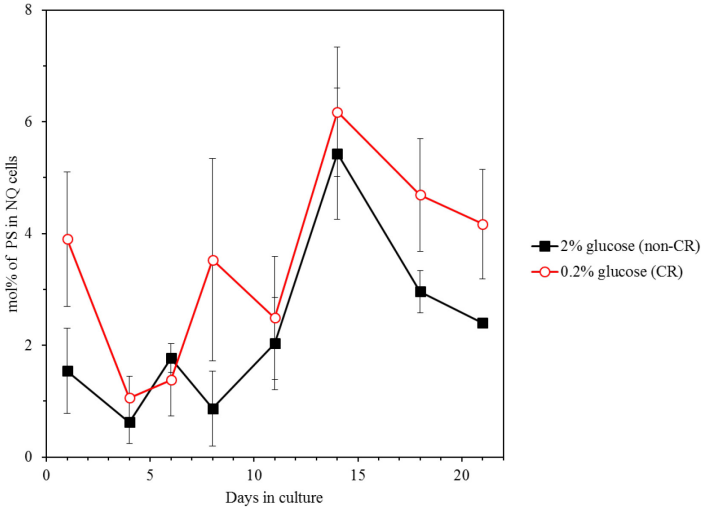

Figure 2.8. CR does not alter PS concentrations in NQ cells recovered at various stages of chronological aging. Cells were cultured in the nutrient-rich YP medium initially containing 0.2% or 2% glucose. Q cells were purified from cell cultures recovered on days 1, 4, 6, 8, 11, 14, 18 or 21 of cell culturing. Extraction of cellular lipids, as well as their mass spectrometric identification and quantitation, were carried out as described in Materials and Methods. Based on these data, the concentrations of PS were calculated in mol%. Data are presented as means ± SEM (n = 2).

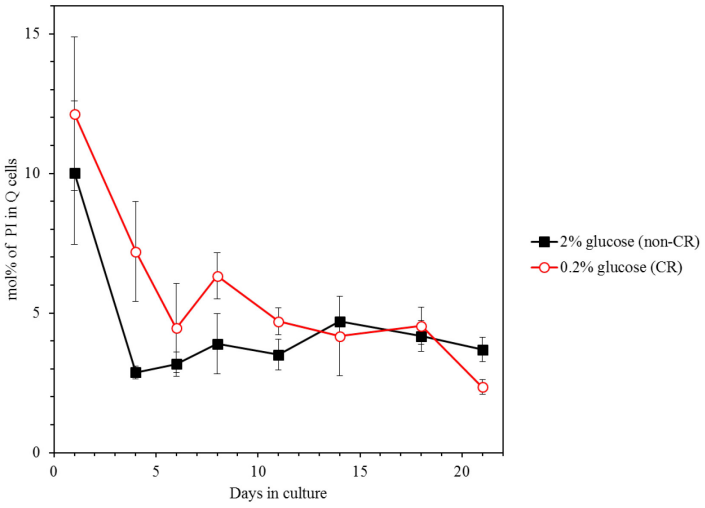

Figure 2.9. CR does not change PI concentrations in Q cells of any chronological age. Cells were cultured in the nutrient-rich YP medium initially containing 0.2% or 2% glucose. Q cells were purified from cell cultures recovered on days 1, 4, 6, 8, 11, 14, 18 or 21 of cell culturing. Extraction of cellular lipids, as well as their mass spectrometric identification and quantitation, were carried out as described in Materials and Methods. Based on these data, the concentrations of PI were calculated in mol%. Data are presented as means ± SEM (n = 2).

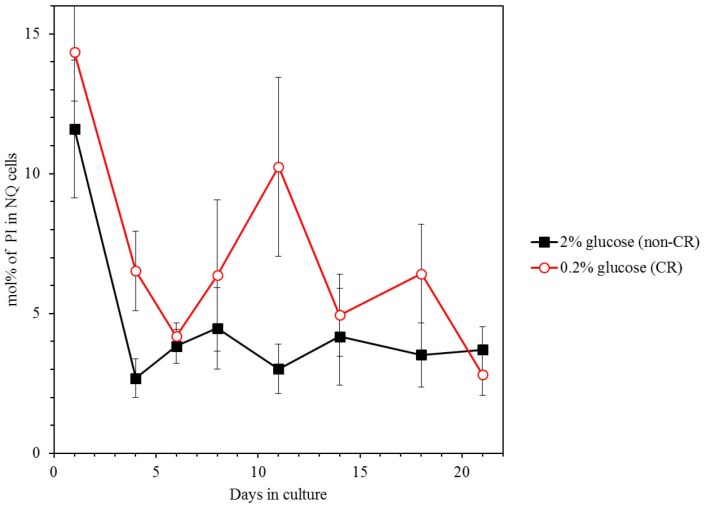

Figure 2.10. CR does not change PI concentrations in NQ cells of any chronological age. Cells were cultured in the nutrient-rich YP medium initially containing 0.2% or 2% glucose. NQ cells were purified from cell cultures recovered on days 1, 4, 6, 8, 11, 14, 18 or 21 of cell culturing. Extraction of cellular lipids, as well as their mass spectrometric identification and quantitation, were carried out as described in Materials and Methods. Based on these data, the concentrations of PI were calculated in mol%. Data are presented as means ± SEM (n = 2).

2.3.5 CR changes the concentrations of phosphatidylethanolamine (PE) within Q and NQ cells and differentially affects the concentrations of phosphatidylcholine (PC) in these cell populations

The glycerophospholipid PE is known to be synthesized from PS in the inner mitochondrial membrane [22-24]. After being transported to the ER via mitochondria-ER junctions, PE serves as a substrate for the synthesis of PC [22-24]. Using quantitative mass spectrometry, I monitored the concentrations of PE and PC in Q and NQ cells purified from yeast cultures progressing through the chronological aging process. I found that the CR diet has the following effects on the cellular concentrations of these two lipid classes in chronologically aging yeast: 1) throughout the chronological lifespan of Q and NQ cells, the cellular concentrations of PE are maintained significantly higher in CR cells than that observed non-CR cells (**Figures 2.11 and 2.12**, respectively); 2) CR increases the concentration of PC in Q cells recovered at various stages of chronological aging (**Figure 2.13**); 3) in chronologically "young" NQ cells that have not entered stationary growth phase on day 6 of culturing, CR increases the concentration of PC (**Figure 2.14**); and 4) in chronologically "old" NQ cells that have entered stationary growth phase, CR does not alter PC concentrations (**Figure 2.14**). My findings suggest that the CR diet may delay aging of Q cells by enabling the maintenance of high concentrations of PE and PC at all stages of chronological aging. Moreover, my observations suggest that the CR diet may delay aging of NQ cells by maintaining high concentration of PE within chronologically "young" and "old" NQ cells and/or by increasing PC concentrations within chronologically "young", but not "old", NQ cells.

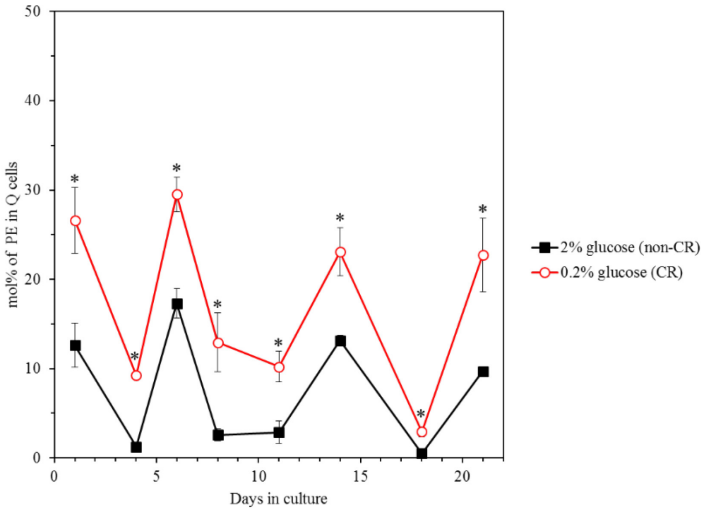

Figure 2.11. CR increases the concentrations of PE throughout the chronological lifespan of Q cells. Cells were cultured in the nutrient-rich YP medium initially containing 0.2% or 2% glucose. Q cells were purified from cell cultures recovered on days 1, 4, 6, 8, 11, 14, 18 or 21 of cell culturing. Extraction of cellular lipids, as well as their mass spectrometric identification and quantitation, were carried out as described in Materials and Methods. Based on these data, the concentrations of PE were calculated in mol%. Data are presented as means ± SEM (n = 2; * $p < 0.05$).

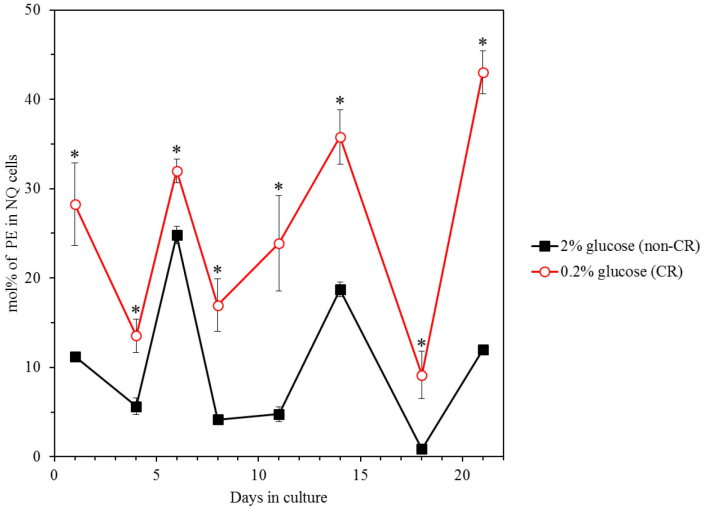

Figure 2.12. CR increases the concentrations of PE in NQ cells recovered at various stages of chronological aging. Cells were cultured in the nutrient-rich YP medium initially containing 0.2% or 2% glucose. NQ cells were purified from cell cultures recovered on days 1, 4, 6, 8, 11, 14, 18 or 21 of cell culturing. Extraction of cellular lipids, as well as their mass spectrometric identification and quantitation, were carried out as described in Materials and Methods. Based on these data, the concentrations of PE were calculated in mol%. Data are presented as means ± SEM (n = 2; * $p < 0.05$).

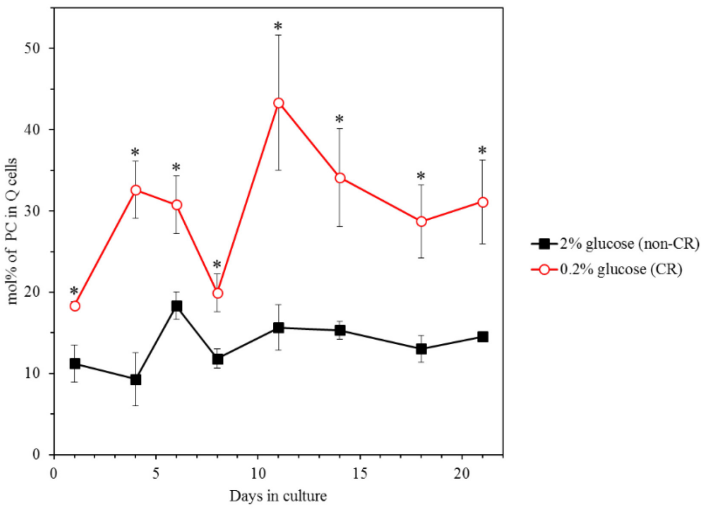

Figure 2.13. CR increases the concentrations of PC throughout the chronological lifespan of Q cells. Cells were cultured in the nutrient-rich YP medium initially containing 0.2% or 2% glucose. Q cells were purified from cell cultures recovered on days 1, 4, 6, 8, 11, 14, 18 or 21 of cell culturing. Extraction of cellular lipids, as well as their mass spectrometric identification and quantitation, were carried out as described in Materials and Methods. Based on these data, the concentrations of PC were calculated in mol%. Data are presented as means ± SEM (n = 2; * $p < 0.05$).

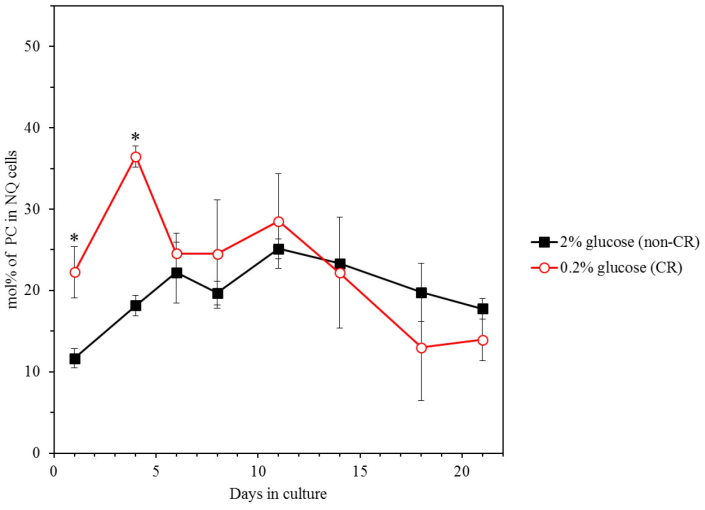

Figure 2.14. In chronologically "young" NQ cells that have not entered stationary growth phase, CR increases the concentration of PC, whereas in chronologically "old" NQ cells that have entered stationary growth phase, this dietary regimen does not alter PC concentrations. Cells were cultured in the nutrient-rich YP medium initially containing 0.2% or 2% glucose. NQ cells were purified from cell cultures recovered on days 1, 4, 6, 8, 11, 14, 18 or 21 of cell culturing. Extraction of cellular lipids, as well as their mass spectrometric identification and quantitation, were carried out as described in Materials and Methods. Based on these data, the concentrations of PC were calculated in mol%. Data are presented as means ± SEM (n = 2; * $p < 0.05$).

2.4 Discussion

Studies described in this chapter of my thesis have demonstrated that the CR diet alters the concentrations of various classes of lipids within Q and NQ cells of chronologically aging yeast. These studies strongly support the notion that this longevity-extending dietary intervention causes a substantial remodeling of lipid metabolism and transport within both Q and NQ cells. Based on observations presented in this chapter, I propose a hypothetical model on how CR may delay yeast chronological aging by altering the age-related dynamics of various lipids in Q and NQ cells. Using the centrifugation-based approach for separating Q and NQ cell populations, I found that yeast cells cultured under CR in 0.2% glucose enter differentiation program leading to formation of ″heavy″ (high-density) Q and ″light″ (low-density) NQ cell subpopulations during the logarithmic (L) growth phase (**Figure 2.15**) - i.e. much earlier than yeast cells cultured under non-CR conditions in 2% glucose and known to differentiate only when they reach stationary (ST) growth phase (**Figure 2.15**) [4, 5, 15-18]. As other graduate students in the Titorenko laboratory have demonstrated, there are two differentiation programs that in chronologically aging yeast link cellular aging to cell cycle regulation, preservation of a Q state, and entry into and advancement through an NQ state (Feldman et al., manuscript in preparation). The differentiation program 1 and the maintenance program 1 function in yeast cultured under CR conditions, whereas the differentiation program 2 and the maintenance program 2 operate in yeast grown under non-CR conditions (**Figure 2.16**). The two differentiation programs and the two maintenance program define longevity of chronologically aging yeast by setting up the following: 1) a growth phase in which G_1 cell cycle arrest occurs, 2) the efficacy with which a stem cell

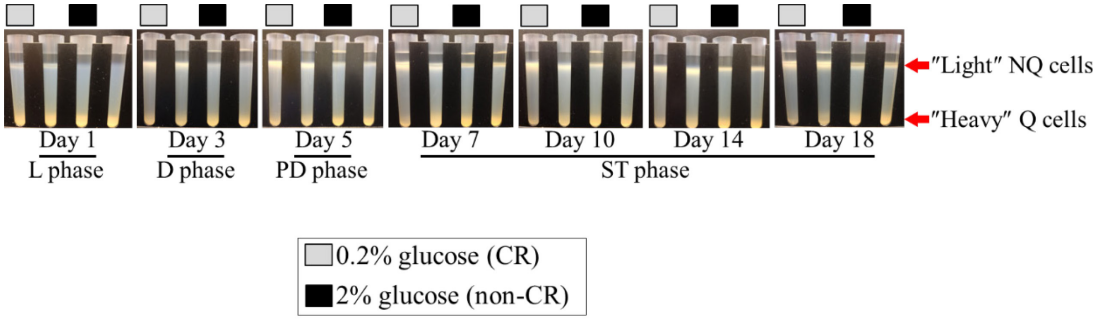

Figure 2.15. Yeast cells grown under CR in 0.2% glucose enter differentiation program leading to formation of ″heavy″ (high-density) Q and ″light″ (low-density) NQ cell subpopulations when a yeast culture reaches L growth phase. Yeast cells were cultured in the complete (nutrient-rich) YEP medium initially containing 0.2% glucose (CR conditions) or 2% glucose (non-CR conditions), recovered from logarithmic (L), diauxic (D), post-diauxic (PD) or stationary (ST) growth phase and subjected to centrifugation in Percoll density gradient as described in ″Materials and Methods″.

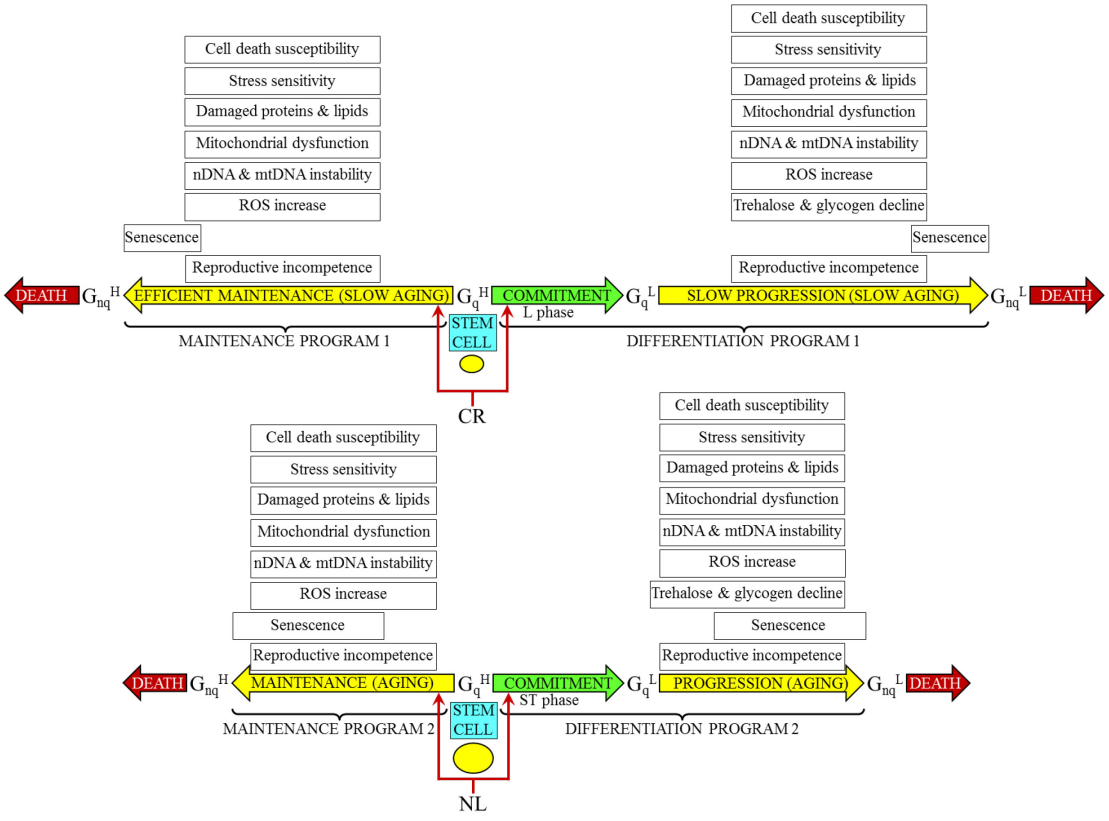

Figure 2.16. A model of two differentiation programs and two maintenance programs that in chronologically aging yeast link cellular aging to cell cycle regulation, preservation of a Q state, and entry into and advancement through an NQ state. See text for more details. Abbreviations: CR, caloric restriction; L, logarithmic; nDNA, nuclear DNA; NL, nutrient limitation; mDNA, mitochondrial DNA; ST, stationary.

niche of heavy Q cells (G_q^H) is maintained and depleted by converting to heavy NQ cells (G_{nq}^H) in an age-related manner, 3) the age-related rate with which heavy Q cells progress through apoptotic and necrosis-like subroutines of programmed death, 4) the age-related rate with which heavy Q cells are converted to light Q cells (G_q^L), 5) the age-related rate with which light Q cells differentiate into light NQ cells (G_{nq}^L), and 6) the age-related rate with which light NQ cells advance through apoptotic and necrosis-like forms of programmed death (**Figure 2.16**) (Feldman et al., manuscript in preparation).

My hypothetical model on how CR may delay yeast chronological aging by altering the age-related dynamics of various lipids in different organelles of Q and NQ cells posits the following: 1) in "young" Q cells, CR reduces the concentration of TAG and CL, possibly by decelerating their synthesis in the ER and mitochondria, respectively (**Figure 2.17**); 2) in "young" Q cells, CR increases the concentrations of PS, PE, and PC, perhaps by stimulating their synthesis and interorganellar transport in the ER and mitochondria (**Figure 2.17**); 3) in "old" Q cells, CR reduces the concentration of TAG, probably by decelerating the synthesis of this neutral lipid in the ER (**Figure 2.18**); 4) in "old" Q cells, CR increases the concentrations of PA, PS, PE, PC and CL, perhaps by stimulating their synthesis and interorganellar transport within the ER and mitochondria (**Figure 2.18**); 5) in "young" NQ cells, CR reduces the concentration of TAG, possibly by decelerating its synthesis in the ER (**Figure 2.19**); 6) in "young" NQ cells, CR increases the concentrations of PE, PC and CL, likely by stimulating their synthesis and interorganellar transport within the ER and mitochondria (**Figure 2.19**); 7) in "old" NQ cells, CR reduces the concentration of TAG, probably by decelerating the synthesis of this neutral lipid in the ER (**Figure 2.20**); and 8) in "old" NQ cells, CR increases the concentrations of PA, PE and

CL, perhaps by stimulating their synthesis and interorganellar transport within the ER and mitochondria (**Figure 2.20**).

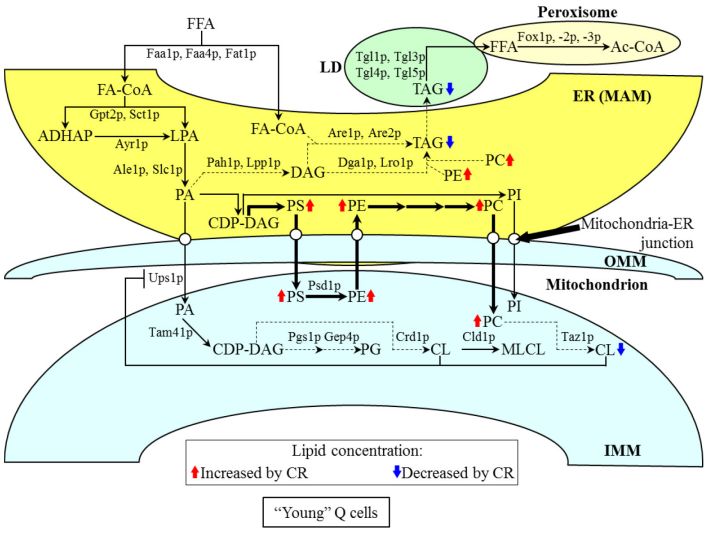

Figure 2.17. A hypothetical model on how CR alters the metabolism and interorganellar transport of some lipids in "young" Q cells. The model is based on mass spectrometric lipidomics of purified Q cells that were recovered from yeast cultures prior to entry into stationary growth phase. From the data of lipidomic analysis, I inferred an outline of the rates and efficiencies of lipid synthesis and transport that were increased (thick solid arrows) or decreased (thin dashed arrows) under CR conditions. Arrows next to the names of lipid classes denote those of them whose concentrations are elevated (red arrows) or reduced (blue arrows) by CR.

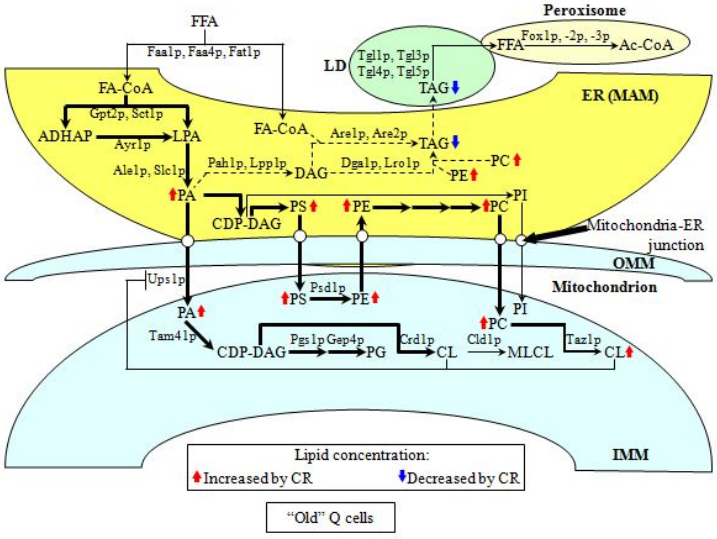

Figure 2.18. A hypothetical model on how CR alters the metabolism and interorganellar transport of some lipids in "old" Q cells. The model is based on mass spectrometric lipidomics of purified Q cells that were recovered from yeast cultures after entry into stationary growth phase. From the data of lipidomic analysis, I inferred an outline of the rates and efficiencies of lipid

synthesis and transport that were increased (thick solid arrows) or decreased (thin dashed arrows) under CR conditions. Arrows next to the names of lipid classes denote those of them whose concentrations are elevated (red arrows) or reduced (blue arrows) by CR.

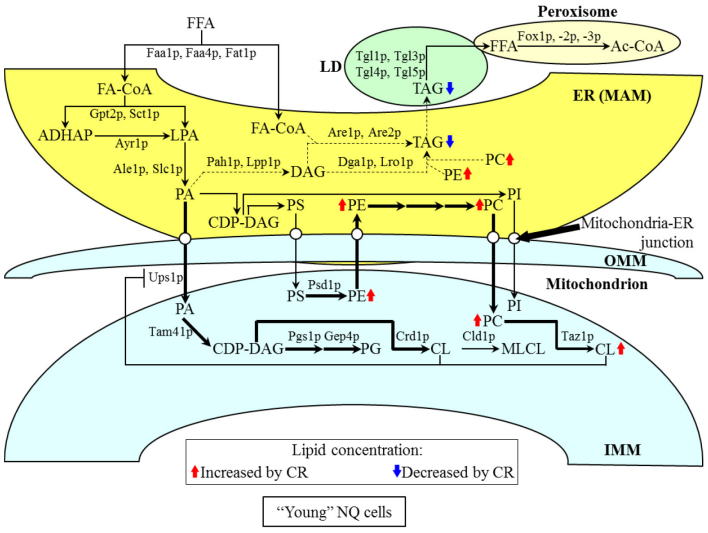

Figure 2.19. A hypothetical model on how CR alters the metabolism and interorganellar transport of some lipids in "young" NQ cells. The model is based on mass spectrometric lipidomics of purified NQ cells that were recovered from yeast cultures prior to entry into stationary growth phase. From the data of lipidomic analysis, I inferred an outline of the rates and efficiencies of lipid synthesis and transport that were increased (thick solid arrows) or decreased (thin dashed arrows) under CR conditions. Arrows next to the names of lipid classes denote those of them whose concentrations are elevated (red arrows) or reduced (blue arrows) by CR.

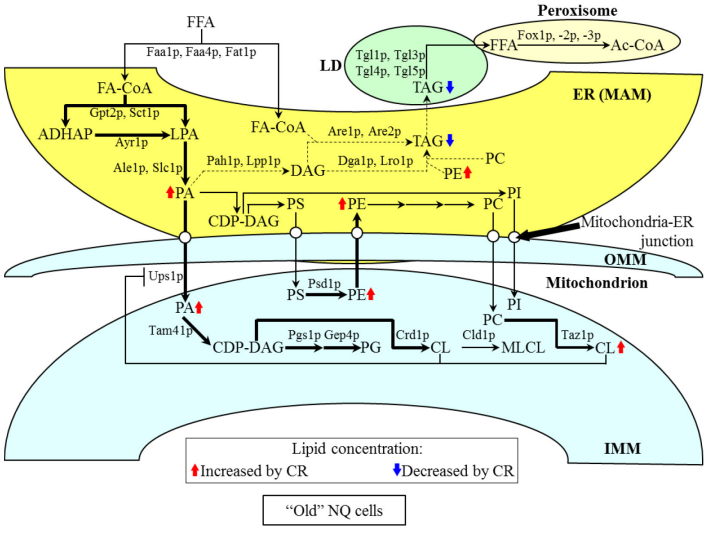

Figure 2.20. A hypothetical model on how CR alters the metabolism and interorganellar transport of some lipids in "old" NQ cells. The model is based on mass spectrometric lipidomics of purified NQ cells that were recovered from yeast cultures after entry into stationary growth phase. From the data of lipidomic analysis, I inferred an outline of the rates and efficiencies of lipid synthesis and transport that were increased (thick solid arrows) or decreased (thin dashed

arrows) under CR conditions. Arrows next to the names of lipid classes denote those of them whose concentrations are elevated (red arrows) or reduced (blue arrows) by CR.

It remains to be determined which of the alterations in lipid concentrations observed in Q and NQ cells are essential for the ability of CR to delay aging of these cell populations; it is possible that some of these alterations just coincide with the progress of chronological aging. To address this key aspect of the proposed model, it will be important in the future to assess how single-gene mutations eliminating enzymes that accelerate individual reactions of lipid metabolism in yeast (**Figures 2.17 – 2.20**) influence the efficiency with which CR slows down yeast chronological aging. Moreover, a challenge remains to understand how the alterations of lipid concentrations seen in chronologically aging Q and NQ cells delay their aging. It is conceivable that, by redirecting the flow of fatty acids from the synthesis of TAG to the formation of glycerophospholipids in the ER and mitochondria, the CR diet increases the efficiencies with which these two organelles support some pro-longevity cellular processes. These longevity-assuring processes may include mitochondrial respiration and ATP synthesis, unfolded protein response in mitochondrial and ER, and/or the modulation of intracellular ROS by oxidative enzymes residing in these organelles.

3 Lithocholic acid, a longevity-extending natural chemical compound, changes lipid compositions of quiescent and non-quiescent cells of chronologically aging yeast

3.1 Abstract

Lithocholic acid (LCA), the most hydrophobic bile acid, has been shown to extend longevity of chronologically aging yeast mainly under CR conditions [15, 26 - 30]. In studies described in this Chapter of my thesis, I used centrifugation in Percoll density gradient to separate quiescent (Q) and non-quiescent (NQ) cells of chronologically aging yeast. The Q and NQ populations of cells were purified from yeast cultured either under CR conditions in 0.2% glucose with or without LCA. Using quantitative mass spectrometry, I assessed how LCA influences age-related changes in the lipid composition of purified populations of Q and NQ yeast grown under CR conditions. My findings imply LCA causes a remodeling of lipid metabolism and transport in both Q and NQ cells limited in calorie supply. Based on these findings, I propose a working hypothesis on how this bile acid delays chronological aging of yeast cells by altering lipid dynamics within different cellular organelles.

3.2 Materials and Methods

Yeast strains, media and growth conditions

The wild-type strain *Saccharomyces cerevisiae* BY4742 (*MATα his3Δ1 leu2Δ0 lys2Δ0 ura3Δ0*) from Thermo Scientific/Open Biosystems was grown in YEP medium (1% yeast extract, 2% peptone; both from Fisher Scientific; #BP1422-2 and #BP1420-2, respectively) initially containing 0.2% or 2% glucose (#D16-10; Fisher Scientific) as carbon source. Cells

were cultured at 30^{o}C with rotational shaking at 200 rpm in Erlenmeyer flasks at a "flask volume/medium volume" ratio of 5:1.

Pharmacological manipulation of chronological lifespan

Chronological lifespan analysis was performed as described above in this section. The lithocholic (LCA) (#L6250) bile acid was from Sigma. The stock solution of LCA in water was made on the day of adding this compound to cell cultures. LCA was added to growth medium in water at the final concentration of 50 μM immediately following cell inoculation into the medium.

Separation of Q and NQ cells by centrifugation in Percoll density gradient

1 mL of 1.5 M NaCl (#S7653; Sigma) was placed into a 50-mL Falcon tube, and 8 mL of the Percoll solution (#P1644; Sigma) was added to this tube. The NaCl and Percoll solution was then mixed by pipetting. To form two Percoll density gradients, 4 mL of the NaCl/Percoll mixture was put into each of the two polyallomer tubes for an MLS-50 rotor for an Optima MAX ultracentrifuge (all from Beckman Coulter). The tubes were centrifuged at 25,000 × g (16,000 rpm) for 15 min at 4^{o}C in an Optima MAX ultracentrifuge. A sample of yeast cells were taken from a culture at a certain time point. A fraction of the sample was diluted in order to determine the total number of cells per mL of culture using a hemacytometer (#0267110; Fisher Scientific). For each Percoll density gradient, 1×10^{9} yeast cells were placed into a 15-mL Falcon tube and pelleted by centrifugation at 5,000 rpm for 7 min at room temperature in a Centra CL2 clinical centrifuge (Thermo IEC). Pelleted cells were resuspended in 500 μL of 50 mM Tris/HCl buffer (pH 7.5), overlaid onto the preformed gradient with a syringe and needle to avoid disrupting the gradient, and centrifuged at 2,300 × g (5,000 rpm) for 30 min at 25^{o}C in an Optima MAX

ultracentrifuge. The upper and lower fractions of cells were removed with a micropipette, discarding the gradient with no visible band of cells and Percoll was removed by washing cells twice with 50 mM Tris/HCl buffer (pH 7.5) and cells were resuspended in 1 mL of 50 mM Tris/HCl buffer (pH 7.5) for cell counts and preparation for freezing of the cell pellet.

Cell number measurement of Q and NQ cells separated by centrifugation in Percoll density gradient and preparation of pellet for storage until lipid extraction

A 50 μL aliquot of the upper or lower fraction of cells recovered and washed from the Percoll gradient were diluted in order to determine the total number of cells per fraction using a hemacytometer (#0267110; Fisher Scientific). 10 μL of serial dilutions (1:10 to $1:10^3$) of cells were applied to the hemacytometer, where each large square is calibrated to hold 0.1 μL. The number of cells in 4 large squares was then counted and an average was taken in order to ensure greater accuracy. The concentration of cells was calculated as follows: number of cells per large square × dilution factor × 10 × 1,000 = total number of cells per mL of fraction. The remaining 950 μL of the cell aliquots were washed twice with 155 mM ammonium bicarbonate (pH 8.0) in preparation for the freezing of the cell pellet at -80°C until the lipid extraction.

Lipid extraction from purified populations of Q and NQ cells

The lipid extraction of purified populations of quiescent and non-quiescent cells used Richard et al.'s modified version of Bligh and Dyer's lipid purification and extraction protocol [31]. The pelleted cell fractions kept at -80°C were thawed on ice before being resuspended in 1mL of cold nanopure water. The volume that contained 5×10^7 cells of each fraction was transferred to the appropriate 15-mL high-strength glass screw top centrifuge tube with a Teflon

lined cap (#0556912; Fisher Scientific). The volume of each sample was topped off to 1 mL with cold nanopure water. To each tube the following was added: 20 µL of the internal standard mix prepared in Chromasolv HPLC (>99.9%) chloroform (Sigma-Aldrich) (**Table 3.1**), 800 uL of 425-600 µM acid-washed glass beads to break open the cells (#G8772; Sigma-Aldrich) and 3 mL of a Chromasolv HPLC (>99.9%) chloroform: methanol mixture (both from Sigma-Aldrich) at a 17:1 ratio. The samples were then vortexed vigorously for 2 hours at 4^{O}C. At room temperature, the samples were then centrifuged in a Centra CL2 clinical centrifuge for 5 minutes separating the upper aqueous and lower organic phase which contained nonpolar lipids TAG, PC, PE and PG. The lower organic layer was transferred to another labelled 15 mL glass high-strength centrifuge tube using a glass Pasteur pipette with careful attention not to disrupt the glass beads or upper aqueous phase. 1.5 mL of 2:1 chloroform: methanol solution was added to the remaining upper aqueous phase allowing the separation of polar lipids PA, PS, PI and CL. The samples were again vortexed vigorously at 4^{O}C for 1 hour. The non-polar organic band was kept at 4^{O}C for the duration of the second vortexing. At the end of 1 hour, the samples were again centrifuged for 5 minutes at 3,000 rpm and the lower organic phase was separated and added to the corresponding non-polar organic phase with a glass Pasteur pipette. With both lower organic phases combined, the solvent was evaporated off by nitrogen gas flow. Once all solvent was evaporated, the remaining lipid film was dissolved and resuspended in 100 µL of 1:2 chloroform: methanol and immediately transferred into 2 mL glass vials with Teflon screw tops to avoid evaporation until samples were analysed by mass spectrometry. Samples were then stored at -20^{O}C and ran on the LTQ Orbitrap Mass Spectrometer within one week of the extraction.

Table 3.1: Internal standard mix composition (modified from reference [31])

Detection Mode	Class of Lipid Standard	Lipid Chain Composition (number carbons: number double bonds on fatty acid chain)	Exact Mass Molecular Weight (g/mol)	M/Z (mass/ion charge)	Concentration in mix (mg/µL)
Negative	CL	14:0 / 14:0 / 14:0 /14:0	1274.9000	619.4157	0.10
	FFA	19:0	298.2872	297.2711	0.02
	PA	14:0 / 14:0	614.3920	591.4026	0.10
	PE	14:0 / 14:0	635.4526	634.4448	0.10
	PG	14:0 / 14:0	688.4290	665.4394	0.10
	PS	14:0 / 14:0	701.4240	678.4271	0.02
Positive	TAG	13:0 / 13:0 / 13:0	680.5955	698.6299	0.10
	PC	13:0 / 13:0	649.4683	650.4761	0.10

Internal Standards CL, PA, PE, PG, PS and PC are all from Avanti Polar Lipid, Alabaster, AL, USA. TAG Internal standard originates from Larodan, Malmo, Sweden.

Lipid identification and quantitation of Q and NQ cells using mass spectrometry

Samples were diluted 1:1 with 1:2 chloroform: methanol and 0.1% ammonium hydroxide for improved ionization efficiency. Samples were injected one at a time using a Thermo Orbitrap Velos Mass Spectrometer equipped with HESI-II ion source (Thermo Scientific) at a flow rate of 5 µL/ minute. The instrument settings for the Orbitrap used the optimized settings listed in Richard's et al.'s tune file (**Table 3.2**).

Table 3.2: Thermo Orbitrap Velos mass spectrometer's tune file instrument settings (from reference [31])

Instrument polarity	Positive	Negative
Source voltage (kV)	3.9	4
Capillary temperature (°C)	275	275
Sheath gas flow	5	5
Aux gas flow	1	1
FT-MS injection time (ms)	100	500
FTMS microscans	3	1

Data was acquired according to the Instrument Method for data-dependent acquisition for 5 minutes in both positive and negative mode by the FTMS analyser at a resolution of 100,000 for both MS and MS/MS data (**Table 3.3**).

Table 3.3: Instrument method for data-dependent acquisition (from reference [31])

Acquisition time	**5 minutes (with a 0.25 minute delay)**	
Instrument polarity	**Positive**	**Negative**
MS (Segment 1)		
Analyzer	FTMS	FTMS
Mass Range	Normal	Normal
Resolution	100,000	100,000
Data Type	Centroid	Centroid
Scan Range	400-1,200	400-1,200
Data dependent MSMS (segments 2-10)		
Analyzer	FTMS	FTMS
Resolution	30,000	30,000
Data Type	Centroid	Centroid
Activation	HCD	HCD
Activation time (ms)	0.1	0.1
Isolation width	1	1
Collision energy	35	65
Mass range	Normal	Normal
Data type	Centroid	Centroid
Scan Range	-	-

Between each sample, the line was flushed with 1:2 chloroform: methanol until the background ion detection steadied and returned back into the baseline level. Diluted internal standard mix was injected multiple times throughout the acquisition to ensure no sensitivity loss throughout the run.

Once all data was acquired, raw files were converted to open mzXML format using ProteoWizard MSConvert software (http://proteowizard.sourceforge.net/), the file format used by the Lipid Identification Software LipidXplorer (https://wiki.mpi-cbg.de/lipidx/Main_Page). Data files were then imported into the software, using the following settings (**Table 3.4**), and all

lipids in the following lipids classes: PA, PC, PE, PI, PS, CL and TAG, were identified with the help of Molecular Fragmentation Query Language (MFQL) files. MFQL files were obtained from the LipidXplorer page listed above and aided in the identification of lipids by their m/z ratio as well as their fragmentation patterns.

LipidXplorer's output data was then opened under a Microsoft Excel file and all detected lipids were quantified by comparison with the intensity of the corresponding lipid class' internal standard's known concentration in the sample. Each quantified lipid had a corresponding internal standard from the same lipid class, allowing the calculation of molar percentage of each identified lipid species and therefore lipid class.

Table 3.4 Lipid identification by LipidXplorer import settings for data acquired under positive and negative mode. (From reference [31])

	Positive Mode	**Negative Mode**
Selection Window (Da)	1	1
Time Range (sec.)	0-350	0-350
Calibration masses		
MS	0	0
MS/MS	0	0
m/z range (m/z-m/z)		
MS	140-1,200	100-400
MS/MS	200-1,400	200-1200
Resolution (FMHW)		
MS	100,000	100,000
MS/MS	30,000	30,000
Tolerance (ppm)		
MS	10	10
MS/MS	10	10
Resolution Gradient (res/(m/z))		
MS	0	-55
MS/MS	0	0
Minimum Occupation (0<1)		
MS	0.5	0.5
MS/MS	0	0
MS1 offset (Da)	0	0

Statistical analysis

Statistical analysis was performed using Microsoft Excel's (2010) Analysis ToolPack-VBA. All data are presented as mean ± SEM. The *p* values were calculated with the help of GraphPad *t* test calculator using an unpaired two-tailed *t* test.

3.3 Results

3.3.1 LCA does not alter the intracellular concentrations of CL, a phospholipid specific for mitochondria, in Q and NQ cell populations of chronologically aging yeast grown under CR conditions

Using quantitative mass spectrometry, I monitored the concentrations of CL in Q and NQ cells of chronologically aging yeast grown under CR conditions in 0.2% glucose. I found that LCA does not change CL concentrations in Q and NQ cell populations of any chronological age (**Figures 3.1 and 3.2**, respectively). My findings suggest that LCA delays aging of Q and NQ cells under CR conditions not by altering the concentration of CL, the signature lipid of mitochondria, within these cells.

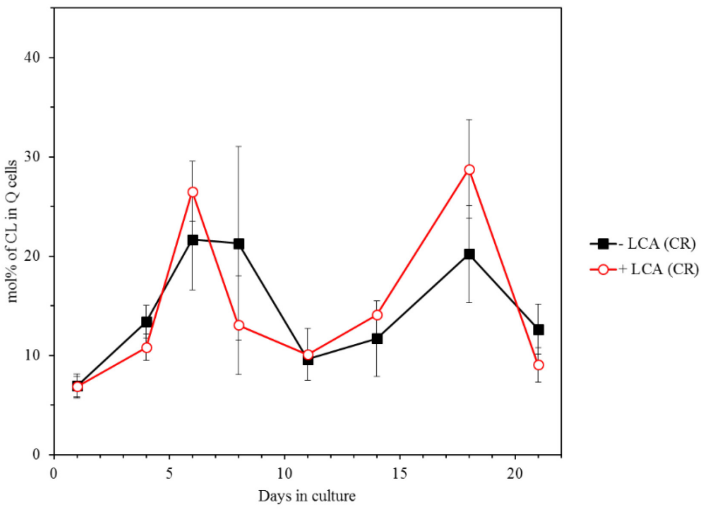

Figure 3.1. LCA does not alter the age-related dynamics of changes in CL concentrations within Q cells under CR conditions. Cells were cultured in the nutrient-rich YP medium initially containing 0.2% glucose with or without LCA. Q cells were purified from cell cultures recovered on days 1, 4, 6, 8, 11, 14, 18 or 21 of cell culturing. Extraction of cellular lipids, as well as their mass spectrometric identification and quantitation, were carried out as described in Materials and Methods. Based on these data, the concentrations of CL were calculated in mol%. Data are presented as means ± SEM (n = 2).

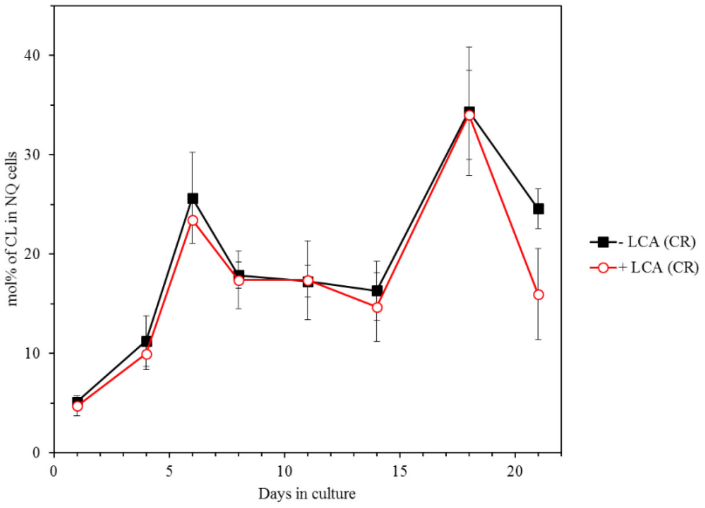

Figure 3.2. LCA does not change the concentrations CL within NQ cells grown under CR conditions. Cells were cultured in the nutrient-rich YP medium initially containing 0.2% glucose with or without LCA. NQ cells were purified from cell cultures recovered on days 1, 4, 6, 8, 11, 14, 18 or 21 of cell culturing. Extraction of cellular lipids, as well as their mass spectrometric identification and quantitation, were carried out as described in Materials and Methods. Based on these data, the concentrations of CL were calculated in mol%. Data are presented as means ± SEM (n = 2).

3.3.2 LCA alters the intracellular concentrations of TAG, a neutral lipid specific for LD, in Q and NQ cell populations of chronologically aging yeast grown under CR conditions

With the help of quantitative mass spectrometry, I assessed how LCA impacts the concentrations of TAG in Q and NQ cells of chronologically aging yeast grown under CR conditions and recovered at various stages of the aging process. I found that LCA has the following effects on the cellular concentrations of TAG in yeast limited in calorie supply: 1) in chronologically "young" (cultured from 1 to 6 days) and "middle-aged" (cultured from 8 to 11 days) Q cells but not in "old" Q cells cultured for 14 days and longer, LCA increases the concentration of TAG (**Figure 3.3**); and 2) only in chronologically "middle-aged" (cultured from 8 to 11 days) NQ cells but not in "young" (cultured from 1 to 6 days) or "old" (cultured for 14 days and longer) NQ cells, LCA significantly increased the concentration of TAG (**Figure 3.4**). These findings suggest that LCA may delay aging of Q cells under CR conditions by enabling these cells to maintain relatively high concentrations of TAG within chronologically "young" and "middle-aged" Q cells. Furthermore, it is conceivable that the ability of LCA to delay aging of NQ cells under CR conditions may be due to its ability to increase the concentration of TAG in "middle-aged" NQ cells.

3.3.3 LCA alters the concentrations of PA only in Q cells of chronologically aging yeast grown under CR conditions

Using quantitative mass spectrometry, I monitored the age-related dynamics of changes in the concentrations of PA in Q and NQ cell populations of chronologically aging yeast

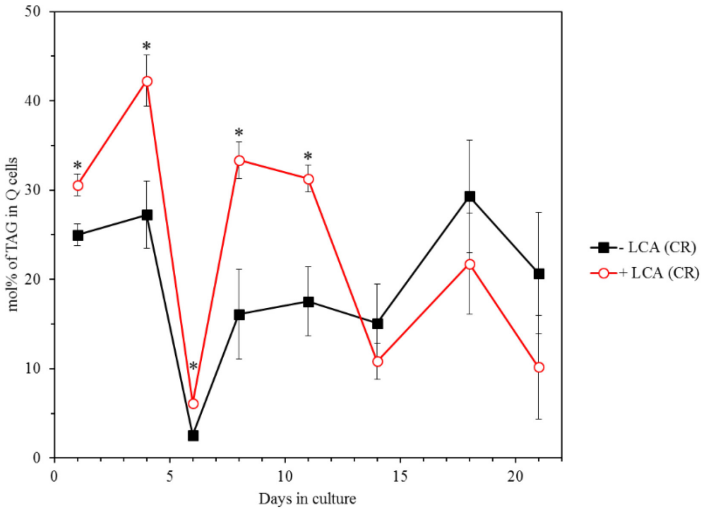

Figure 3.3. LCA increases the concentration of TAG in chronologically "young" (cultured from 1 to 6 days) and "middle-aged" (cultured from 8 to 11 days) Q cells but not in "old" Q cells cultured for 14 days and longer. Cells were cultured in YP medium initially containing 0.2% glucose with or without LCA. Q cells were purified from cell cultures recovered on days 1, 4, 6, 8, 11, 14, 18 or 21 of culturing. Extraction of cellular lipids, as well as their mass spectrometric identification and quantitation, were carried out as described in Materials and Methods. Based on these data, the concentrations of TAG were calculated in mol%. Data are presented as means ± SEM (n = 2; * $p < 0.05$).

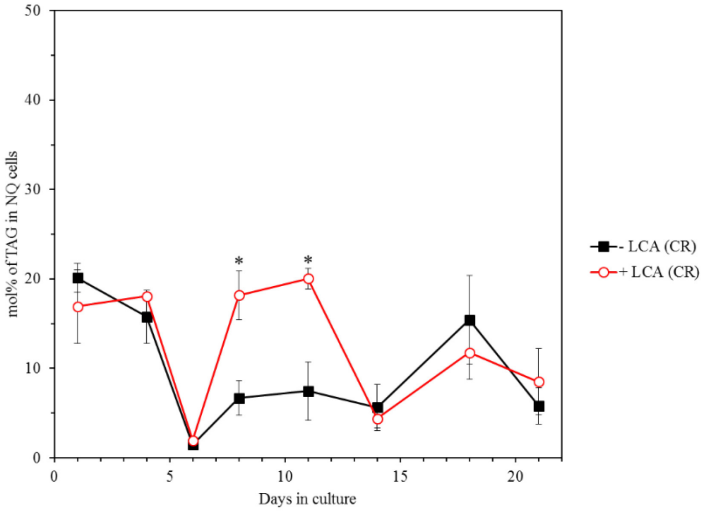

Figure 3.4. LCA increases the concentration of TAG only in chronologically "middle-aged" (cultured from 8 to 11 days) NQ cells but not in "young" (cultured from 1 to 6 days) or "old" (cultured for 14 days and longer) NQ cells. Cells were cultured in YP medium initially containing 0.2% glucose with or without LCA. NQ cells were purified from cell cultures recovered on days 1, 4, 6, 8, 11, 14, 18 or 21 of culturing. Extraction of cellular lipids, as well as their mass spectrometric identification and quantitation, were carried out as described in Materials and Methods. Based on these data, the concentrations of TAG were calculated in mol%. Data are presented as means ± SEM (n = 2; * $p < 0.05$).

grown under CR conditions in the presence or absence of LCA. I discovered that LCA has the following effects on the cellular concentrations of PA in yeast limited in calorie supply: 1) in chronologically "young" (cultured from 1 to 6 days) and "middle-aged" (cultured from 8 to 11 days) Q cells, but not in "old" Q cells, cultured for 14 days and longer, LCA decreases the concentration of PA (**Figure 3.5**); and 2) LCA does not change PA concentrations in NQ cells of any chronological age (**Figure 3.6**). My findings suggest that the ability of LCA to delay chronological aging of yeast limited in calorie supply may be due to the ability of this bile acid to decrease the concentration of PA within chronologically "young" and "middle-aged" Q cells. My findings also imply that LCA does not alter the concentration of PA within NQ cells when delaying aging of NQ cells under CR conditions.

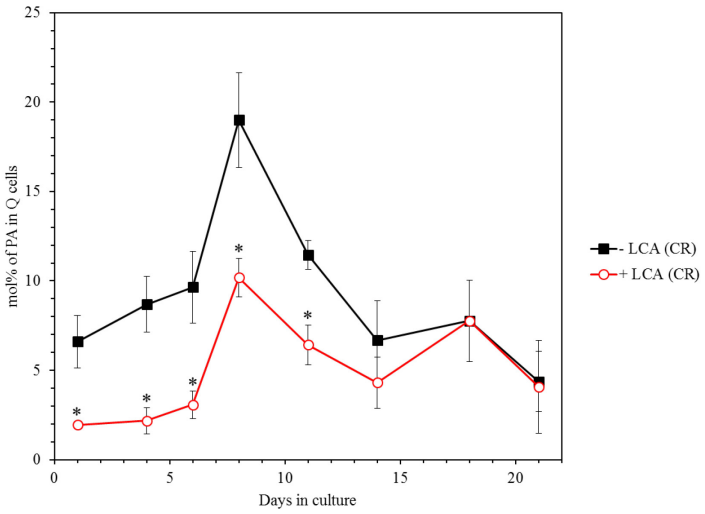

Figure 3.5. LCA decreases the concentration of PA in chronologically "young" (cultured from 1 to 6 days) and "middle-aged" (cultured from 8 to 11 days) Q cells but not in "old" Q cells cultured for 14 days and longer. Cells were cultured in YP medium initially containing 0.2% glucose with or without LCA. Q cells were purified from cell cultures recovered on days 1, 4, 6, 8, 11, 14, 18 or 21 of culturing. Extraction of cellular lipids, as well as their mass spectrometric identification and quantitation, were carried out as described in Materials and Methods. Based on these data, the concentrations of PA were calculated in mol%. Data are presented as means ± SEM (n = 2; * $p < 0.05$).

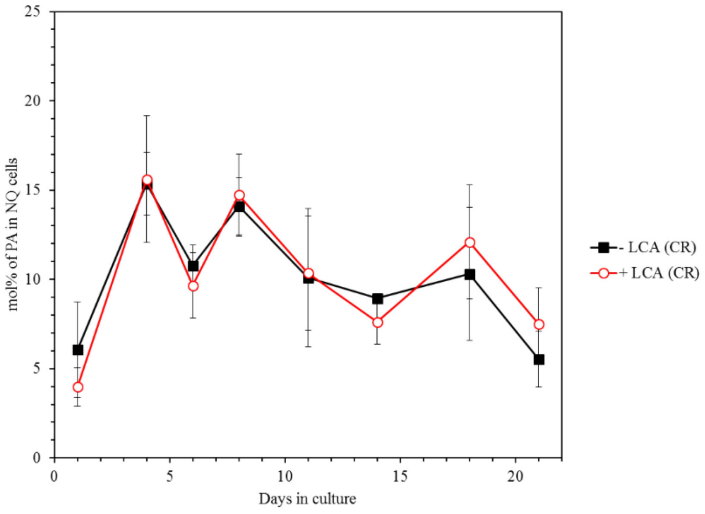

Figure 3.6. LCA does not change PA concentrations in NQ cells of any chronological age. Cells were cultured in YP medium initially containing 0.2% glucose with or without LCA. NQ cells were purified from cell cultures recovered on days 1, 4, 6, 8, 11, 14, 18 or 21 of culturing. Extraction of cellular lipids, as well as their mass spectrometric identification and quantitation, were carried out as described in Materials and Methods. Based on these data, the concentrations of PA were calculated in mol%. Data are presented as means ± SEM (n = 2).

3.3.4 LCA alters the concentrations of PI only in "old" Q cells and does not change PS concentrations in Q and NQ cells of chronologically aging yeast grown under CR conditions

With the help of quantitative mass spectrometry, I assessed how LCA impacts the concentrations of PS and PI in Q and NQ cells of chronologically aging yeast cultured under CR conditions. I found that LCA does not change PS concentrations in Q or NQ cells of any chronological age (**Figures 3.7 and 3.8,** respectively). Moreover, I discovered that LCA has the following effects on the cellular concentrations of PI in yeast limited in calorie supply: 1) in chronologically "middle-aged" (cultured from 11 to 14 days) and "old" (cultured for 14 days and longer) Q cells but not in chronologically "young" (cultured from 1 to 8 days) Q cells, LCA increases the concentration of PI

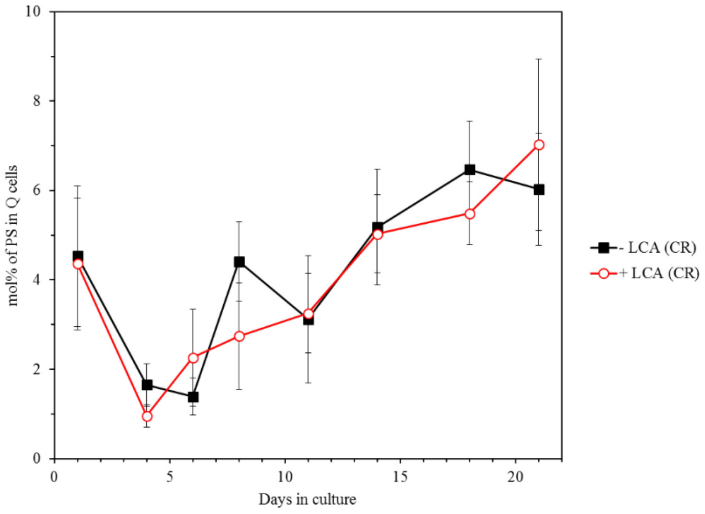

Figure 3.7. LCA does not change PS concentrations in Q cells of any chronological age. Cells were cultured in YP medium initially containing 0.2% glucose with or without LCA. Q cells were purified from cell cultures recovered on days 1, 4, 6, 8, 11, 14, 18 or 21 of culturing. Extraction of cellular lipids, as well as their mass spectrometric identification and quantitation, were carried out as described in Materials and Methods. Based on these data, the concentrations of PS were calculated in mol%. Data are presented as means ± SEM (n = 2).

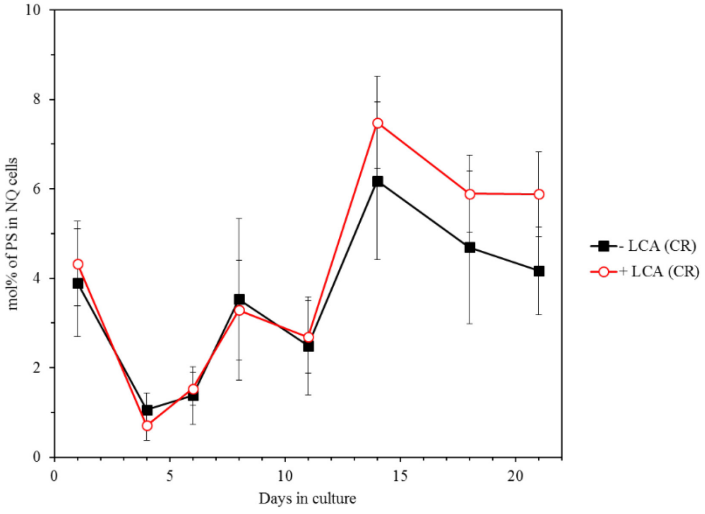

Figure 3.8. LCA does not change PS concentrations in NQ cells of any chronological age. Cells were cultured in YP medium initially containing 0.2% glucose with or without LCA. NQ cells were purified from cell cultures recovered on days 1, 4, 6, 8, 11, 14, 18 or 21 of culturing. Extraction of cellular lipids, as well as their mass spectrometric identification and quantitation, were carried out as described in Materials and Methods. Based on these data, the concentrations of PS were calculated in mol%. Data are presented as means ± SEM (n = 2).

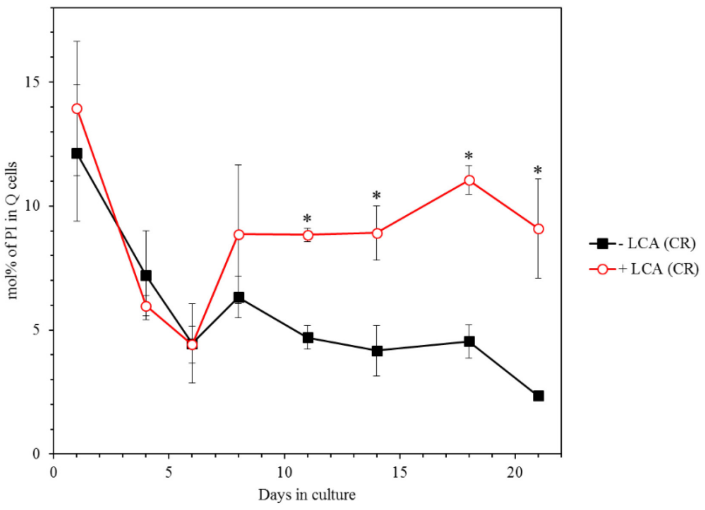

Figure 3.9. LCA increases the concentration of PI in chronologically "middle-aged" (cultured from 11 to 14 days) and "old" (cultured for 14 days and longer) Q cells but not in chronologically "young" (cultured from 1 to 8 days) Q cells. Cells were cultured in YP medium initially containing 0.2% glucose with or without LCA. Q cells were purified from cell cultures recovered on days 1, 4, 6, 8, 11, 14, 18 or 21 of culturing. Extraction of cellular lipids, as well as their mass spectrometric identification and quantitation, were carried out as described in Materials and Methods. Based on these data, the concentrations of PI were calculated in mol%. Data are presented as means ± SEM (n = 2; * $p < 0.05$).

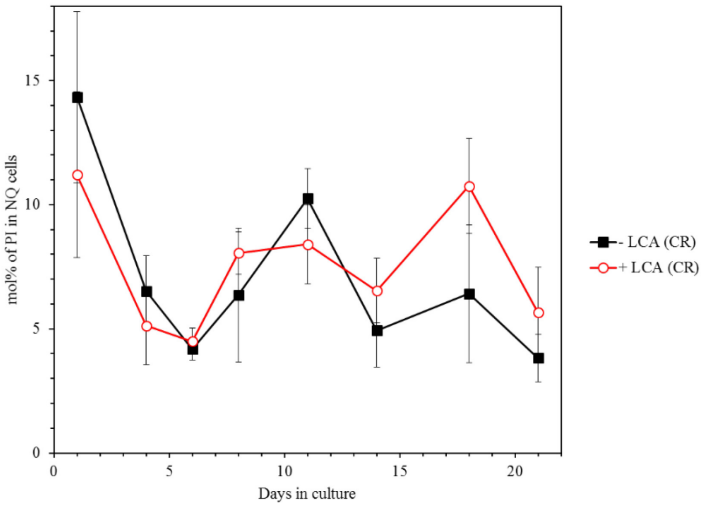

Figure 3.10. LCA does not change PI concentrations in NQ cells of any chronological age. Cells were cultured in YP medium initially containing 0.2% glucose with or without LCA. NQ cells were purified from cell cultures recovered on days 1, 4, 6, 8, 11, 14, 18 or 21 of culturing. Extraction of cellular lipids, as well as their mass spectrometric identification and quantitation, were carried out as described in Materials and Methods. Based on these data, the concentrations of PI were calculated in mol%. Data are presented as means ± SEM (n = 2).

(**Figure 3.9**); and 2) LCA does not change PI concentrations in NQ cells of any chronological age (**Figure 3.10**). These observations suggest that LCA delays aging of Q and NQ cells limited in calorie supply not by altering the concentrations of PS in these cells. Furthermore, the ability of LCA to delay aging of NQ cells under CR conditions is unlikely to be caused by any changes in concentration of PI in these cells. Moreover, it seems that LCA may delay aging of Q cells limited in calorie supply by increasing the concentration of PI in chronologically "middle-aged" (cultured from 11 to 14 days) and "old" (cultured for 14 days and longer) Q cells but not in chronologically "young" (cultured from 1 to 8 days) Q cells.

3.3.5 LCA does not change the concentrations of PE and PC within Q and NQ cells of chronologically aging yeast grown under CR conditions

Using quantitative mass spectrometry, I monitored the concentrations of PE and PC in Q and NQ cells purified from chronologically aging yeast cultured under CR conditions. I discovered that LCA does not alter PE and PC concentrations in Q and NQ cells of any chronological age (**Figures 3.11, 3.12, 3.13 and 3.14,** respectively). These findings imply that LCA delays aging of Q and NQ cells limited in calorie supply by a mechanism that does not alter the concentrations of PE and PC in these cells.

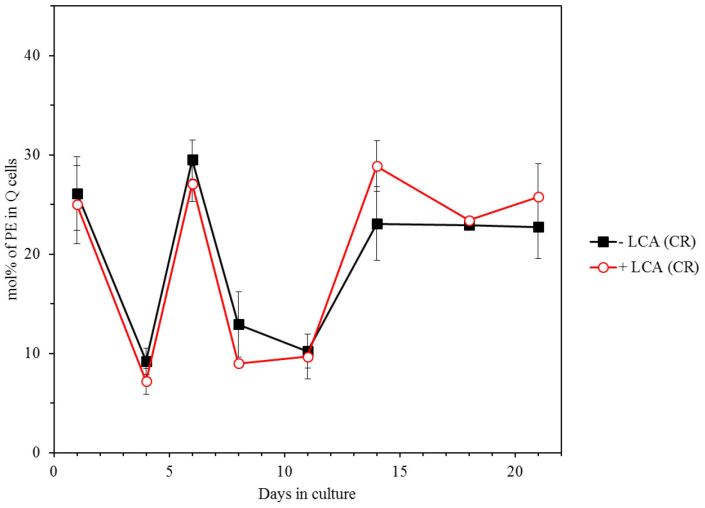

Figure 3.11. LCA does not change PE concentrations in Q cells of any chronological age. Cells were cultured in YP medium initially containing 0.2% glucose with or without LCA. Q cells were purified from cell cultures recovered on days 1, 4, 6, 8, 11, 14, 18 or 21 of culturing. Extraction of cellular lipids, as well as their mass spectrometric identification and quantitation, were carried out as described in Materials and Methods. Based on these data, the concentrations of PE were calculated in mol%. Data are presented as means ± SEM (n = 2).

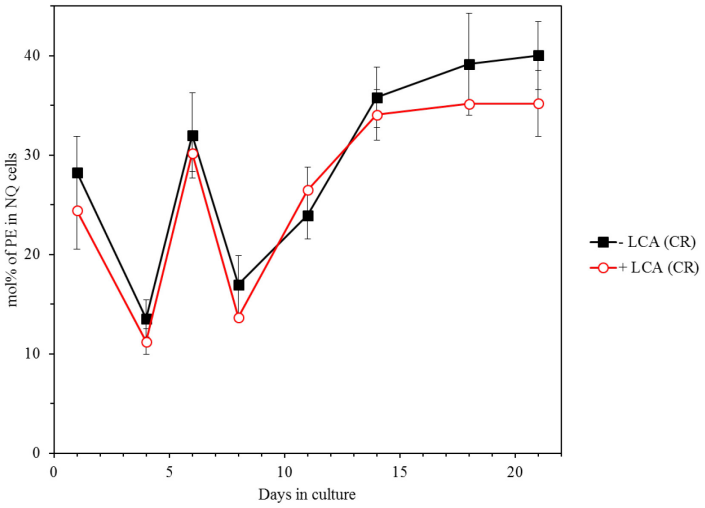

Figure 3.12. LCA does not change PE concentrations in NQ cells of any chronological age. Cells were cultured in YP medium initially containing 0.2% glucose with or without LCA. NQ cells were purified from cell cultures recovered on days 1, 4, 6, 8, 11, 14, 18 or 21 of culturing. Extraction of cellular lipids, as well as their mass spectrometric identification and quantitation, were carried out as described in Materials and Methods. Based on these data, the concentrations of PE were calculated in mol%. Data are presented as means ± SEM (n = 2).

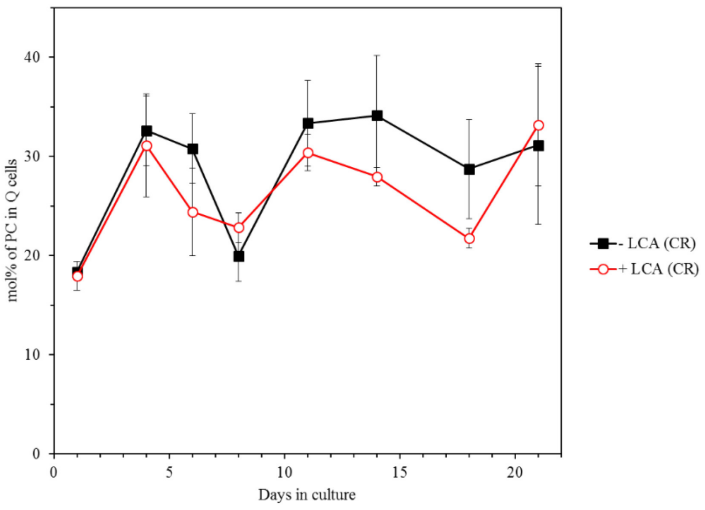

Figure 3.13. LCA does not change PC concentrations in Q cells of any chronological age. Cells were cultured in YP medium initially containing 0.2% glucose with or without LCA. Q cells were purified from cell cultures recovered on days 1, 4, 6, 8, 11, 14, 18 or 21 of culturing. Extraction of cellular lipids, as well as their mass spectrometric identification and quantitation, were carried out as described in Materials and Methods. Based on these data, the concentrations of PC were calculated in mol%. Data are presented as means ± SEM (n = 2).

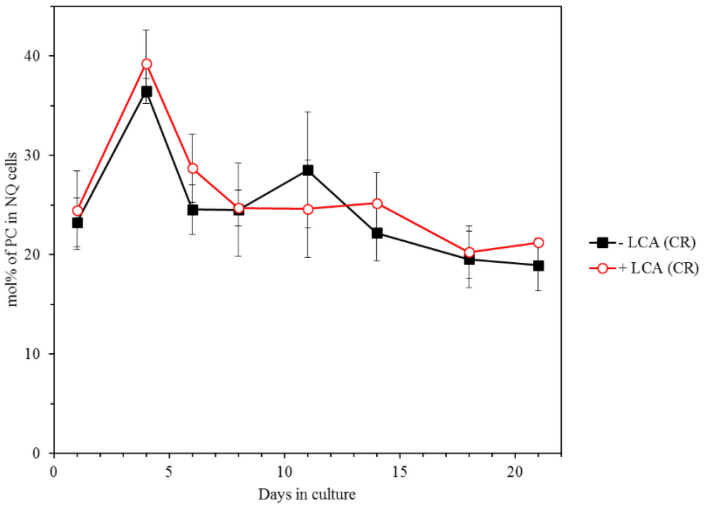

Figure 3.14. LCA does not change PC concentrations in NQ cells of any chronological age. Cells were cultured in YP medium initially containing 0.2% glucose with or without LCA. Q cells were purified from cell cultures recovered on days 1, 4, 6, 8, 11, 14, 18 or 21 of culturing. Extraction of cellular lipids, as well as their mass spectrometric identification and quantitation, were carried out as described in Materials and Methods. Based on these data, the concentrations of PC were calculated in mol%. Data are presented as means ± SEM (n = 2).

3.4 Discussion

Studies described in this chapter of my thesis have demonstrated that in yeast limited in calorie supply LCA causes a remodeling of lipid metabolism and transport within both Q and NQ cells. My findings imply that the LCA-driven remodeling of lipid dynamics in each of these cell populations differs substantially from the one observed in Q and NQ cells subjected to CR in the absence of LCA. Based on observations presented in this chapter, I propose a hypothetical model on how LCA, a longevity-extending natural chemical compound, may delay yeast chronological aging by altering the age-related dynamics of various lipids in Q and NQ cells progressing through consecutive stages of the aging process. My model posits the following: 1) in "young" Q cells, LCA increases the concentration of TAG, perhaps by intensifying its synthesis from PA and/or CoA-esters of free fatty acids in the ER (**Figure 3.15**); 2) in "young" Q cells, LCA reduces the concentration of PA, probably by decelerating the synthesis of this glycerophospholipid and/or accelerating its incorporation into TAG in the ER (**Figure 3.15**); 3) in "middle-aged" Q cells, LCA elevates the concentrations of TAG and PI, likely by stimulating their synthesis in the ER (**Figure 3.16**); 4) in "middle-aged" Q cells, LCA decreases the concentration of PA, perhaps by slowing down its synthesis and/or speeding up its incorporation into TAG in the ER (**Figure 3.16**); 5) in "old" Q cells, LCA increases the concentration of PI, possibly by stimulating its formation in the ER (**Figure 3.17**); 6) in "young" NQ cells, LCA does not alter the concentrations of lipids (**Figure 3.18**); 7) in "middle-aged" NQ cells, LCA increases the concentration of TAG, probably by activating its synthesis from CoA-esters of free fatty acids in the ER (**Figure 3.19**); and 8) in "old" NQ cells, LCA does not change the concentrations of lipids (**Figure 3.20**).

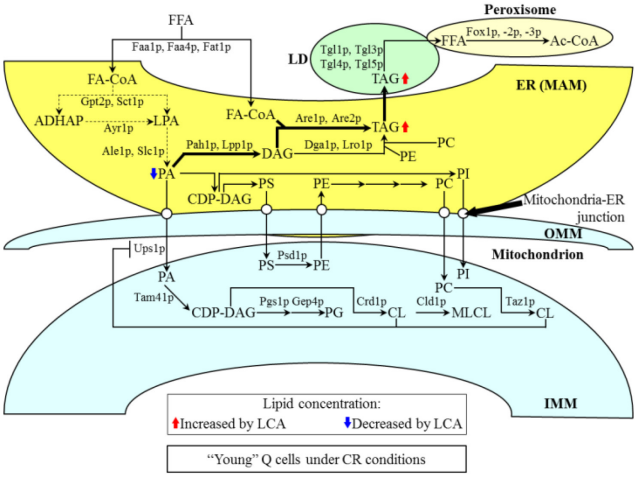

Figure 3.15. A hypothetical model on how LCA alters the metabolism of TAG and PA in "young" Q cells. The model is based on mass spectrometric lipidomics of purified Q cells that were recovered from yeast cultured from 1 to 6 days prior to entry into stationary growth phase under CR conditions in 0.2% glucose. From the data of lipidomic analysis, I inferred an outline of the rates and efficiencies of lipid metabolism that were increased (thick solid arrows) or decreased (thin dashed arrows) by LCA under CR conditions. Arrows next to the names of lipid classes denote those of them whose concentrations are elevated (red arrows) or reduced (blue arrows) by LCA in cells limited in calorie supply.

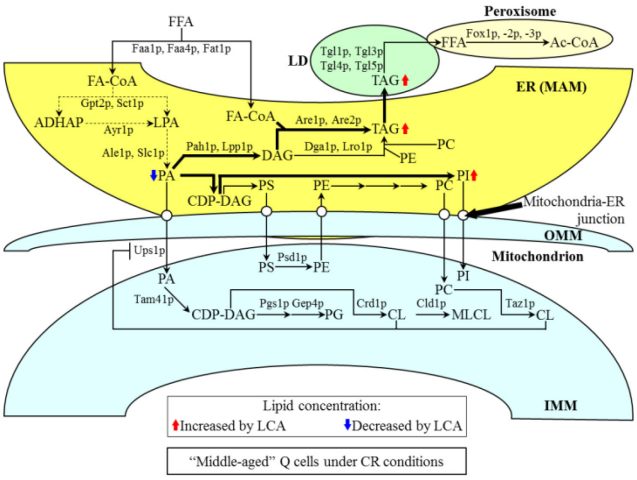

Figure 3.16. A hypothetical model on how LCA alters the metabolism of TAG, PA and PI in "middle-aged" Q cells. The model is based on mass spectrometric lipidomics of purified Q cells that were recovered from yeast cultured from 8 to 11 days under CR conditions in 0.2% glucose. From the data of lipidomic analysis, I inferred an outline of the rates and efficiencies of lipid metabolism that were increased (thick solid arrows) or decreased (thin dashed arrows) by LCA under CR conditions. Arrows next to the names of lipid classes denote those of them whose concentrations are elevated (red arrows) or reduced (blue arrows) by LCA in cells limited in calorie supply.

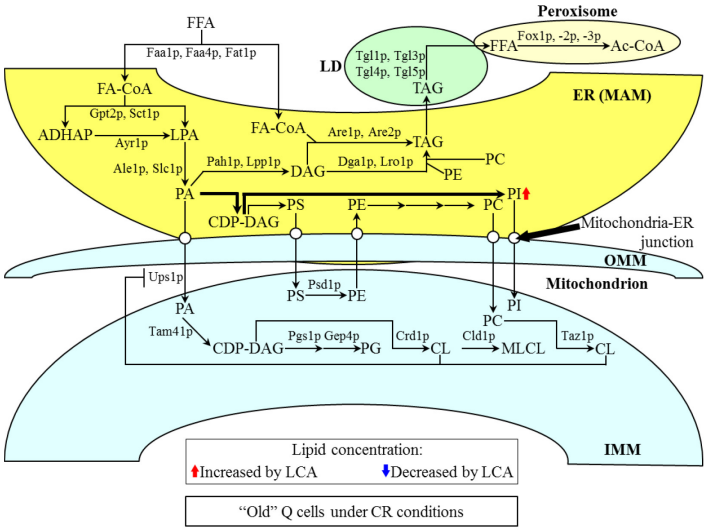

Figure 3.17. A hypothetical model on how LCA alters the metabolism of PI in "old" Q cells. The model is based on mass spectrometric lipidomics of purified Q cells that were recovered from yeast cultured for 14 days and longer under CR conditions in 0.2% glucose. From the data of lipidomic analysis, I inferred an outline of the rates and efficiencies of lipid metabolism that were increased (thick solid arrows) by LCA under CR conditions. A red arrow next to the name of PI indicates that its concentration is elevated by LCA in cells limited in calorie supply.

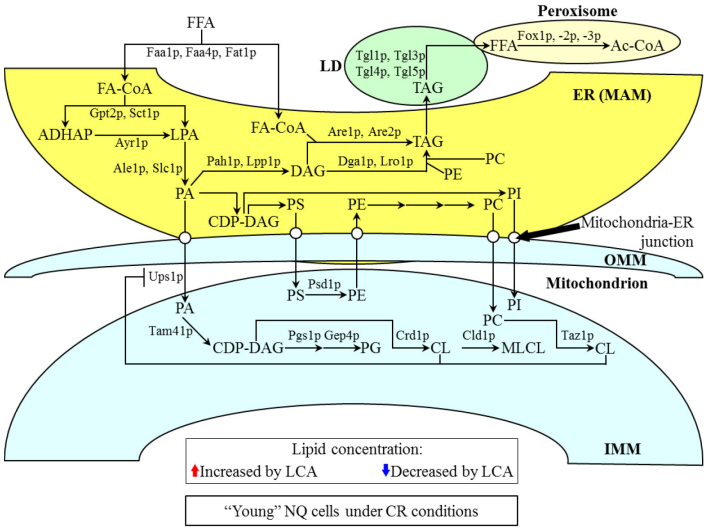

Figure 3.18. A hypothetical model on how LCA influences lipid metabolism in "young" NQ cells. The model is based on mass spectrometric lipidomics of purified NQ cells that were recovered from yeast cultured from 1 to 6 days prior to entry into stationary growth phase under CR conditions in 0.2% glucose. From the data of lipidomic analysis, I inferred that LCA does not alter the concentrations of lipids in "young" NQ cells limited in calorie supply.

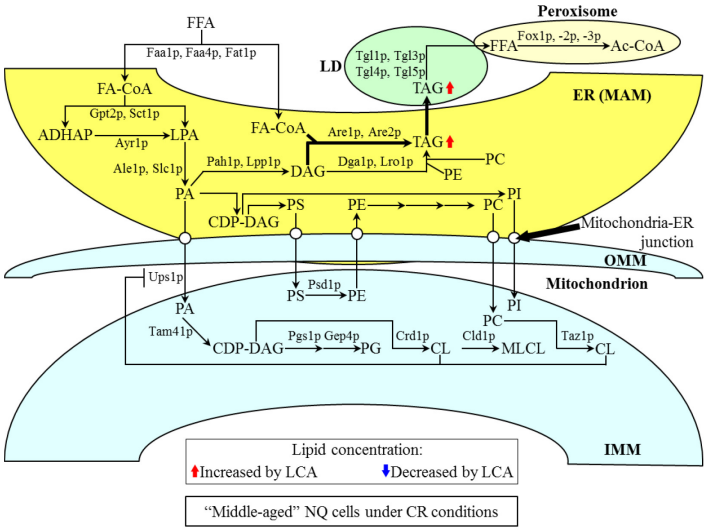

Figure 3.19. A hypothetical model on how LCA alters the metabolism of TAG in "middle-aged" NQ cells. The model is based on mass spectrometric lipidomics of purified NQ cells that were recovered from yeast cultured from 8 to 11 days under CR conditions in 0.2% glucose. From the data of lipidomic analysis, I inferred an outline of the rates and efficiencies of lipid metabolism that were increased (thick solid arrows) by LCA under CR conditions. Arrows next to the names of TAG indicates that its concentration is elevated by LCA in cells limited in calorie supply.

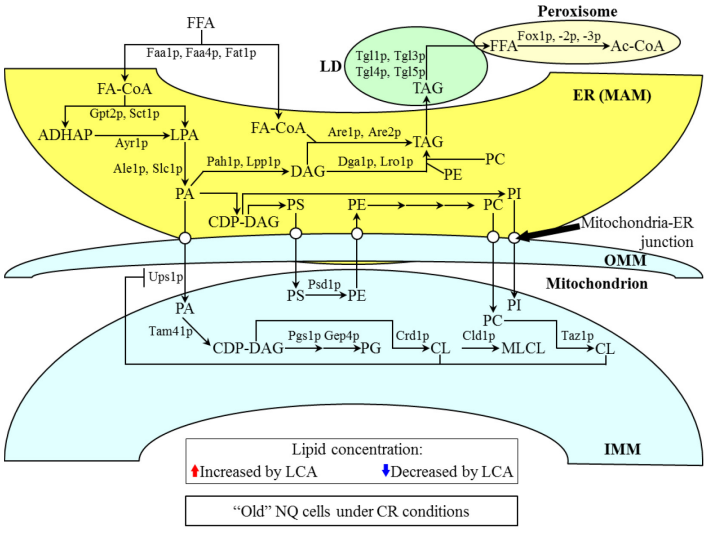

Figure 3.20. A hypothetical model on how LCA influences lipid metabolism in "old" NQ cells. The model is based on mass spectrometric lipidomics of purified NQ cells that were recovered from yeast cultured for 14 days and longer under CR conditions in 0.2% glucose. From the data of lipidomic analysis, I inferred that LCA does not alter the concentrations of lipids in "old" NQ cells limited in calorie supply.

Taken together, my findings imply that the pattern of age-related changes in lipid concentrations seen in Q and NQ cells treated with LCA under CR conditions differs substantially from the pattern observed in Q and NQ cells subjected to CR in the absence of LCA. Thus, it seems that there are at least two different ways of delaying yeast chronological aging by altering lipid metabolism and transport in Q and NQ cells; these two ways are outlined in **Figures 2.17-2.20** and **3.15-3.20**.

Future studies will address the key question of which alterations in lipid concentrations observed in Q and NQ cells are important for the ability of LCA to delay aging of these cell populations under CR conditions. Of note, it is possible that some of these alterations just coincide with the progress of chronological aging. To address this challenging question, it will be necessary to examine how single-gene mutations eliminating enzymes that accelerate individual reactions of lipid metabolism in yeast (**Figures 3.15 – 3.20**) influence the efficiency with which LCA delays yeast chronological aging under CR conditions. Moreover, a challenge remains to understand how the alterations of lipid concentrations seen in chronologically aging Q and NQ cells treated with LCA delay their aging under CR conditions. It is conceivable that, by stimulating the incorporation of fatty acids into TAG, LCA may protect yeast cells from an age-related form of cell death called liponecrosis [35, 36].

4 Lack of the nutrient-sensing protein kinase Tor1, a pro-aging master regulator, alters lipid compositions of quiescent and non-quiescent cells of chronologically aging yeast

4.1 Abstract

The nutrient-sensing protein kinase Tor1 is a longevity-shortening master regulator [1, 2, 5]. In yeast, Tor1 is known to activate the pro-aging process of protein synthesis in the cytosol and also to inhibit such anti-aging processes as transcription of numerous stress-response genes, autophagy and protein synthesis in mitochondria [1, 2, 5, 20, 21]. Tor1 can modulate all these longevity-defining cellular processes and accelerate chronological aging only under non-CR conditions [1, 2, 5]. In studies described in this Chapter of my thesis, I used Percoll density gradient centrifugation to separate quiescent (Q) and non-quiescent (NQ) cells of chronologically aging yeast. The Q and NQ populations of cells were purified from wild-type cells as well as from *tor1Δ* mutant cells lacking Tor1. These cells were cultured under non-CR conditions on 2% glucose without LCA. With the help of quantitative mass spectrometry, I monitored how the *tor1Δ* mutation influences age-related changes in the lipid composition of purified populations of Q and NQ yeast grown under non-CR conditions. My findings imply that the *tor1Δ* mutation, which extends yeast chronological lifespan, causes a remodeling of lipid metabolism and transport in both Q and NQ cells under non-CR conditions. Based on these findings, I propose a working hypothesis on how Tor1 can accelerate chronological aging of yeast cells by altering lipid dynamics within different cellular organelles.

4.2 Materials and Methods

Yeast strains, media and growth conditions

The wild-type strain *Saccharomyces cerevisiae* BY4742 (*MATα his3Δ1 leu2Δ0 lys2Δ0 ura3Δ0*) and the single-gene-deletion mutant strain *tor1Δ* (*MATα his3Δ1 leu2Δ0 lys2Δ0 ura3Δ0 tor1::kanMX4*) from Thermo Scientific/Open Biosystems were grown in YEP medium (1% yeast extract, 2% peptone; both from Fisher Scientific; #BP1422-2 and #BP1420-2, respectively) initially containing 2% glucose (#D16-10; Fisher Scientific) as carbon source. Cells were cultured at 30^{o}C with rotational shaking at 200 rpm in Erlenmeyer flasks at a "flask volume/medium volume" ratio of 5:1.

Separation of Q and NQ cells by centrifugation in Percoll density gradient

1 mL of 1.5 M NaCl (#S7653; Sigma) was placed into a 50-mL Falcon tube, and 8 mL of the Percoll solution (#P1644; Sigma) was added to this tube. The NaCl and Percoll solution was then mixed by pipetting. To form two Percoll density gradients, 4 mL of the NaCl/Percoll mixture was put into each of the two polyallomer tubes for an MLS-50 rotor for an Optima MAX ultracentrifuge (all from Beckman Coulter). The tubes were centrifuged at 25,000 × g (16,000 rpm) for 15 min at 4^{o}C in an Optima MAX ultracentrifuge. A sample of yeast cells were taken from a culture at a certain time point. A fraction of the sample was diluted in order to determine the total number of cells per mL of culture using a hemacytometer (#0267110; Fisher Scientific). For each Percoll density gradient, 1×10^{9} yeast cells were placed into a 15-mL Falcon tube and pelleted by centrifugation at 5,000 rpm for 7 min at room temperature in a Centra CL2 clinical centrifuge (Thermo IEC). Pelleted cells were resuspended in 500 μL of 50 mM Tris/HCl buffer (pH 7.5), overlaid onto the preformed gradient with a syringe and needle to avoid disrupting the gradient, and centrifuged at 2,300 × g (5,000 rpm) for 30 min at 25^{o}C in an Optima MAX

ultracentrifuge. The upper and lower fractions of cells were removed with a micropipette, discarding the gradient with no visible band of cells and Percoll was removed by washing cells twice with 50 mM Tris/HCl buffer (pH 7.5) and cells were resuspended in 1 mL of 50 mM Tris/HCl buffer (pH 7.5) for cell counts and preparation for freezing of the cell pellet.

Cell number measurement of Q and NQ cells separated by centrifugation in Percoll density gradient and preparation of pellet for storage until lipid extraction

A 50 μL aliquot of the upper or lower fraction of cells recovered and washed from the Percoll gradient were diluted in order to determine the total number of cells per fraction using a hemacytometer (#0267110; Fisher Scientific). 10 μL of serial dilutions (1:10 to $1:10^3$) of cells were applied to the hemacytometer, where each large square is calibrated to hold 0.1 μL. The number of cells in 4 large squares was then counted and an average was taken in order to ensure greater accuracy. The concentration of cells was calculated as follows: number of cells per large square × dilution factor × 10 × 1,000 = total number of cells per mL of fraction. The remaining 950 μL of the cell aliquots were washed twice with 155 mM ammonium bicarbonate (pH 8.0) in preparation for the freezing of the cell pellet at -80°C until the lipid extraction.

Lipid extraction from purified populations of Q and NQ cells

The lipid extraction of purified populations of quiescent and non-quiescent cells used Richard et al.'s modified version of Bligh and Dyer's lipid purification and extraction protocol [31]. The pelleted cell fractions kept at -80°C were thawed on ice before being resuspended in 1mL of cold nanopure water. The volume that contained 5×10^7 cells of each fraction was transferred to the appropriate 15-mL high-strength glass screw top centrifuge tube with a Teflon

lined cap (#0556912; Fisher Scientific). The volume of each sample was topped off to 1 mL with cold nanopure water. To each tube the following was added: 20 µL of the internal standard mix prepared in Chromasolv HPLC (>99.9%) chloroform (Sigma-Aldrich) (**Table 4.1**), 800 uL of 425-600 µM acid-washed glass beads to break open the cells (#G8772; Sigma-Aldrich) and 3 mL of a Chromasolv HPLC (>99.9%) chloroform: methanol mixture (both from Sigma-Aldrich) at a 17:1 ratio. The samples were then vortexed vigorously for 2 hours at 4^{O}C. At room temperature, the samples were then centrifuged in a Centra CL2 clinical centrifuge for 5 minutes separating the upper aqueous and lower organic phase which contained nonpolar lipids TAG, PC, PE and PG. The lower organic layer was transferred to another labelled 15 mL glass high-strength centrifuge tube using a glass Pasteur pipette with careful attention not to disrupt the glass beads or upper aqueous phase. 1.5 mL of 2:1 chloroform: methanol solution was added to the remaining upper aqueous phase allowing the separation of polar lipids PA, PS, PI and CL. The samples were again vortexed vigorously at 4^{O}C for 1 hour. The non-polar organic band was kept at 4^{O}C for the duration of the second vortexing. At the end of 1 hour, the samples were again centrifuged for 5 minutes at 3,000 rpm and the lower organic phase was separated and added to the corresponding non-polar organic phase with a glass Pasteur pipette. With both lower organic phases combined, the solvent was evaporated off by nitrogen gas flow. Once all solvent was evaporated, the remaining lipid film was dissolved and resuspended in 100 µL of 1:2 chloroform: methanol and immediately transferred into 2 mL glass vials with Teflon screw tops to avoid evaporation until samples were analysed by mass spectrometry. Samples were then stored at -20^{O}C and ran on the LTQ Orbitrap Mass Spectrometer within one week of the extraction.

Table 4.1: Internal standard mix composition (modified from reference [31])

Detection Mode	Class of Lipid Standard	Lipid Chain Composition (number carbons: number double bonds on fatty acid chain)	Exact Mass Molecular Weight (g/mol)	M/Z (mass/ion charge)	Concentration in mix (mg/µL)
Negative	CL	14:0 / 14:0 / 14:0 /14:0	1274.9000	619.4157	0.10
	FFA	19:0	298.2872	297.2711	0.02
	PA	14:0 / 14:0	614.3920	591.4026	0.10
	PE	14:0 / 14:0	635.4526	634.4448	0.10
	PG	14:0 / 14:0	688.4290	665.4394	0.10
	PS	14:0 / 14:0	701.4240	678.4271	0.02
Positive	TAG	13:0 / 13:0 / 13:0	680.5955	698.6299	0.10
	PC	13:0 / 13:0	649.4683	650.4761	0.10

Internal Standards CL, PA, PE, PG, PS and PC are all from Avanti Polar Lipid, Alabaster, AL, USA. TAG Internal standard originates from Larodan, Malmo, Sweden.

Lipid identification and quantitation of Q and NQ cells using mass spectrometry

Samples were diluted 1:1 with 1:2 chloroform: methanol and 0.1% ammonium hydroxide for improved ionization efficiency. Samples were injected one at a time using a Thermo Orbitrap Velos Mass Spectrometer equipped with HESI-II ion source (Thermo Scientific) at a flow rate of 5 µL/ minute. The instrument settings for the Orbitrap used the optimized settings listed in Richard's et al.'s tune file (**Table 4.2**).

Table 4.2: Thermo Orbitrap Velos mass spectrometer's tune file instrument settings (from reference [31])

Instrument polarity	Positive	Negative
Source voltage (kV)	3.9	4
Capillary temperature (°C)	275	275
Sheath gas flow	5	5
Aux gas flow	1	1
FT-MS injection time (ms)	100	500
FTMS microscans	3	1

Data was acquired according to the Instrument Method for data-dependent acquisition for 5 minutes in both positive and negative mode by the FTMS analyser at a resolution of 100,000 for both MS and MS/MS data (**Table 4.3**).

Table 4.3: Instrument method for data-dependent acquisition (from reference [31])

Acquisition time	**5 minutes (with a 0.25 minute delay)**	
Instrument polarity	**Positive**	**Negative**
MS (Segment 1)		
Analyzer	FTMS	FTMS
Mass Range	Normal	Normal
Resolution	100,000	100,000
Data Type	Centroid	Centroid
Scan Range	400-1,200	400-1,200
Data dependent MSMS (segments 2-10)		
Analyzer	FTMS	FTMS
Resolution	30,000	30,000
Data Type	Centroid	Centroid
Activation	HCD	HCD
Activation time (ms)	0.1	0.1
Isolation width	1	1
Collision energy	35	65
Mass range	Normal	Normal
Data type	Centroid	Centroid
Scan Range	-	-

Between each sample, the line was flushed with 1:2 chloroform: methanol until the background ion detection steadied and returned back into the baseline level. Diluted internal standard mix was injected multiple times throughout the acquisition to ensure no sensitivity loss throughout the run.

Once all data was acquired, raw files were converted to open mzXML format using ProteoWizard MSConvert software (http://proteowizard.sourceforge.net/), the file format used by the Lipid Identification Software LipidXplorer (https://wiki.mpi-cbg.de/lipidx/Main_Page). Data files were then imported into the software, using the following settings (**Table 4.4**), and all

lipids in the following lipids classes: PA, PC, PE, PI, PS, CL and TAG, were identified with the help of Molecular Fragmentation Query Language (MFQL) files. MFQL files were obtained from the LipidXplorer page listed above and aided in the identification of lipids by their m/z ratio as well as their fragmentation patterns.

LipidXplorer's output data was then opened under a Microsoft Excel file and all detected lipids were quantified by comparison with the intensity of the corresponding lipid class' internal standard's known concentration in the sample. Each quantified lipid had a corresponding internal standard from the same lipid class, allowing the calculation of molar percentage of each identified lipid species and therefore lipid class.

Table 4.4 Lipid identification by LipidXplorer import settings for data acquired under positive and negative mode. (From reference [31])

	Positive Mode	**Negative Mode**
Selection Window (Da)	1	1
Time Range (sec.)	0-350	0-350
Calibration masses		
MS	0	0
MS/MS	0	0
m/z range (m/z-m/z)		
MS	140-1,200	100-400
MS/MS	200-1,400	200-1200
Resolution (FMHW)		
MS	100,000	100,000
MS/MS	30,000	30,000
Tolerance (ppm)		
MS	10	10
MS/MS	10	10
Resolution Gradient (res/(m/z))		
MS	0	-55
MS/MS	0	0
Minimum Occupation (0<1)		
MS	0.5	0.5
MS/MS	0	0
MS1 offset (Da)	0	0

Statistical analysis

Statistical analysis was performed using Microsoft Excel's (2010) Analysis ToolPack-VBA. All data are presented as mean ± SEM. The *p* values were calculated with the help of GraphPad *t* test calculator using an unpaired two-tailed *t* test.

4.3 Results

4.3.1 The *tor1Δ* mutation alters the intracellular concentrations of CL, a phospholipid specific for mitochondria, in Q and NQ cell populations of chronologically aging yeast grown under non-CR conditions

Using quantitative mass spectrometry, I assessed how the *tor1Δ* mutation influences the concentrations of CL in Q and NQ cells of chronologically aging yeast grown under non-CR conditions in 2% glucose. I found that this mutation caused the following effects on the cellular concentrations of CL: 1) in chronologically "young" Q and NQ cells cultured from 1 to 4 days, the *tor1Δ* mutation significantly increases CL concentration (**Figures 4.1 and 4.2**, respectively); and 2) in chronologically "middle-aged" (cultured from 6 to 11 days) and "old" (cultured for 14 days and longer) Q and NQ cells, the *tor1Δ* mutation substantially decreases CL concentration (**Figures 4.1 and 4.2**, respectively). My findings suggest that the ability of the *tor1Δ* mutation to alter cellular concentrations of CL in Q and NQ cells throughout chronological lifespan may be responsible in part for the ability of this mutation to delay chronological aging of both these cell populations.

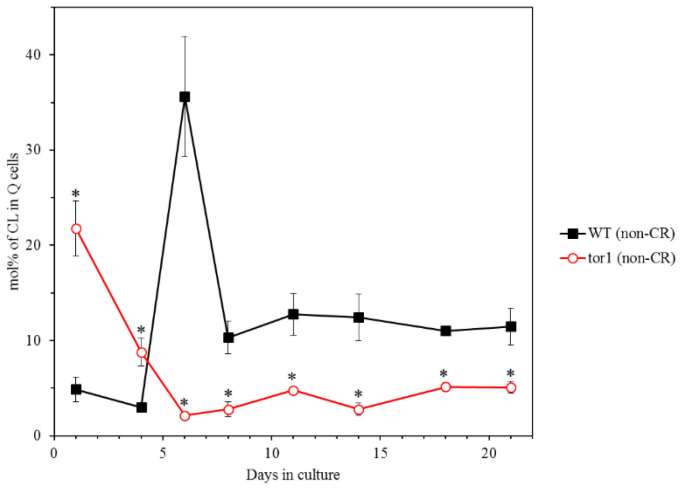

Figure 4.1. The *tor1Δ* mutation alters the age-related dynamics of changes in CL concentrations within Q cells under non-CR conditions. Cells were cultured in the nutrient-rich YP medium initially containing 2% glucose. Q cells were purified from cell cultures recovered on days 1, 4, 6, 8, 11, 14, 18 or 21 of cell culturing. Extraction of cellular lipids, as well as their mass spectrometric identification and quantitation, were carried out as described in Materials and Methods. Based on these data, the concentrations of CL were calculated in mol%. Data are presented as means ± SEM (n = 2; * $p < 0.05$).

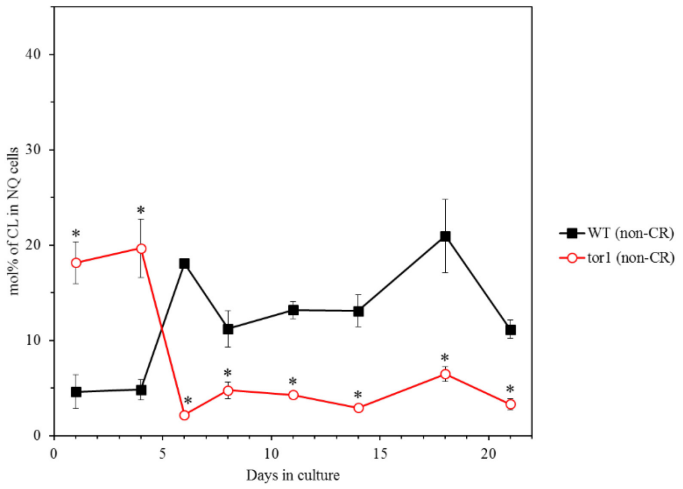

Figure 4.2. The *tor1Δ* mutation alters the age-related dynamics of changes in CL concentrations within NQ cells under non-CR conditions. Cells were cultured in the nutrient-rich YP medium initially containing 2% glucose. NQ cells were purified from cell cultures recovered on days 1, 4, 6, 8, 11, 14, 18 or 21 of cell culturing. Extraction of cellular lipids, as well as their mass spectrometric identification and quantitation, were carried out as described in Materials and Methods. Based on these data, the concentrations of CL were calculated in mol%. Data are presented as means ± SEM (n = 2; * $p < 0.05$).

4.3.2 The *tor1Δ* mutation increases the intracellular concentrations of TAG in Q and NQ cell populations of chronologically aging yeast grown under non-CR conditions, but for a limited period of chronological age

With the help of quantitative mass spectrometry, I examined how the *tor1Δ* mutation influences the concentrations of TAG in Q and NQ cells of chronologically aging yeast grown under non-CR conditions in 2% glucose. I discovered that this mutation caused the following effects on the cellular concentrations of TAG: 1) in chronologically "young" Q and NQ cells cultured from 1 to 4 days, the *tor1Δ* mutation does not alter TAG concentration (**Figures 4.3 and 4.4**, respectively); 2) during a transition from the "young" to the "middle" chronological age (from day 4 to day 6 of culturing), the *tor1Δ* mutation substantially increases TAG concentration in Q and NQ cells (**Figures 4.3 and 4.4**, respectively); and 3) in chronologically "middle-aged" (cultured from 6 to 11 days) and "old" (cultured for 14 days and longer) Q and NQ cells, the *tor1Δ* mutation does not change TAG concentration (**Figures 4.3 and 4.4**, respectively). These observations suggest that the abilities of the *tor1Δ* mutation to increase the concentrations of TAG in Q and NQ cells for a limited period of chronological age, during a transition from the "young" to the "middle" chronological age of these cells, may underlie the delay of chronological aging for both these cell populations known to be caused by the *tor1Δ* mutation.

4.3.3 The *tor1Δ* mutation increases the concentrations of PA only in "old" Q and NQ cells of chronologically aging yeast grown under non-CR conditions

Using quantitative mass spectrometry, I assessed the effects of the *tor1Δ* mutation on the

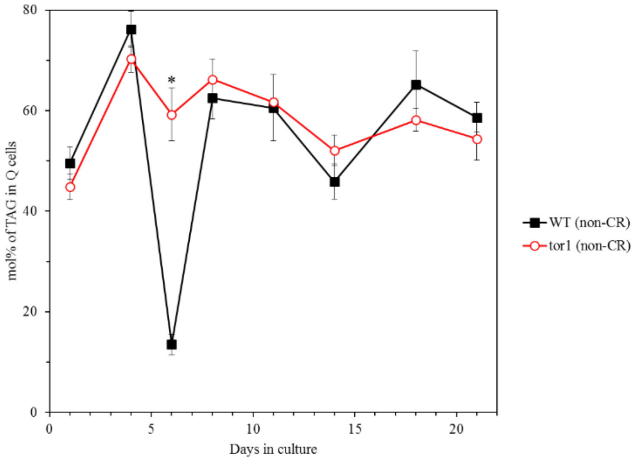

Figure 4.3. The *tor1Δ* mutation increases TAG concentration within Q cells under non-CR conditions for a limited period of chronological age, during a transition from the "young" to the "middle" chronological age (from day 4 to day 6 of culturing). Cells were cultured in the nutrient-rich YP medium initially containing 2% glucose. Q cells were purified from cell cultures recovered on days 1, 4, 6, 8, 11, 14, 18 or 21 of cell culturing. Extraction of cellular lipids, as well as their mass spectrometric identification and quantitation, were carried out as described in Materials and Methods. Based on these data, the concentrations of TAG were calculated in mol%. Data are presented as means ± SEM (n = 2; * $p < 0.05$).

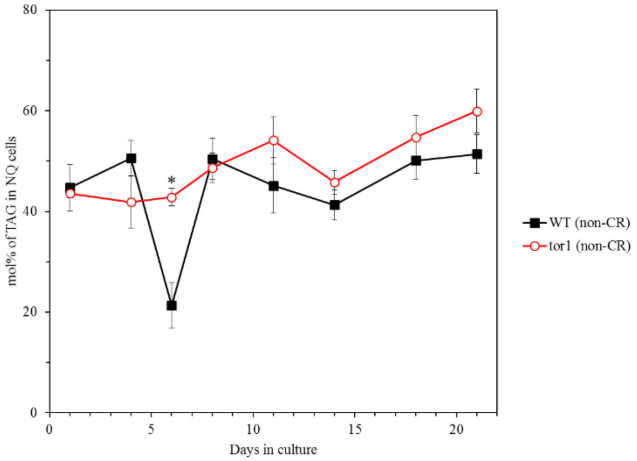

Figure 4.4. The *tor1Δ* mutation increases TAG concentration within NQ cells under non-CR conditions for a limited period of chronological age, during a transition from the "young" to the "middle" chronological age (from day 4 to day 6 of culturing). Cells were cultured in the nutrient-rich YP medium initially containing 2% glucose. NQ cells were purified from cell cultures recovered on days 1, 4, 6, 8, 11, 14, 18 or 21 of cell culturing. Extraction of cellular lipids, as well as their mass spectrometric identification and quantitation, were carried out as described in Materials and Methods. Based on these data, the concentrations of TAG were calculated in mol%. Data are presented as means ± SEM (n = 2; * $p < 0.05$).

concentrations of PA in Q and NQ cells of chronologically aging yeast grown under non-CR conditions in 2% glucose. I found that this mutation does not alter the concentrations of PA in "young" and "middle-aged" Q and NQ cells of chronologically aging yeast grown under non-CR conditions on 2% glucose (**Figures 4.5 and 4.6**, respectively). However, the *tor1Δ* mutation significantly increases the concentrations of PA in "old" (cultured for 14 days and longer) Q and NQ cells of chronologically aging yeast grown under non-CR conditions (**Figures 4.5 and 4.6**, respectively). My findings suggest that the abilities of the *tor1Δ* mutation to increase the concentrations of PA only in chronologically "old" Q and NQ cells may cause the significant extensions of their longevities known to be elicited by the *tor1Δ* mutation.

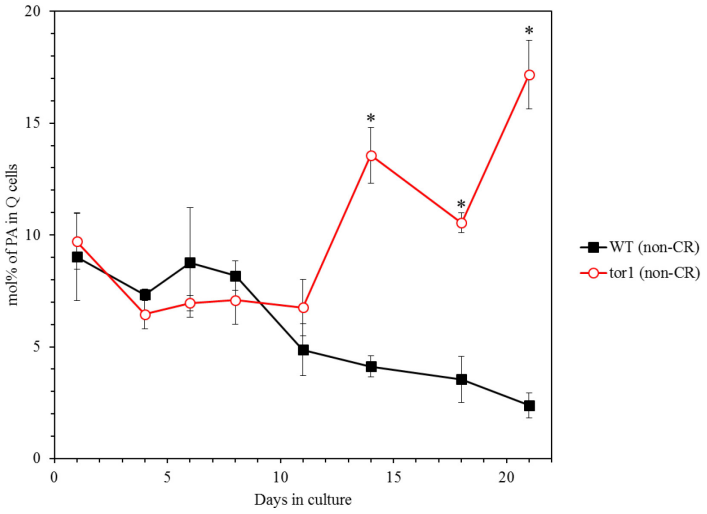

Figure 4.5. The *tor1Δ* mutation increases the concentrations of PA only in "old" Q cells of chronologically aging yeast grown under non-CR conditions. Cells were cultured in the nutrient-rich YP medium initially containing 2% glucose. Q cells were purified from cell cultures recovered on days 1, 4, 6, 8, 11, 14, 18 or 21 of cell culturing. Extraction of cellular lipids, as well as their mass spectrometric identification and quantitation, were carried out as described in Materials and Methods. Based on these data, the concentrations of PA were calculated in mol%. Data are presented as means ± SEM (n = 2; * $p < 0.05$).

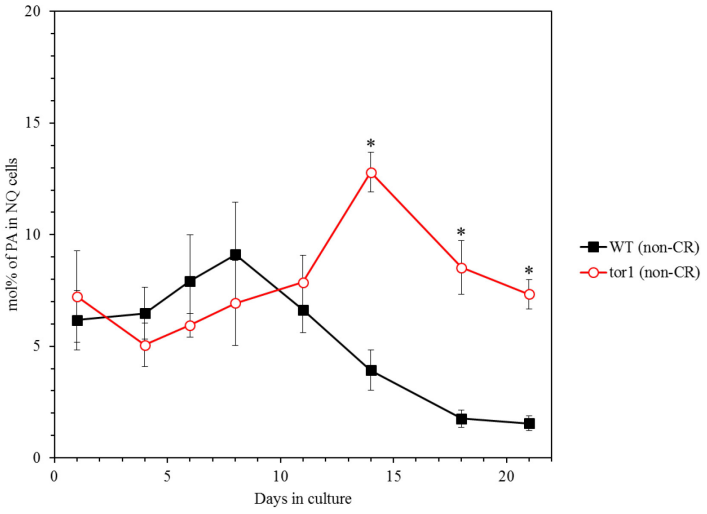

Figure 4.6. The *tor1Δ* mutation increases the concentrations of PA only in "old" NQ cells of chronologically aging yeast grown under non-CR conditions. Cells were cultured in the nutrient-rich YP medium initially containing 2% glucose. NQ cells were purified from cell cultures recovered on days 1, 4, 6, 8, 11, 14, 18 or 21 of cell culturing. Extraction of cellular lipids, as well as their mass spectrometric identification and quantitation, were carried out as described in Materials and Methods. Based on these data, the concentrations of PA were calculated in mol%. Data are presented as means ± SEM (n = 2; * $p < 0.05$).

4.3.4 The *tor1Δ* mutation increases the concentrations of PS in "young" and "middle-aged" Q and NQ cells, as well as decreases the concentrations of PI in "young" cells of both cell types of chronologically aging yeast grown under non-CR conditions

Using quantitative mass spectrometry, I assessed the effects of the *tor1Δ* mutation on the concentrations of PS and PI in Q and NQ cells of chronologically aging yeast grown under non-CR conditions on 2% glucose. I discovered that this mutation caused the following effects on the cellular concentrations of PS and PI: 1) in chronologically "young" (cultured from 1 to 6 days) and "middle-aged" (cultured from 8 to 11 days) Q and NQ cells, the *tor1Δ* mutation significantly increases the concentrations of PS (**Figures 4.7 and 4.8**, respectively); 2) in chronologically "old" (cultured for 14 days and

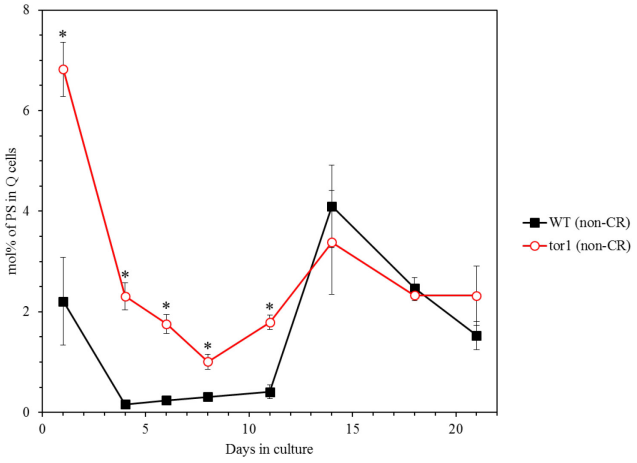

Figure 4.7. The *tor1Δ* mutation increases the concentrations of PS in chronologically "young" (cultured from 1 to 6 days) and "middle-aged" (cultured from 8 to 11 days) Q cells of chronologically aging yeast grown under non-CR conditions. Cells were cultured in the nutrient-rich YP medium initially containing 2% glucose. Q cells were purified from cell cultures recovered on days 1, 4, 6, 8, 11, 14, 18 or 21 of cell culturing. Extraction of cellular lipids, as well as their mass spectrometric identification and quantitation, were carried out as described in Materials and Methods. Based on these data, the concentrations of PS were calculated in mol%. Data are presented as means ± SEM (n = 2; * $p < 0.05$).

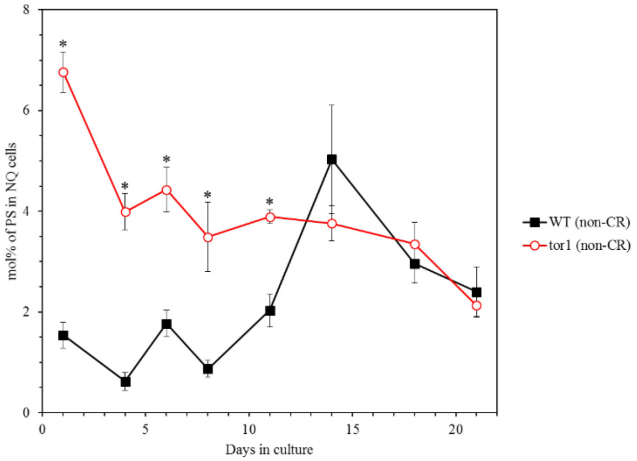

Figure 4.8. The *tor1Δ* mutation increases the concentrations of PS in chronologically "young" (cultured from 1 to 6 days) and "middle-aged" (cultured from 8 to 11 days) NQ cells of chronologically aging yeast grown under non-CR conditions. Cells were cultured in the nutrient-rich YP medium initially containing 2% glucose. NQ cells were purified from cell cultures recovered on days 1, 4, 6, 8, 11, 14, 18 or 21 of cell culturing. Extraction of cellular lipids, as well as their mass spectrometric identification and quantitation, were carried out as described in Materials and Methods. Based on these data, the concentrations of PS were calculated in mol%. Data are presented as means ± SEM (n = 2; * $p < 0.05$).

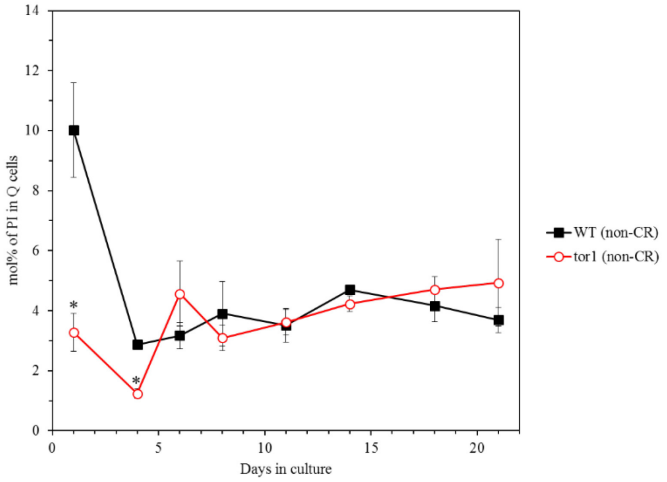

Figure 4.9. The *tor1Δ* mutation decreases the concentrations of PI in chronologically "young" (cultured from 1 to 4 days) Q cells of chronologically aging yeast grown under non-CR conditions. Cells were cultured in the nutrient-rich YP medium initially containing 2% glucose. Q cells were purified from cell cultures recovered on days 1, 4, 6, 8, 11, 14, 18 or 21 of cell culturing. Extraction of cellular lipids, as well as their mass spectrometric identification and quantitation, were carried out as described in Materials and Methods. Based on these data, the concentrations of PI were calculated in mol%. Data are presented as means ± SEM (n = 2; * $p < 0.05$).

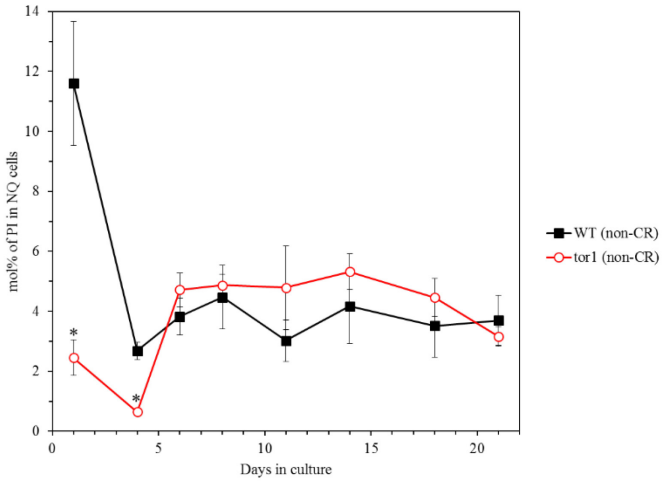

Figure 4.10. The *tor1Δ* mutation decreases the concentrations of PI in chronologically "young" (cultured from 1 to 4 days) NQ cells of chronologically aging yeast grown under non-CR conditions. Cells were cultured in the nutrient-rich YP medium initially containing 2% glucose. NQ cells were purified from cell cultures recovered on days 1, 4, 6, 8, 11, 14, 18 or 21 of cell culturing. Extraction of cellular lipids, as well as their mass spectrometric identification and quantitation, were carried out as described in Materials and Methods. Based on these data, the concentrations of PI were calculated in mol%. Data are presented as means ± SEM (n = 2; * $p < 0.05$).

longer) Q and NQ cells, the *tor1Δ* mutation does not change PS concentration (**Figures 4.7 and 4.8**, respectively); 3) in chronologically "young" (cultured from 1 to 4 days) Q and NQ cells, the *tor1Δ* mutation substantially decreases the concentrations of PI (**Figures 4.9 and 4.10**, respectively); and 4) in chronologically "middle-aged" (cultured from 6 to 11 days) and "old" (cultured for 14 days and longer) Q and NQ cells, the *tor1Δ* mutation does not change PI concentration (**Figures 4.9 and 4.10**, respectively). These findings suggest that the abilities of the *tor1Δ* mutation to increase PS concentrations in "young" and "middle-aged" Q and NQ cells, as well its abilities to decrease PI concentrations in "young" cells of both cell types, may be responsible in part for the significant delays of aging of Q and NQ cells known to be elicited by the *tor1Δ* mutation.

4.3.5 The *tor1Δ* mutation increases the concentrations of PE in "middle-aged" Q and NQ cells, as well as decreases the concentrations of PC in "middle-aged" and "old" NQ cells, of chronologically aging yeast grown under non-CR conditions

With the help of quantitative mass spectrometry, I examined how the *tor1Δ* mutation influences the concentrations of PE and PC in Q and NQ cells of chronologically aging yeast grown under non-CR conditions in 2% glucose. I found that the *tor1Δ* mutation caused the following effects on the cellular concentrations of PE and PC: 1) in chronologically "middle-aged" (cultured from 8 to 11 days) Q and NQ cells, the *tor1Δ* mutation significantly increases the concentrations of PE (**Figures 4.11 and 4.12**, respectively); 2) in chronologically "young" (cultured from 1 to 6 days) and "old" (cultured for 14 days and longer) Q and NQ cells, the *tor1Δ* mutation does not change PE concentration (**Figures 4.11 and 4.12**, respectively); 3) the *tor1Δ* mutation does not change PC concentrations in Q cells of any chronological age (**Figure 4.13**);

and 4) the *tor1Δ* mutation decreases the concentrations of PC in "middle-aged" (cultured from 8 to 11 days) and "old" (cultured for 14 days and longer) NQ cells (**Figure 4.14**). My findings suggest that the abilities of the *tor1Δ* mutation to increase the concentrations of PE in "middle-aged" Q and NQ cells, as well as its abilities to decrease the concentrations of PC in "middle-aged" and "old" NQ cells, may be responsible in part for the significant delays of aging of Q and NQ cells known to be caused by the *tor1Δ* mutation.

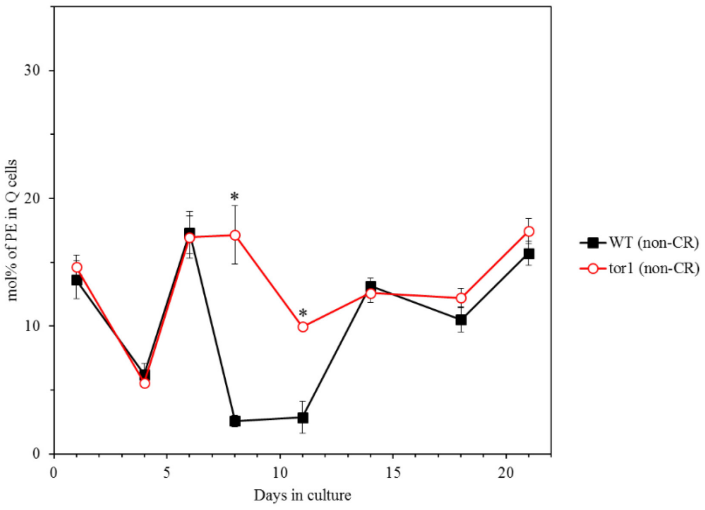

Figure 4.11. The *tor1Δ* mutation increases the concentrations of PE in chronologically "middle-aged" (cultured from 8 to 11 days) Q cells of chronologically aging yeast grown under non-CR conditions. Cells were cultured in the nutrient-rich YP medium initially containing 2% glucose. Q cells were purified from cell cultures recovered on days 1, 4, 6, 8, 11, 14, 18 or 21 of cell culturing. Extraction of cellular lipids, as well as their mass spectrometric identification and quantitation, were carried out as described in Materials and Methods. Based on these data, the concentrations of PE were calculated in mol%. Data are presented as means ± SEM (n = 2; * $p < 0.05$).

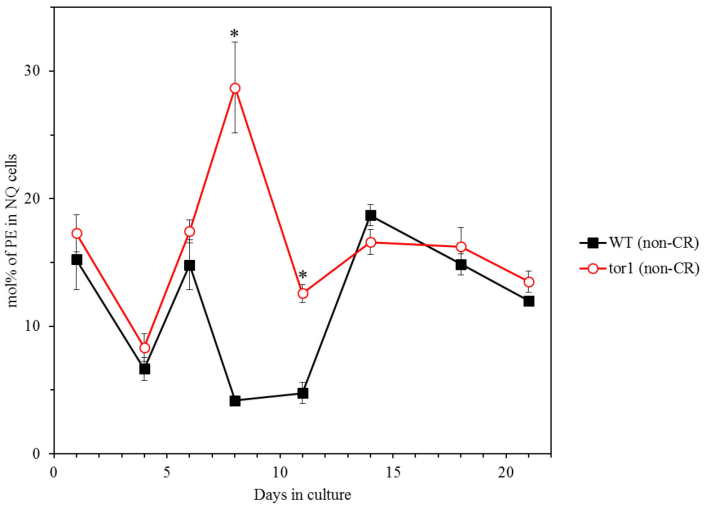

Figure 4.12. The *tor1Δ* mutation increases the concentrations of PE in chronologically "middle-aged" (cultured from 8 to 11 days) NQ cells of chronologically aging yeast grown under non-CR conditions. Cells were cultured in the nutrient-rich YP medium initially containing 2% glucose. NQ cells were purified from cell cultures recovered on days 1, 4, 6, 8, 11, 14, 18 or 21 of cell culturing. Extraction of cellular lipids, as well as their mass spectrometric identification and quantitation, were carried out as described in Materials and Methods. Based on these data, the concentrations of PE were calculated in mol%. Data are presented as means ± SEM (n = 2; * $p < 0.05$).

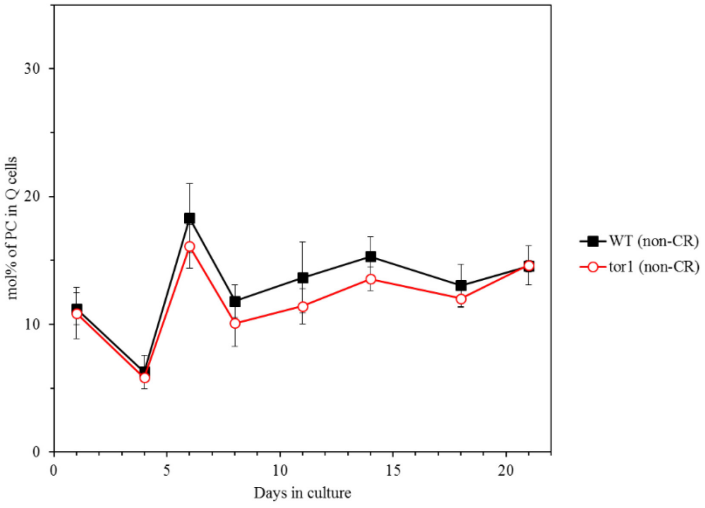

Figure 4.13. The *tor1Δ* mutation does not change PC concentrations in Q cells of any chronological age in yeast grown under non-CR conditions. Cells were cultured in the nutrient-rich YP medium initially containing 2% glucose. Q cells were purified from cell cultures recovered on days 1, 4, 6, 8, 11, 14, 18 or 21 of cell culturing. Extraction of cellular lipids, as well as their mass spectrometric identification and quantitation, were carried out as described in Materials and Methods. Based on these data, the concentrations of PC were calculated in mol%. Data are presented as means ± SEM (n = 2).

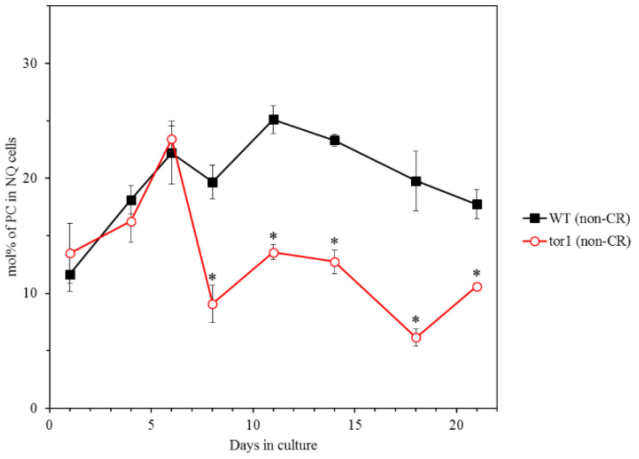

Figure 4.14. The *tor1Δ* mutation decreases the concentrations of PC in "middle-aged" (cultured from 8 to 11 days) and "old" (cultured for 14 days and longer) NQ cells of chronologically aging yeast grown under non-CR conditions. Cells were cultured in the nutrient-rich YP medium initially containing 2% glucose. NQ cells were purified from cell cultures recovered on days 1, 4, 6, 8, 11, 14, 18 or 21 of cell culturing. Extraction of cellular lipids, as well as their mass spectrometric identification and quantitation, were carried out as described in Materials and Methods. Based on these data, the concentrations of PC were calculated in mol%. Data are presented as means ± SEM (n = 2; * $p < 0.05$).

4.4 Discussion

Studies described in this chapter of my thesis have demonstrated that in yeast cultured under non-CR conditions the *tor1Δ* mutation causes a remodeling of lipid metabolism and transport within both Q and NQ cells. My findings imply that the remodeling of lipid dynamics elicited by the *tor1Δ* mutation in each of these cell populations differs substantially from the ones observed in Q and NQ cells subjected to CR in the absence of LCA or in Q and NQ cells treated with LCA under CR conditions. Based on findings presented in this chapter, I propose a hypothetical model on how the *tor1Δ* mutation, a longevity-extending genetic intervention, may delay yeast chronological aging by altering the age-related dynamics of various lipids in Q and NQ cells progressing through consecutive stages of the aging process. My model posits the following: 1) in "young" Q cells, the *tor1Δ* mutation increases the concentration of PS and CL, perhaps by intensifying their synthesis in the ER and mitochondria, respectively (**Figure 4.15**);

2) in “young” Q cells, the *tor1Δ* mutation reduces the concentration of PI, perhaps by slowing down its synthesis in the ER (**Figure 4.15**); 3) in “middle-aged” Q cells, the *tor1Δ* mutation elevates the concentrations of TAG, PS and PE, likely by stimulating their synthesis in the ER and mitochondria (**Figure 4.16**); 4) in “middle-aged” Q cells, the *tor1Δ* mutation decreases the concentration of CL, perhaps by slowing down its synthesis in mitochondria (**Figure 4.16**); 5) in “old” Q cells, the *tor1Δ* mutation increases the concentration of PA, possibly by stimulating its formation in the ER (**Figure 4.17**); 6) in “old” Q cells, the *tor1Δ* mutation decreases the concentration of CL, likely by decelerating its synthesis in mitochondria (**Figure 4.17**); 7) in “young” NQ cells, the *tor1Δ* mutation increases the concentration of PS and CL, perhaps by intensifying their synthesis in the ER and mitochondria, respectively (**Figure 4.18**); 8) in “young” NQ cells, the *tor1Δ* mutation reduces the concentration of PI, perhaps by slowing down its synthesis in the ER (**Figure 4.18**); 9) in “middle-aged” NQ cells, the *tor1Δ* mutation elevates the concentrations of TAG, PS and PE, likely by stimulating their synthesis in the ER and mitochondria (**Figure 4.19**); 10) in “middle-aged” NQ cells, the *tor1Δ* mutation decreases the concentrations of PC and CL, perhaps by slowing down their synthesis in the ER and mitochondria, respectively (**Figure 4.19**); 11) in “old” NQ cells, the *tor1Δ* mutation increases the concentration of PA, possibly by stimulating its formation in the ER (**Figure 4.20**); and 12) in “old” NQ cells, the *tor1Δ* mutation decreases the concentration of PC and CL, likely by decelerating their synthesis in the ER and mitochondria, respectively (**Figure 4.20**).

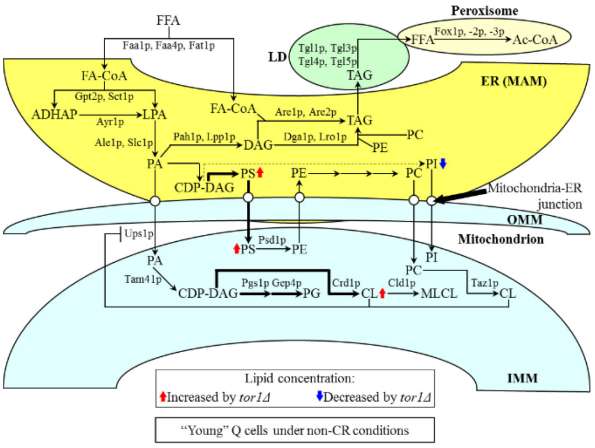

Figure 4.15. A hypothetical model on how the *tor1Δ* mutation alters the metabolism of PS, PI and CL in "young" Q cells. The model is based on mass spectrometric lipidomics of purified Q cells that were recovered from yeast cultured from 1 to 4 days prior to entry into stationary growth phase under non-CR conditions in 2% glucose. From the data of lipidomic analysis, I inferred an outline of the rates and efficiencies of lipid metabolism that were increased (thick solid arrows) or decreased (thin dashed arrows) by the *tor1Δ* mutation under non-CR conditions. Arrows next to the names of lipid classes denote those of them whose concentrations are elevated (red arrows) or reduced (blue arrows) by the *tor1Δ* mutation in cells under non-CR conditions.

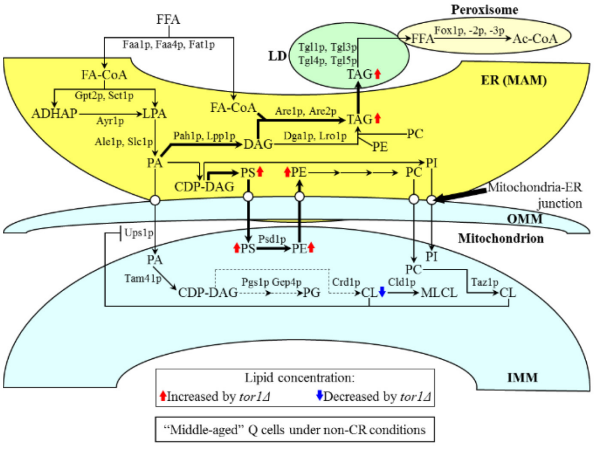

Figure 4.16. A hypothetical model on how the *tor1Δ* mutation alters the metabolism of TAG, PS, PE and CL in "middle-aged" Q cells. The model is based on mass spectrometric lipidomics of purified Q cells that were recovered from yeast cultured from 6 to 11 days under non-CR conditions in 2% glucose. From the data of lipidomic analysis, I inferred an outline of the rates and efficiencies of lipid metabolism that were increased (thick solid arrows) or decreased (thin dashed arrows) by the *tor1Δ* mutation under non-CR conditions. Arrows next to the names of lipid classes denote those of them whose concentrations are elevated (red arrows) or reduced (blue arrows) by the *tor1Δ* mutation in cells under non-CR conditions.

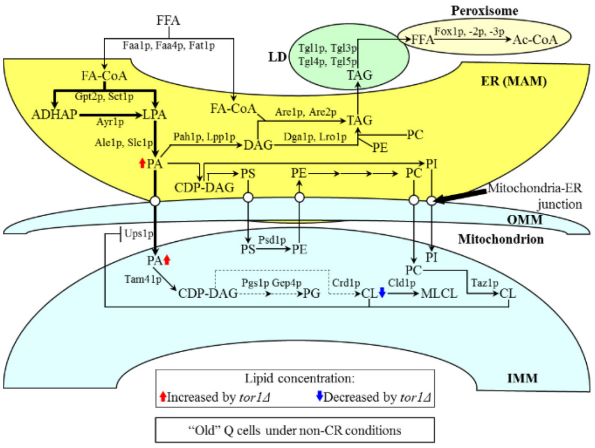

Figure 4.17. A hypothetical model on how the *tor1Δ* mutation alters the metabolism of PA and CL in "old" Q cells. The model is based on mass spectrometric lipidomics of purified Q cells that were recovered from yeast cultured for 14 days and longer under non-CR conditions in 2% glucose. From the data of lipidomic analysis, I inferred an outline of the rates and efficiencies of lipid metabolism that were increased (thick solid arrows) or decreased (thin dashed arrows) by the *tor1Δ* mutation under non-CR conditions. Arrows next to the names of lipid classes denote those of them whose concentrations are elevated (red arrows) or reduced (blue arrows) by the *tor1Δ* mutation in cells under non-CR conditions.

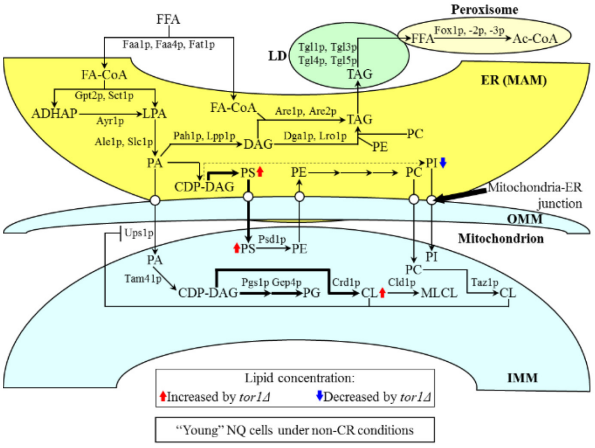

Figure 4.18. A hypothetical model on how the *tor1Δ* mutation alters the metabolism of PS, PI and CL in "young" NQ cells. The model is based on mass spectrometric lipidomics of purified NQ cells that were recovered from yeast cultured from 1 to 4 days prior to entry into stationary growth phase under non-CR conditions in 2% glucose. From the data of lipidomic analysis, I inferred an outline of the rates and efficiencies of lipid metabolism that were increased (thick solid arrows) or decreased (thin dashed arrows) by the *tor1Δ* mutation under non-CR conditions. Arrows next to the names of lipid classes denote those of them whose concentrations are elevated (red arrows) or reduced (blue arrows) by the *tor1Δ* mutation in cells under non-CR conditions.

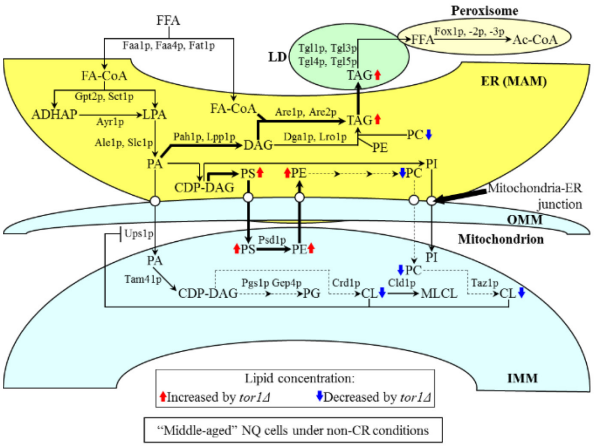

Figure 4.19. A hypothetical model on how the *tor1Δ* mutation alters the metabolism of TAG, PC, PS, PE and CL in "middle-aged" NQ cells. The model is based on mass spectrometric lipidomics of purified NQ cells that were recovered from yeast cultured from 6 to 11 days under non-CR conditions on 2% glucose. From the data of lipidomic analysis, I inferred an outline of the rates and efficiencies of lipid metabolism that were increased (thick solid arrows) or decreased (thin dashed arrows) by the *tor1Δ* mutation under non-CR conditions. Arrows next to the names of lipid classes denote those of them whose concentrations are elevated (red arrows) or reduced (blue arrows) by the *tor1Δ* mutation in cells under non-CR conditions.

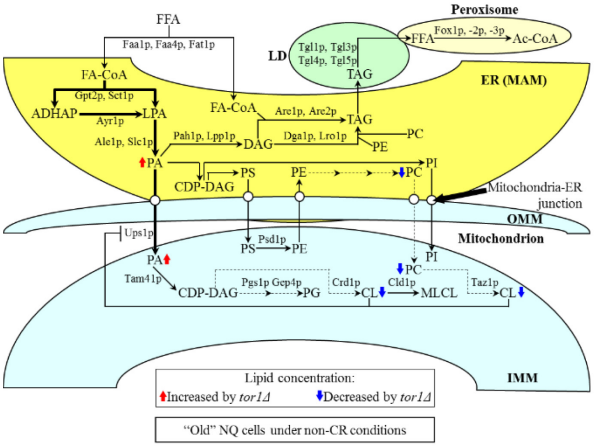

Figure 4.20. A hypothetical model on how the *tor1Δ* mutation alters the metabolism of PA, PC and CL in "old" NQ cells. The model is based on mass spectrometric lipidomics of purified NQ cells that were recovered from yeast cultured from 6 to 11 days under non-CR conditions on 2% glucose. From the data of lipidomic analysis, I inferred an outline of the rates and efficiencies of lipid metabolism that were increased (thick solid arrows) or decreased (thin dashed arrows) by the *tor1Δ* mutation under non-CR conditions. Arrows next to the names of lipid classes denote those of them whose concentrations are elevated (red arrows) or reduced (blue arrows) by the *tor1Δ* mutation in cells under non-CR conditions.

In sum, my findings imply that the pattern of age-related changes in lipid concentrations seen in Q and NQ cells carrying the *tor1Δ* mutation differs substantially from the patterns observed in Q and NQ cells either subjected to CR in the absence of LCA or treated with LCA under CR conditions. Thus, it seems that there are at least three different ways of delaying yeast chronological aging by altering lipid metabolism and transport in Q and NQ cells; these three ways are outlined in **Figures 2.17-2.20, 3.15-3.20** and **4.15-4.20**.

Future studies will address the key question which of the alterations in lipid concentrations observed in Q and NQ cells are essential for the ability of the *tor1Δ* mutation to delay aging of these cell populations under non-CR conditions. It is conceivable that some of these alterations just coincide with the progress of chronological aging. To address this challenging question, it will be necessary to examine how single-gene mutations eliminating enzymes that accelerate individual reactions of lipid metabolism in yeast (**Figures 4.15 – 4.20**) impact the efficiency with which the *tor1Δ* mutation delays yeast chronological aging under non-CR conditions. Moreover, a challenge remains to understand how the alterations of lipid concentrations seen in chronologically aging Q and NQ cells carrying the *tor1Δ* mutation delay their aging under non-CR conditions.

5 References

1. Longo VD, Shadel GS, Kaeberlein M, Kennedy B. Replicative and Chronological Aging in *Saccharomyces cerevisiae.* Cell Metab 2012; 16:18-31.

2. Kaeberlein M. Lessons on longevity from budding yeast. Nature 2010; 464:513-519.

3. Gray JV, Petsko GA, Johnston GC, Ringe D, Singer R, Werner-Washburne M. "Sleeping Beauty": Quiescence in *Saccharomyces cerevisiae.* Microbiol and Mol Biol Rev 2004; 68:187-206.

4. Werner-Washburne M, Roy S, Davidson GS. Aging and the survival of quiescent and non-quiescent cells in yeast stationary-phase cultures. Subcell Biochem 2012; 57:123-143.

5. Arlia-Ciommo A, Leonov A, Piano A, Svistkova V, Titorenko VI. Cell-autonomous mechanisms of chronological aging in yeast *Saccharomyces cerevisiae*. Microbial Cell 2014; 1:163-178.

6. Botstein D, Fink GF. Yeast: an experimental organism for 21st century biology. Genetics 2011; 18:695-704.

7. Lee SS, Avalos Vizcarra I, Huberts DH, Lee LP, Heinemann M. Whole lifespan microscopic observation of budding yeast aging through a microfluidic dissection platform. Proc Natl Acad Sci USA; 109:4916-4920.

8. Sutphin GL, Olsen BA, Kennedy BK, Kaeberlein M. Genome-wide analysis of yeast aging. Subcell Biochem 2012; 57:251-289.

9. Arlia-Ciommo A, Piano A, Leonov A, Svistkova V, Titorenko VI. Quasi-programmed aging of budding yeast: a trade-off between programmed processes of cell proliferation, differentiation, stress response, survival and death defines yeast lifespan. Cell Cycle 2014; 13:3336-3349.

10. Denoth Lippuner A, Julou T, Barral Y. Budding Yeast as a model organism to study the effects of age. FEMS Microbiol Rev 2014; 38:300-325.

11. Steffen KK, Kennedy BK, Kaeberlein M. Measuring replicative life span in budding yeast. J Vis Exp 28:1209.

12. Longo VD, Fabrizio P. Chronological aging in *Saccharomyces cerevisiae.* Subcell Biochem 2012; 57:101-121.

13. Hu J, Wei M, Mirisola MG, Longo VD. Assessing chronological aging in *Saccharomyces cerevisiae*. Methods Mol Bio 2013; 965:463-472.

14. Fontana L, Partridge L, Longo VD. Extending healthy lifespan- from yeast to humans. Science 2010; 328:321-326.

15. Burstein MT, Kyryakov P, Beach A, Richard VR, Koupaki O, Gomez-Perez A, Leonov A, Levy S, Noohi F, Titorenko V. Lithocholic acid extends longevity of chronologically aging yeast only if added at certain critical periods of their lifespan. Cell Cycle 2012; 11:3443-3462.

16. Allen C, Büttner S, Aragon AD, Thomas JA, Meirelles O, Jaetao JE, Benn D, Ruby SW, Veenhuis M, Madeo F, Werner-Washburne M. Isolation of quiescent and nonquiescent cells from yeast stationary-phase cultures. J Cell Biol 2006; 174:89-100.

17. Aragon AD, Rodriguez AL, Meirelles O, Roy S, Davidson GS, Tapia PH, Allen C, Benn D, Werner-Washburne M. Characterization of differentiated quiescent and nonquiescent cells in yeast stationary phase cultures. Mol Biol Cell 2008; 19:1217-1280.

18. De Virgilio C. The essence of quiescence. FEMS Microbiol Rev 2012; 36:306-339.

19. Smets B, Ghillebert R, De Snijder P, Binda M, Swinnen E, De Virgilio C, Winderickx J. Life in the midst of scarcity: adaptations to nutrient availability in *Saccharomyces cerevisiae*. Curr Genet 2010; 56:1-32.

20. Conrad M, Schothorst J, Kankipati HN, Van Zeebroeck G, Rubio-Texeira M, Thevelein JM. Nutrient sensing and signalling in yeast *Saccharomyces cerevisiae*. FEMS Microbiol Rev 2014; 38:254-299.

21. Swinnen E, Ghillebert R, Wilms T, Winderickx J. Molecular mechanisms linking the evolutionary conserved TORC1-Sch9 nutrient signalling branch to lifespan regulation in *Saccharomyces cerevisiae*. FEMS Yeast Res 2014; 14:17-32.

22. Henry SA, Kohlwein SD, Carman GM. Metabolism and Regulation of Glycerolipids in the Yeast *Saccharomyces cerevisiae*. Genetics 2012; 190:317-349.

23. Carman GM, Han G. Regulation of Phospholipid Synthesis in the Yeast *Saccharomyces cerevisiae*. Annu Rev Biochem 2011; 80:859-883.

24. Klug L, Daum G. Yeast lipid metabolism at a glance. FEMS Yeast Res 2014; 14:369-388.

25. Klose C, Surma MA, Gerl MJ, Meyenhofer F, Shevchenko A, Simons K. Flexibility of a Eukaryotic Lipidome- Insights from Yeast Lipidomics. PLoS ONE 2012; 7:1-11.

26. Arlia-Ciommo A, Piano A, Svistkova V, Mohtashami S, Titorenko VI. Mechanisms Underlying the Anti-Aging and Anti-Tumor Effects of Lithocholic Bile Acid. Int J Mol Sci 2014; 15:16522-16543.

27. Goldberg AA, Bourque SD, Kyryakov P, Gregg C, Boukh-Viner T, Beach A, Burstein MT, Machkalyan G, Richard V, Rampersad S, Cyr D, Milijevic S, Titorenko VI. Effect of calorie restriction on the metabolic history of chronologically aging yeast. Exp Gerontol 2009; 44:555-571.

28. Beach A, Titorenko VI. In search of housekeeping pathways that regulate longevity. Cell Cycle 2011; 10:3042-3044.

29. Goldberg AA, Richard VR, Kyryakov P, Bourque SD, Beach A, Burstein MT, Glebov A, Koupaki O, Boukh-Viner T, Gregg C, Juneau M, English AM, Thomas DY, Titorenko VI. Chemical genetic screen identifies lithocholic acid as an anti-aging compound that extends yeast chronological life span in a TOR-independent manner, by modulating housekeeping longevity assurance processes. Aging 2010; 2:393-414.

30. Burstein MT, Titorenko VI. A mitochondrially targeted compound delays aging in yeast through a mechanism linking mitochondrial membrane lipid metabolism to mitochondrial redox biology. Redox Biol 2014; 2:305-307.

31. Richard VR, Bourque SD, Titorenko VI. Metabolomic and lipidomic analyses of chronologically aging yeast. In: Yeast Genetics. Methods and Protocols. Eds. Smith JS and Burke DJ. Humana Press USA. 2014; 359-373.

32. Osman C, Voelker DR, Langer T. Making heads or tails of phospholipids in mitochondria. J Cell Biol 2011; 192:7-16.

33. Tamura Y, Harada Y, Nishikawa S, Yamano K, Kamiya M, Shiota T, Kuroda T, Kuge O, Sesaki H, Imai K, Tomii K, Endo T. Tam41 is a CDP-diacylglycerol synthase required for cardiolipin biosynthesis in mitochondria. Cell Metab 2013; 17:709-718.

34. Goldberg AA, Bourque SD, Kyryakov P, Boukh-Viner T, Gregg C, Beach A, Burstein MT, Machkalyan G, Richard V, Rampersad S, Titorenko VI. A novel function of lipid droplets in regulating longevity. Biochem Soc Trans 2009; 37:1050-1055.

35. Richard VR, Beach A, Piano A, Leonov A, Feldman R, Burstein MT, Kyryakov P, Gomez-Perez A, Arlia-Ciommo A, Baptista S, Campbell C, Goncharov D, Pannu S, Patrinos D, Sadri B, Svistkova V, Victor A, Titorenko VI. Mechanism of liponecrosis, a distinct mode of programmed cell death. Cell Cycle 2014; 13:3707-3726.

36. Sheibani S, Richard VR, Beach A, Leonov A, Feldman R, Mattie S, Khelghatybana L, Piano A, Greenwood M, Vali H, Titorenko VI. Macromitophagy, neutral lipids synthesis, and peroxisomal fatty acid oxidation protect yeast from "liponecrosis", a previously unknown form of programmed cell death. Cell Cycle 2014; 13:138-147.